Copyright Warning & Restrictions

The copyright law of the United States (Title 17, United States Code) governs the making of photocopies or other reproductions of copyrighted material.

Under certain conditions specified in the law, libraries and archives are authorized to furnish a photocopy or other reproduction. One of these specified conditions is that the photocopy or reproduction is not to be "used for any purpose other than private study, scholarship, or research." If a, user makes a request for, or later uses, a photocopy or reproduction for purposes in excess of "fair use" that user may be liable for copyright infringement,

This institution reserves the right to refuse to accept a copying order if, in its judgment, fulfillment of the order would involve violation of copyright law.

Please Note: The author retains the copyright while the New Jersey Institute of Technology reserves the right to distribute this thesis or dissertation

Printing note: If you do not wish to print this page, then select "Pages from: first page # to: last page #" on the print dialog screen

ABSTRACT

DEVELOPMENT OF A MATHEMATICAL MODEL OF GAIT DYNAMICS

by
Tae Ho Choi

There exists hypothesis that gait selection is strongly correlated with mechanical energy efficiency in normal subjects. The hypothesis is experimentally proven, and intuitively taken for granted. However, it is not mathematically proven that the minimum energy consumption hypothesis is the underlying principle for the normal human gait. To prove the hypothesis we have developed a mathematical model of human walking, in which it is possible to predict an optimal gait at any given speed of walking based on the principle of minimum mechanical energy consumption.

This improved model, which includes the double-support phase of walking as well as the swing phase, is an extension to the previous model studied in the author's master thesis which included only the swing phase; with this improved model it is possible to calculate the mechanical energy loss during an entire walking cycle. This permits the unique determination of an optimal gait for any given speed of walking which minimizes the mechanical energy loss per unit length of motion. The hypothesis that minimum energy is consumed in normal gait is tested by comparing the predicted gait with that actually observed experimentally. Reasonable results are obtained and it is confirmed that minimum energy consumption is the underlying principle determining the characteristics of human gait. Nevertheless, there is some discrepancy between the theoretical and empirical data; to reduce the discrepancy it will be necessary to develop a more detailed model which permits, for example, the stance leg to bend, and the foot of the swing leg to move as an independent segment. To facilitate this task a generalized model of walking is developed and recommended for future research.

DEVELOPMENT OF A MATHEMATICAL MODEL OF GAIT DYNAMICS

by
Tae Ho Choi

A Dissertation
Submitted to the Faculty of
New Jersey Institute of Technology
in Partial Fulfillment of the Requirements for the Degree of
Doctor of Philosophy

Department of Electrical and Computer Engineering

May 1997

APPROVAL PAGE

DEVELOPMENT OF A MATHEMATICAL MODEL OF GAIT DYNAMICS

Tae Ho Choi

Dr. H. Michael Lacker, Dissertation Co-Adviser — Date
Professor of Applied Mathematics, NJIT

Dr. Peter Engler, Dissertation Co-Adviser — Date
Associate Professor of Electrical and Computer Engineering, NJIT

Dr. Stanley S. Reisman, Committee Member — Date
Professor of Electrical and Computer Engineering, NJIT

Dr. Timothy Chang, Committee Member — Date
Associate Professor of Electrical and Computer Engineering, NJIT

Dr. Judy Deutsch, Committee Member — Date
Assistant Professor of Physical Therapy, UMDNJ-SHRP

BIOGRAPHICAL SKETCH

Author: Tae Ho Choi

Degree: Doctor of Philosophy

Date: May 1997

Undergraduate and Graduate Education:

- Doctor of Philosophy in Electrical Engineering,
  New Jersey Institute of Technology, Newark, NJ, 1997
- Master of Science in Electrical Engineering,
  New Jersey Institute of Technology, Newark, NJ, 1993
- Master of Science in Electrical Engineering,
  Korea Advanced Institute of Science and Technology, Seoul, Korea, 1979
- Bachelor of Science in Electronic Engineering,
  Seoul National University, Seoul, Korea, 1977

Major: Electrical Engineering

Presentations and Publications:

Lacker, H.M., H. Chaudry, T.H. Choi, W. Boda, W.N. Tapp, S.S. Reisman, T. Findley, and P. Engler "Calculation of Mechanical Energy Cost in a simple Model of Human Walking." *19th IEEE Annual Northeast Bioengineering Conference.* Newark, NJ, March 18-19, 1993.

This dissertation is dedicated to
Jesus Christ

ACKNOWLEDGMENT

I would like to thank the people who helped me to complete my research. With all the helps together the problem, which is to prove the minimum energy gait hypothesis mathematically, has turned out as a simple and easy problem even though it looked formidable to me about five years ago.

Heartily thanks to Dr. Peter Engler for his kind advice, and sincere eagerness to help me to do research. Extreme thanks to Dr. H. Michael Lacker for his advice, kindness and ability in mathematics. I was impressed by his methods to try to solve problems, and learned many things from his attitude doing research. Those things will give me invaluable effect in my future life. Thanks to Dr. Sue Ann Sisto and Dr. Judy Redling for their help in getting experimental data. Thanks to my research colleagues. While discussing with them many things could be understood. Finally, I have to give the greatest thanks to Jesus Christ. Whenever I was fronted with problems seemingly not solvable, I prayed and he gave me answers. At this moment apparently finishing my research, a new and interesting question arises in my mind. That is why and how he answered all of my questions.

All of these things were made possible in sincere academic atmosphere in NJIT to find out truth. Like many other students I want to express my thanks to favors and benefits I received from NJIT during my research. Those were the most important resources to my survival for the past years in school.

TABLE OF CONTENTS

TABLE OF CONTENTS
(Continued)

Chapter **Page**

TABLE OF CONTENTS
(Continued)

Chapter **Page**

TABLE OF CONTENTS
(Continued)

Chapter **Page**

LIST OF TABLES

LIST OF FIGURES

Figure **Page**

LIST OF FIGURES
(Continued)

Figure **Page**

LIST OF FIGURES
(Continued)

Figure **Page**

CHAPTER 1

INTRODUCTION

1.1 Objective

Human walking may appear simple, but it is controlled by complicated coordination between various elements, and there are numerous theories and mathematical models in the literature for analysis of human body dynamics using rigid-body idealization. The theories and models say that the swing leg acts as a free pendulum and muscular control is not necessary during the swing phase, that there are many other forces and moments acting on the swing leg in addition to gravity(Fenn 1930; Beckett and Chang 1968) and that it seems reasonable to expect the movement of the legs would be made in such a way as to reduce the muscular effort to a minimum consistent with physical conditions imposed on the walker (e.g. constant walking speed, step length or step frequency) (Inman 1966). Experimentally it is found that the energy consumption per unit walking distance is a minimum at a particular chosen step frequency(Elftman 1966; Ralston 1974). This result led Inman(1966) to describe locomotion as the translation of the mass center through space along a path requiring the least expenditure of energy. Beckett and Chang(1968) solved for joint moment effects in the swing leg that produces a prescribed swing phase gait in such a way as to give a minimum expenditure of energy. Mochon and McMahon(1980) have developed a mathematical model to predict the form of swing period vs. walking speed relationship. Lacker et al.(1993) have extended the coupled pendulum model of Mochon and McMahon(1980) to include joint viscosity, and improved the model resulting in output characteristics that better match the experimental data. Nevertheless, neither the Mochon and McMahon's model nor Lacker et al.'s extension to it, include the double-support phase. Therefore, an improved model incorporating the double-support phase as well as the swing phase is to be proposed in this dissertation.

1.2 Outline

In this research we have developed a mathematical model of human walking including both the swing phase and the double-support phase. In this two dimensional three angle model the body is represented by a three-coupled pendulum system, one inverted pendulum for the stance leg and two for the thigh and shank of the swing leg, respectively.(See Figure 2.1) The foot of the swing leg is rigidly attached to the shank at a right angle. It is assumed that the muscles act only to establish an initial velocity of the limbs at the beginning of the swing phase and the double-support phase. The swing leg and the rest of the body then moves through the remainder of the swing and double-support phases entirely under the influence of gravity and joint viscosity.

There are 11 independent structural parameters in the model. They are the lengths of the thigh, shank and foot, the masses of thigh, shank and upper body, the mass centers of the thigh and shank, and the viscous coefficients of the ankle, hip and knee joints. Total body mass and limb lengths are readily measured; masses and mass centers of limbs are taken from data published by Dempster(Veau 1977). With these information we can write the dynamic equations with the joint viscous coefficients as unknown parameters. The Downhill Simplex method(Press 1992) is then used to estimate joint viscous coefficients by a least square curve fitting procedure that minimizes the difference between the measured and modeled angle vs. time curves.

To validate this simple and primitive model and to test the minimum-energy-consumption hypothesis it is necessary to compare theoretical data with experimental data in normal subjects. The theoretically derived angle vs. time history is compared with tracings measured on a Vicon 370 Motion Analysis System. Then the particular gait parameters at a specific walking speed that consumes the minimum energy are identified and compared to the measured data.

We surveyed all the possible solutions for various values of the ratio between swing and double-support duration, step length and toe-off angle. These parameters vary with

walking speed. Thus a gait space is identified to produce a complete ensemble of model walks, consistent with a given model individual(set of structural parameters). And at each gait a two-point boundary value problem algorithm is used to solve the dynamic equations to match the two point configurations, which are the toe-off and heel-strike configurations. From the solution we can determine the dynamic variable values at each instant during the walking cycle and the net muscle forces required at the beginning of the swing and double-support phases. From these dynamic variables the energy loss during the walking cycle can be calculated. Mechanical energy losses are due to joint viscosities, impacts at heel-strike and full range of joint motion. The total energy loss is the energy the body must re-supply for the subsequent walking cycle. In addition the model predicts relationships between parameters(swing duration, double-support duration, step length and toe-off angle) and walking speed based on the hypothesis that gait selection is strongly correlated with mechanical energy efficiency in normal subjects. Finally, an attempt was made by comparing the theoretical and experimental data about consumed energy during walking to verify that the gait selected by a subject is the most efficient gait energetically.

In addition a generalized 2-D(two dimensional) walking model is proposed which generates the dynamic equation for a system of any number of segments. In this method the relation matrix(R), viscous matrix(B) and mass matrix(M) are defined. The relation matrix shows the relationship of segment connections, and contains the information about the length of every segment and the mass center of every point mass. The viscous matrix gives information about the joint viscosity between any two segments, and the mass matrix contains information about the mass of each point mass. If these three matrices are known, then we can get the dynamic equations of the system without the long and tedious derivation using the Lagrangean. With the Lagrangean, if the number of variables are no greater than three, the derivation is relatively simple. But, when the number of variables is greater than three, the derivation is not simple. It is proposed that the model developed in this dissertation be expanded by adding more segments to the foot, thigh and shank, and

by incorporating provision for bending the foot and stance leg. The methodology in this dissertation can be readily be expanded toward that effect.

The theoretical results will be compared with experimental results to validate the significance of the proposed mathematical model. In addition to adding more segments to the present model in the future we will also improve the present two phase model to incorporate multiple phases. In multiple phase model, the energy input from impulsive muscular force occurs at more than two points in the walking cycle at the beginnings of the swing phase and the double-support phase; this model is expected to produce better results.

CHAPTER 2

PREVIOUS WORK DONE

As explained above, Mochon's model(1980) includes both the swing leg and the stance leg. Beckett's model(1968) includes only the swing leg, negating the possibility of energy transfers between legs. In Mochon's model energy is conserved during the swing phase, but in Beckett's model energy is not conserved. Beckett's idea is that forces and moments that are imposed at the joints of the leg may produce motion that is consistent with the geometrical constraints and in such a way as to yield minimum energy expenditure. Consequently, Lacker and et al.(1993) have modified Mochon's model with Beckett's concept, and extended it using an algorithm which calculates the mechanical energy losses during the swing phase and at heel strike due to velocity dependent dissipating forces, i.e. viscous, and impact forces on the joints. However, Lacker's(1993) model did not consider the double-support phase, and therefore the energy losses that take place over an entire walking cycle(the swing phase and the double-support phase) could not be calculated. In this thesis work the model has been improved to include the double-support phase, and the total amount of mechanical energy that needs to be re-supplied during each step of a periodic walking cycle has been calculated.

2.1 Dempster's Anthropometric Data

The mathematical model requires anthropometric data for the evaluation of the parameters which are used in the equations. In their research Mochon and McMahon(1980) used Dempster's data(Veau 1977); Dempster's data are summarized in Appendix A. In our research the lengths of limbs are taken from experimental data, but masses and mass centers of limbs are estimated from the Dempster's data.

Dempster's data was derived from eight male cadavers of "more or less medium" build. They ranged in age from 52 to 83 years. Heights ranged from 61.1 to 73.5 inches and weights from 109.25 to 159.5 lb(Veau 1977).

2.2 Three Angle Model for the Swing Phase

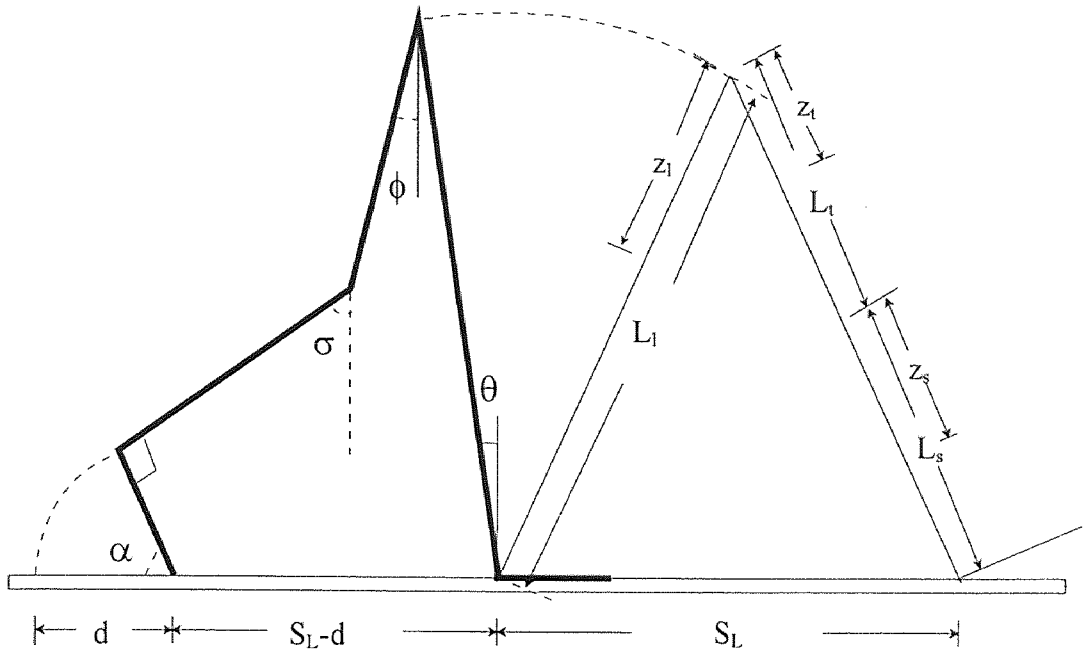

Figure 2.1 Schematic representation of the model during the swing phase; the solid line represents the initial configuration, and the regular line the final configuration.

Mochon and McMahon(1980) model introduced a mathematical model of the swing phase of walking. This model is two dimensional, and ballistic in the sense that, after the initial velocity of a limb is prescribed, the subsequent swing phase motion solution is obtained by assuming that it is entirely the consequence of "free-fall" in a constant gravitational field without any energy losses. The body is represented by three links, one for the stance leg and two for the thigh and shank of the swing leg. The foot of the swing leg is rigidly attached to the distal link by a 90 degree angle, and therefore does not constitute a separate link. It is assumed that the muscles act only to establish an initial configuration and velocity of the limbs at the beginning of the swing phase. The swing leg and the rest

of the body then move throughout the remainder of the swing phase entirely under the action of gravity. The toe-off and heel-strike configurations are shown in Figure 2.1 where the step-length is represented as S_L, and the length of the foot as d.

The mathematical equation of the model has a nonlinear form as follows:

$$\begin{bmatrix} c_{11} & c_{12} & c_{13} \\ c_{21} & c_{22} & c_{23} \\ c_{31} & c_{32} & c_{33} \end{bmatrix} \begin{bmatrix} \ddot{\theta} \\ \ddot{\phi} \\ \ddot{\sigma} \end{bmatrix} + \begin{bmatrix} 0 & c_{12}^* & c_{13}^* \\ c_{21}^* & 0 & c_{23}^* \\ c_{31}^* & c_{32}^* & 0 \end{bmatrix} \begin{bmatrix} \dot{\theta}^2 \\ \dot{\phi}^2 \\ \dot{\sigma}^2 \end{bmatrix} = \begin{bmatrix} w_1 \sin\theta \\ w_2 \sin\phi \\ w_3 \sin\sigma \end{bmatrix} \tag{2.1}$$

where

$$c_{ij} = \bar{c}_{ij} \cos(\varphi_i - \varphi_j) \qquad i, j = 1, 2, 3 \text{ and } (\varphi_1, \varphi_2, \varphi_3) = (\theta, \phi, \sigma)$$

$$c_{ij}^* = \bar{c}_{ij} \sin(\varphi_i - \varphi_j)$$

$$(\bar{c}_{11},\ \bar{c}_{22},\ \bar{c}_{33}) = (M_T L_l^2 - 2M_l L_l z_l + M_l z_l^2,\ M_t z_t^2 + M_s L_t^2,\ M_s z_s^2)$$

$$(\bar{c}_{12},\ \bar{c}_{13},\ \bar{c}_{23}) = (-M_t L_l z_t - M_s L_l L_t,\ -M_s L_l z_s,\ M_s L_t z_s)$$

$$(\bar{c}_{21},\ \bar{c}_{31},\ \bar{c}_{32}) = (-M_t L_l z_t - M_s L_l L_t,\ -M_s L_l z_s,\ M_s L_t z_s)$$

$$(w_1,\ w_2,\ w_3) = (M_T L_l g - M_l z_l g,\ -M_t z_t g - M_s L_l g,\ -M_s z_s g)$$

L_l, L_t, L_s Lengths of the leg, thigh and shank, respectively.

z_l, z_t, z_s Distances of mass center of the leg, thigh and shank, respectively.

M_T, M_l, M_t, M_s Masses of the body, leg, thigh and shank, respectively.

θ, ϕ, σ Angles that the leg, thigh and shank make with the vertical, respectively.

The theoretical time history of angles θ, ϕ and σ are obtained by solving equation(2.1) with parameter values given in Tables 2.1, 2.2 and 2.3 when the step-length is 0.57916 (m) and the the swing time is 51 x (1/120)sec. The theoretical output is compared with experimental data in Figure 2.2.

Table 2.1 Lengths of limbs

Limb	Leg(L_l)	Thigh(L_t)	Shank(L_s)	Foot(L_f)
Length(m)	0.74471	0.37533	0.36938	0.19068

Table 2.2 Mass centers of limbs from proximal joints

Limb	Leg(Z_l)	Thigh(Z_t)	Shank(Z_s)
Mass center(m)	0.30553	0.16252	0.16142

Table 2.3 Normalized masses of limbs to total body mass(M_t = 1.0 kg)

Limb	Leg(Z_l)	Thigh(Z_t)	Shank(Z_s)
Mass(kg)	0.157	0.097	0.06

Figure 2.2 demonstrates that the theoretical curve(solid) of the stance leg matches the experimental curve(regular) very well, but the theoretical curve of the shank of the swing leg has large discrepancy from the experimental curve. It says that the theoretical shank kicks abnormally high in the air during the swing phase.

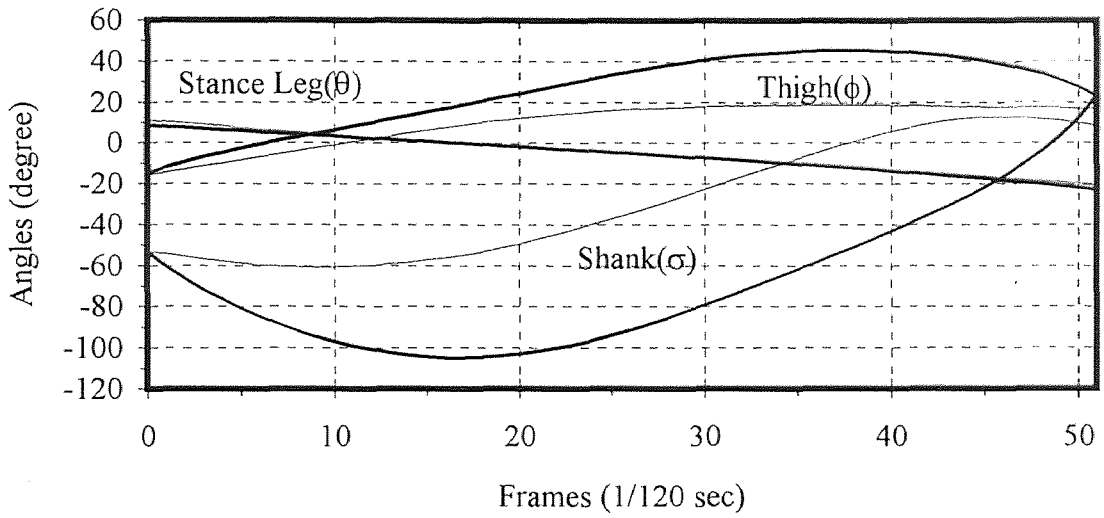

Figure 2.2 Comparison of the theoretical and experimental of the swing phase using equation(2.1): solid lines represent the theoretical data, and regular lines represent the experimental data.

2.3 Joint Viscous Effects

Lacker and et al(1993) improved Mochon's model and expanded the mathematical equations to include energy loss due to viscous effects at the ankle, knee and hip joints, and energy losses from impacts at full-leg extension and heel-strike. When these energy

losses are taken into account, the qualitative as well as quantitative theoretical predictions are in closer agreement with experimental findings of the swing phase.

The mathematical equations of the model including joint viscous effects are represented in equation(2.2).

$$\begin{bmatrix} c_{11} & c_{12} & c_{13} \\ c_{21} & c_{22} & c_{23} \\ c_{31} & c_{32} & c_{33} \end{bmatrix} \begin{bmatrix} \ddot{\theta} \\ \ddot{\phi} \\ \ddot{\sigma} \end{bmatrix} + \begin{bmatrix} 0 & c_{12}^{*} & c_{13}^{*} \\ c_{21}^{*} & 0 & c_{23}^{*} \\ c_{31}^{*} & c_{32}^{*} & 0 \end{bmatrix} \begin{bmatrix} \dot{\theta}^2 \\ \dot{\phi}^2 \\ \dot{\sigma}^2 \end{bmatrix} = \begin{bmatrix} w_1 \sin\theta \\ w_2 \sin\phi \\ w_3 \sin\sigma \end{bmatrix} + \begin{bmatrix} -a-b & b & 0 \\ b & -b-c & c \\ 0 & c & -c \end{bmatrix} \begin{bmatrix} \dot{\theta} \\ \dot{\phi} \\ \dot{\sigma} \end{bmatrix} \quad (2.2)$$

where (a, b, c) are the joint viscous coefficients of the ankle, hip and knee joints. By adjusting the values of a, b and c the theoretical curves are fitted to the experimental curves. The optimum theoretical output of equation(2.2) with a = b = c = 0.012379 (N·m·sec) is compared with the experimental data in Figure 2.3. The solid lines are the theoretical data, and the regular lines the experimental data. Figure 2.3 demonstrates that the shank does not kick as high as in Figure 2.2. In this case the theoretical curves match the experimental curves better than in the case with no joint viscous effects, and it suggests that the model has been improved.

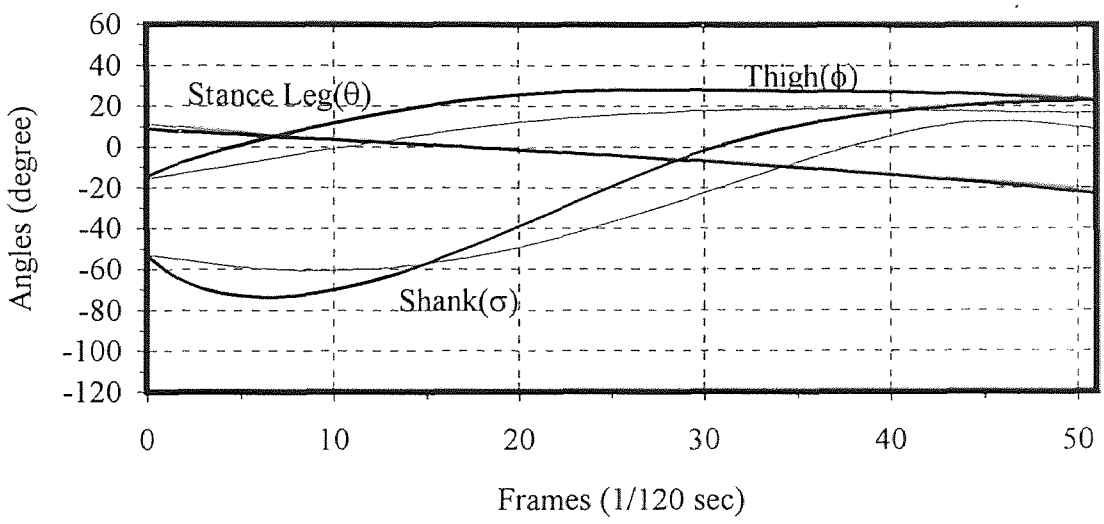

Figure 2.3 Comparison of the theoretical and experimental data of the swing phase using equation(2.2) with the joint viscous coefficients a = b = c = 0.012379 (N•m•sec): solid lines represent the theoretical data, and regular lines represent the experimental data.

2.4 Energy Expenditure Curve During Walking

The ultimate source of energy for skeletal work is the oxidation of foodstuffs. Consequently, the measurement of the oxygen consumption provides a measure of the metabolic energy expenditure of the body. After analyzing experimental data, Passmore and Draper(1965) recommended the following relationship between metabolic energy expenditure(E), ventilation rate(V) and the percent oxygen concentration of expired air (Oe) :

$$E = \frac{4.92V}{100}(20.93 - Oe) \tag{2.3}$$

where E is in Kcal/min, and V is the volume of air expired in liters per minute (liter/min). During walking, a great increase in energy expenditure occurs compared to the basal metabolic rate, reflecting the metabolic cost of moving the body against gravity, and of accelerating and decelerating the various segments. Ralston(1974) showed that an empirical quadratic equation of the form

$$Ew = b + mv^2 \tag{2.4}$$

adequately predicted the energy cost of walking at speeds up to about 100m/min(3.73 mile/h). Ew is the metabolic energy expenditure in cal/min/kg, v is walking speed in m/min, and b and m are constants. Data from various investigations were used to derive the equation, and b = 32 and m = 0.0050 were determined empirically. The curve is shown in Figure 2.4. Dividing Ew by the walking speed v yields the curve Em (top curve on Figure 2.4) which measures the metabolic energy cost per unit walking distance (normalized by body weight) as a function of walking speed. This curve is concave upward, and while fairly flat over a broad range of speeds(65-100 m/min), still exhibits an energetically optimal walking speed. The equation of the curve is given by

$$E_m = \frac{E_w}{v} = \frac{32}{v} + 0.0050v \tag{2.5}$$

where Em is expressed as cal/m/kg. Differentiating Em with respect to v and equating to zero, yields a minimal value of Em equal to 0.80 cal/m/kg, corresponding to an optimal

speed equal to 80 m/min. Ralston also showed that a person's natural walk tends to adopt a speed close to this energetically optimal speed. After we develop a mathematical model of the whole walking cycle including the swing and double-support phases, these curves will be compared with theoretical model predictions.

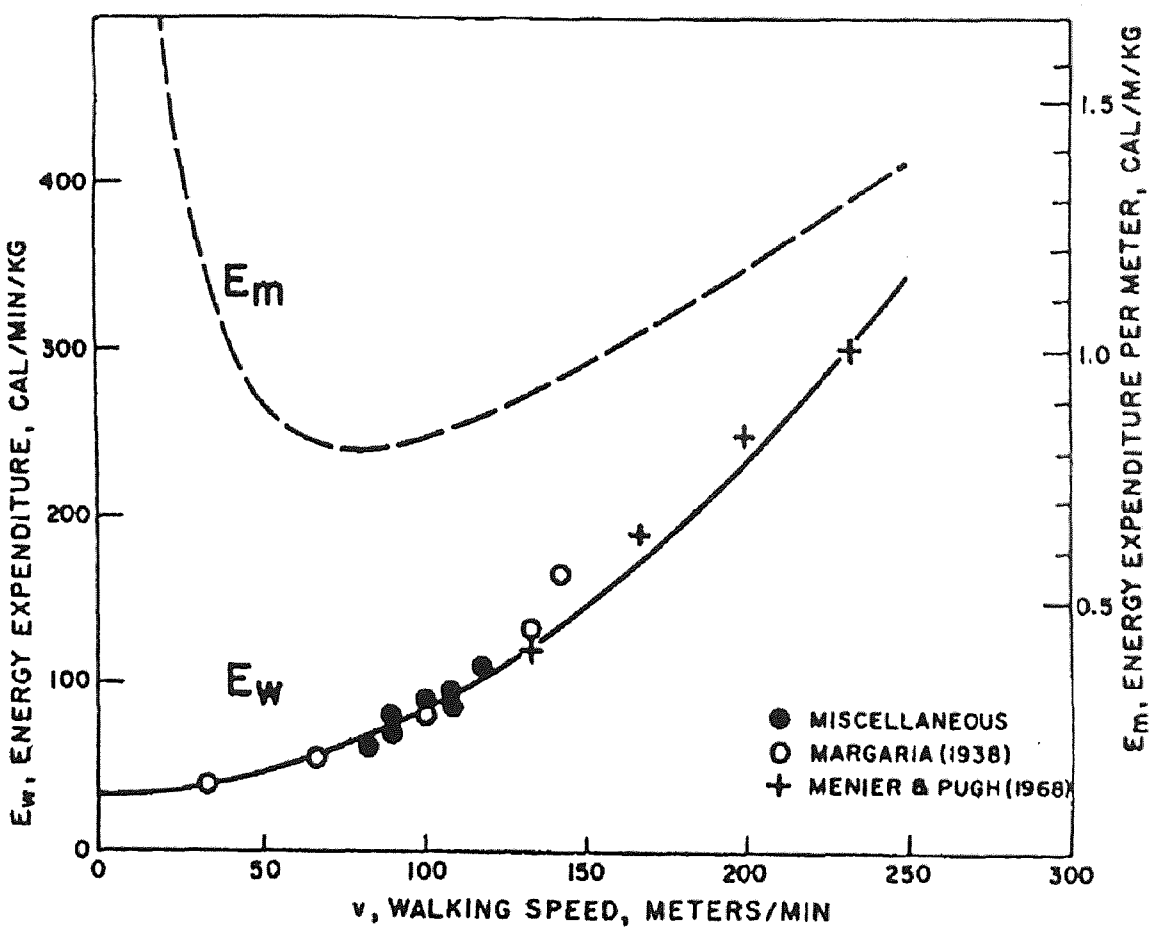

Figure 2.4 Energy expenditure per unit distance during walking (solid line relation between Ew and v calculated from Eq. (2.4); dashed line relation between Em and v, calculated from Eq. (2.5).)

CHAPTER 3

RESEARCH PROCEDURE

3.1 Assumptions

Human walking is a complex phenomenon. Therefore, idealizations are needed to develop a walking model. There are three elements in our walking model. One is the stance leg, and other two are the thigh and shank of the swing leg. The foot of the swing leg is rigidly attached to the shank. The upper body is represented as a mass which is concentrated at the hip. The entire mass of each limb segment is represented as a point mass located at the mass center. The mass of the foot is incorporated in the mass of the shank. There are three energy dissipating terms. They are 1) the energy losses from joint contact at full knee extension, 2) ground impact losses at heel-strike, and 3) the damping effects at the joints that are assumed to be proportional to joint angular velocity. Joint viscous coefficients(the constant of proportionalities) are assumed to be independent of walking speed. Mechanical energy inputs to the body by muscles occur only at the beginning of the swing and double-support phases. Left and right parameters are assumed to be the same, which means that the model is assumed to be symmetric. At heel-strike it is assumed that the swing leg is not bent so that the swing leg assumes a straight line(full knee extension). We can draw the heel-strike configuration if step-length and leg length are known.

3.2 Generalized 2-D Mathematical Walking Model

The development of the dynamic equations of a walking model usually involve the derivation of a complex set of equations. When the number of variables are larger than three, the derivation process is tedious and subject to numerous sources of error. In this dissertation a general method is introduced which can systematically produce the dynamic equations of a simple and error free two dimensional walking model with arbitrary

branching pattern. The derivation of this generalized 2-D mathematical walking model is shown in Appendix C. This general derivation is designed to be flexible and amenable to expansion.

Equation(3.1) in Appendix C is the relation matrix **R** which contains the information of segment connections and limb lengths, equation(3.2) is the mass matrix **M** containing the masses of each segment, and equation(3.3) is the matrix **B** in which the viscous coefficients of the joints are represented. With these matrices the dynamical equations of a walking model can be obtained systematically. If the dynamical equations are compared with the dynamical equations which were obtained from the long process of equation derivation using the Lagrangian, we can see that the results are the same. The derivation process of equations using the Lagrangian is shown for the three variable case in Appendix B. The systematic sequence of obtaining the dynamic equations of a walking model with a specific number of segments is explained in Appendix C, and summarized in the six steps below. It is assumed that there are S number of segments and P number of point masses in the system.

Step 1:

The relation matrix **R** is P x S and is formed as follows(see Appendix C.1). Consider the p-th point mass on the i-th segment of the system. Then, the i-th segment is the last segment of the path to the p-th point mass from the origin, and all other segments of the path are called forefather segments of the i-th segment.

$$\mathbf{R} = \begin{bmatrix} r_{11} & r_{12} & \cdots & r_{1S} \\ r_{21} & r_{22} & \cdots & r_{2S} \\ \vdots & \vdots & \ddots & \vdots \\ r_{P1} & r_{P2} & \cdots & r_{PS} \end{bmatrix} \tag{3.1}$$

where each element of **R** is given by

$$r_{ps} = \begin{cases} z_p & \text{if } s = i, \\ L_s & \text{if the } s\text{-th segment is a forefather segment of the } i\text{-th segment,} \\ 0 & \text{otherwise.} \end{cases}$$

In the mass matrix **M,** m_p is the mass of the p-th point mass(see Appendix C.2).

$$\mathbf{M} = \begin{bmatrix} m_1 & 0 & \cdots & 0 \\ 0 & m_2 & \cdots & 0 \\ \vdots & \vdots & \ddots & \vdots \\ 0 & 0 & \cdots & m_P \end{bmatrix} \tag{3.2}$$

The joint viscous coefficients are represented in matrix **B**(see Appendix C.4.1.2).

$$\mathbf{B} = \begin{bmatrix} b_{11} & b_{12} & \cdots & b_{1S} \\ b_{21} & b_{22} & \cdots & b_{2S} \\ \vdots & \vdots & \cdots & \vdots \\ b_{S1} & b_{S2} & \cdots & b_{SS} \end{bmatrix} \tag{3.3}$$

$$b_{ii} = -\sum_{j=0,\ j\neq i}^{S} b_{ij}$$

where b_{ij} is the joint viscous coefficient between the i-th and j-th segments, and b_{i0} is the viscous coefficient of the joint with which the i-th segment is connected to the origin of the system when the i -th segment does not have forefather segments. The origin is shown as (0, 0) in Figure 3.1.

Step 2:

Determine the coefficient matrices **C, C** * and **C**** for Lagrangian equations(see Appendix C.3).

$$\mathbf{C} = [c_{ij}] = \mathbf{R}^T \cdot \mathbf{M} \cdot \mathbf{R} \tag{3.4}$$

$$\mathbf{C}^* = [c_{ij}^*] = [c_{ij} \cos(\theta_i - \theta_j)] \tag{3.5}$$

$$\mathbf{C}^{**} = [c_{ij}^{**}] = [c_{ij} \sin(\theta_i - \theta_j)] \tag{3.6}$$

where θ_i is the angle each segment makes with the horizontal line.

Step 3:

Determine the generalized gravitational forces $\mathbf{F}_{grv}$(see Appendix C.4.1.1).

$$\mathbf{F}_{grv} = -\underline{\cos\Theta} \cdot \mathbf{P} \tag{3.7}$$

where

$$\mathbf{P} = [p_i] = g \cdot \mathbf{R}^T \cdot \mathbf{M} \cdot \begin{bmatrix} 1 & 1 & \cdots & 1 \end{bmatrix}^T \tag{3.8}$$

$$\underline{\cos\Theta} = \begin{bmatrix} \cos\theta_1 & 0 & \cdots & 0 \\ 0 & \cos\theta_2 & \cdots & 0 \\ \vdots & \vdots & \ddots & \vdots \\ 0 & 0 & \cdots & \cos\theta_S \end{bmatrix}.$$

Step 4:

determine the generalized joint viscous forces $\mathbf{F}_{vis}$(see Appendix C.4.1.2).

$$\mathbf{F}_{vis} = \mathbf{B} \cdot \underline{\dot{\theta}} \tag{3.9}$$

where

$$\underline{\dot{\theta}} = \begin{bmatrix} \dot{\theta}_1 & \dot{\theta}_2 & \cdots & \dot{\theta}_S \end{bmatrix}^T$$

Step 5:

Using equations(3.5), (3.6), (3.7) and (3.9) the dynamic equations of a walking model for the swing phase can be obtained as follows(see Appendix C.4.2):

$$\mathbf{C}^* \cdot \underline{\ddot{\theta}} + \mathbf{C}^{**} \cdot \underline{\dot{\theta}}^2 = -\underline{\cos\Theta} \cdot \mathbf{P} + \mathbf{B} \cdot \underline{\dot{\theta}} \ . \tag{3.10}$$

which can be rewritten as:

$$\mathbf{C}^* \cdot \underline{\ddot{\theta}} = -\mathbf{C}^{**} \cdot \underline{\dot{\theta}}^2 - \underline{\cos\Theta} \cdot \mathbf{P} + \mathbf{B} \cdot \underline{\dot{\theta}} \ . \tag{3.11}$$

Step 6:

Using the constraint $\mathbf{h}(\underline{\theta}) = 0$ which the dynamical equations satisfy (for example the toe of the swing leg should be on the ground during the double-support phase) calculate $\mathbf{H}$(see Appendix C.4.3):

$$\mathbf{H} = \nabla \cdot \nabla^T \mathbf{h} \tag{3.12}$$

where

$$\nabla = \begin{bmatrix} \dfrac{\partial}{\partial \theta_1} & \dfrac{\partial}{\partial \theta_2} & \dfrac{\partial}{\partial \theta_3} \end{bmatrix}$$

The dynamic equations of a walking model for the double-support phase are:

$$\begin{bmatrix} \mathbf{C}^* & -(\nabla \mathbf{h})^T \\ \nabla \mathbf{h} & \mathbf{0} \end{bmatrix} \begin{bmatrix} \ddot{\underline{\theta}} \\ \underline{\lambda} \end{bmatrix} = \begin{bmatrix} -\mathbf{C}^{**} \cdot \dot{\underline{\theta}}^2 - \underline{\cos\Theta} \cdot \mathbf{P} + \mathbf{B} \cdot \dot{\underline{\theta}} \\ -\dot{\underline{\theta}}^T \cdot \mathbf{H} \cdot \dot{\underline{\theta}} \end{bmatrix}. \tag{3.13}$$

where $\lambda(t)$ is the time dependent Lagrange multiplier that enforces the mechanical connstraints. With this procedure it becomes straightforward and systematic to write dynamic equations of the mathematical walking model. In the following section the procedure will be applied to the three-angle walking model.

3.3 Complete Three Angle Model for the Swing and Double-Support Phases

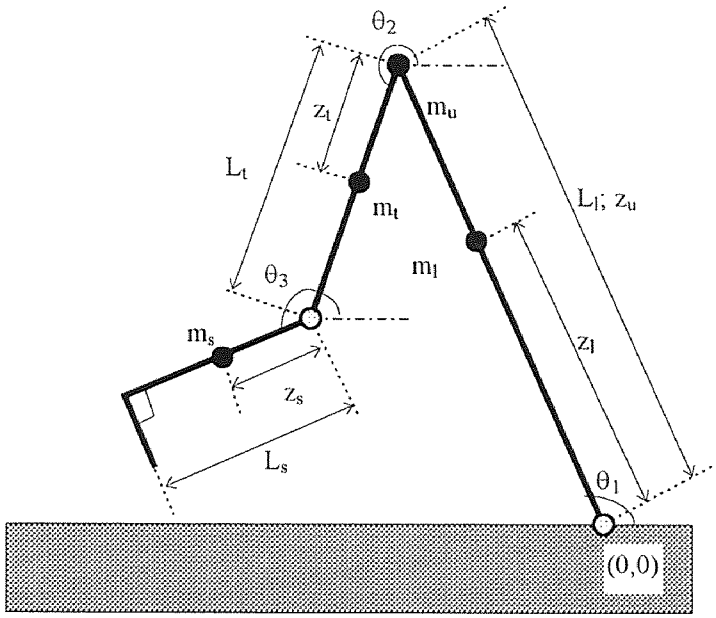

Figure 3.1 The three-angle walking model; θ_1 is the angle of the stance leg, and θ_2 and θ_3 are the angles of the thigh and shank of the swing leg, with respect to the horizontal.

3.3.1 Swing Phase

In the three-angle walking model there are three segments and four point masses. The three segments are the stance leg(L_l), the thigh and shank of the swing leg(L_t, L_s). The four point masss are the mass of the stance leg(m_l), the mass of the upper body(m_u), and the masses of the thigh and shank of the swing leg(m_t, m_s). The schematic diagram is shown in Figure 3.1. With this diagram we will follow the steps outlined in the previous section, and derive the dynamic equations of the walking model.

According to equation(3.1) the relation matrix for the three angle model is:

$$\mathbf{R} = \begin{bmatrix} z_l & 0 & 0 \\ z_u & 0 & 0 \\ L_l & z_t & 0 \\ L_l & L_t & z_s \end{bmatrix}$$

where z_l is the mass center of the stance leg, z_u of the upper body, and z_t and z_s of the thigh and shank of the swing leg. The mass centers are shown in Figure 3.1.

According to equation(3.2) the mass matrix is:

$$\mathbf{M} = \begin{bmatrix} m_l & 0 & 0 & 0 \\ 0 & m_u & 0 & 0 \\ 0 & 0 & m_t & 0 \\ 0 & 0 & 0 & m_s \end{bmatrix}$$

According to equation(3.3) the joint viscous coefficient matrix is obtained as follows:

$$\mathbf{B} = \begin{bmatrix} -a-b & b & 0 \\ b & -b-c & c \\ 0 & c & -c \end{bmatrix}$$

where a, b and c are joint viscous coefficients of the ankle, hip and knee, respectively.

From equation(3.4) the coefficient matrix is:

$$\mathbf{C} = \begin{bmatrix} z_l & z_u & L_l & L_l \\ 0 & 0 & z_t & L_t \\ 0 & 0 & 0 & z_s \end{bmatrix} \begin{bmatrix} m_l & 0 & 0 & 0 \\ 0 & m_u & 0 & 0 \\ 0 & 0 & m_t & 0 \\ 0 & 0 & 0 & m_s \end{bmatrix} \begin{bmatrix} z_l & 0 & 0 \\ z_u & 0 & 0 \\ L_l & z_t & 0 \\ L_l & L_t & z_s \end{bmatrix}.$$

which can be written:

$$\begin{bmatrix} c_{11} & c_{12} & c_{13} \\ c_{21} & c_{22} & c_{23} \\ c_{31} & c_{32} & c_{33} \end{bmatrix} = \begin{bmatrix} m_l z_l^2 + m_u z_u^2 + m_t L_l^2 + m_s L_l^2 & m_t L_l z_t + m_s L_l L_t & m_s L_l z_s \\ m_t z_t L_l + m_s L_t L_l & m_t z_t^2 + m_s L_t^2 & m_s L_t z_s \\ m_s z_s L_l & m_s z_s L_t & m_s z_s^2 \end{bmatrix}. \quad (3.14)$$

From equations(3.5) and (3.6) the values $\mathbf{C}^*$ and $\mathbf{C}^{**}$ are obtained:

$$\mathbf{C}^* = [c_{ij}^*] = [c_{ij} \cos(\theta_i - \theta_j)] \quad (3.15)$$

$$\mathbf{C}^{**} = [c_{ij}^{**}] = [c_{ij} \sin(\theta_i - \theta_j)] \quad (3.16)$$

From equation(3.8) **P** is:

$$\mathbf{P} = g \begin{bmatrix} z_l & z_u & L_l & L_l \\ 0 & 0 & z_t & L_t \\ 0 & 0 & 0 & z_s \end{bmatrix} \begin{bmatrix} m_l \\ m_u \\ m_t \\ m_s \end{bmatrix}$$

$$\begin{bmatrix} p_1 \\ p_2 \\ p_3 \end{bmatrix} = g \begin{bmatrix} m_l z_l + m_u z_u + m_t L_l + m_s L_l \\ m_t z_t + m_s L_t \\ m_s z_s \end{bmatrix}. \quad (3.17)$$

From equation(3.7) generalized gravitational force $\mathbf{F}_{grv}$ is:

$$\begin{aligned} \mathbf{F}_{grv} &= -\begin{bmatrix} \cos\theta_1 & 0 & 0 \\ 0 & \cos\theta_2 & 0 \\ 0 & 0 & \cos\theta_3 \end{bmatrix} \cdot \begin{bmatrix} p_1 \\ p_2 \\ p_3 \end{bmatrix} \\ &= -\begin{bmatrix} p_1 \cos\theta_1 \\ p_2 \cos\theta_2 \\ p_2 \cos\theta_3 \end{bmatrix} \end{aligned} \quad (3.18)$$

From equation(3.9) generalized joint viscous force $\mathbf{F}_{vis}$ is:

$$\mathbf{F}_{vis} = \begin{bmatrix} -a-b & b & 0 \\ b & -b-c & c \\ 0 & c & -c \end{bmatrix} \cdot \begin{bmatrix} \dot{\theta}_1 \\ \dot{\theta}_2 \\ \dot{\theta}_3 \end{bmatrix}$$

From equation(3.11) the dynamic equations of the walking model for the swing phase:

$$\begin{bmatrix} c_{11}^{*} & c_{12}^{*} & c_{13}^{*} \\ c_{21}^{*} & c_{22}^{*} & c_{23}^{*} \\ c_{31}^{*} & c_{32}^{*} & c_{33}^{*} \end{bmatrix} \begin{bmatrix} \ddot{\theta}_1 \\ \ddot{\theta}_2 \\ \ddot{\theta}_3 \end{bmatrix} = \begin{bmatrix} -c_{12}^{**}\dot{\theta}_2^{\,2} - c_{13}^{**}\dot{\theta}_3^{\,2} - p_1 \cos\theta_1 - a\dot{\theta}_1 - b(\dot{\theta}_1 - \dot{\theta}_2) \\ -c_{21}^{**}\dot{\theta}_1^{\,2} - c_{23}^{**}\dot{\theta}_3^{\,2} - p_2 \cos\theta_2 - b(\dot{\theta}_2 - \dot{\theta}_1) - c(\dot{\theta}_2 - \dot{\theta}_3) \\ -c_{31}^{**}\dot{\theta}_1^{\,2} - c_{32}^{**}\dot{\theta}_2^{\,2} - p_3 \cos\theta_3 - c(\dot{\theta}_3 - \dot{\theta}_2) \end{bmatrix} \quad (3.19)$$

Some modifications are necessary before these equations can be compared to the ones in Appendix B. The changes are necessitated due to differences in Figure 3.1 and Figure B.1 in Appendix B. In Figure 3.1 angles(θ_1, θ_2, θ_3) are measured counter-clockwise with respect to the positive horizontal line to make the result more general. In Figure B.1 angles(θ, ϕ, σ) are measured counter-clockwise with respective to the vertical line to make the maximum magnitude of the angles less than 90 degrees. Another difference is the mass center of the leg. In Figure 3.1 the mass center of the stance leg is measured from the origin. In Figure B.1 the mass center of the stance leg is measured from the proximal joint to the body. Therefore, the mass center of the leg, z_l, in Figure 3.1 is equal to L_l-z_l in Figure B.1. The differences are summarized in the Table 3.1. With these differences accounted for, equations (3.15), (3.16), (3.18) and (3.19) above are identical equations (B.5), (B.6), (B.7) and (B.9), respectively.

Table 3.1 The differences of variables and parameters in Figure 3.1 and Figure B.1.

	In Figure 3.1	In Figure B.1
Angle of the leg	θ_1 (= θ + 90°)	θ
Angle of the thigh	θ_2 (= ϕ - 90°)	ϕ
Angle of the shank	θ_3 (= σ - 90°)	σ
Mass center of the leg	z_l (= L_l - z_l)	z_l

3.3.2 Double-Support Phase

There is a constraint that the toe of the swing leg remains on the ground during the double-support phase. As shown in Appendix B this constraint results in one more dynamic variable(θ_1, θ_2, θ_3) equation for the double-support phase. The constraint of the double-support phase - the toe of the swing leg should be on the ground - is obtained as equation(B.10) in Appendix B.

$$\begin{aligned} h(\theta_1,\theta_2,\theta_3) &= L_l^2 + L_t^2 + L_s^2 \\ &\quad - 2L_lL_t\cos(\theta_1-\theta_2) - 2L_lL_s\cos(\theta_1-\theta_3) + 2L_tL_s\cos(\theta_2-\theta_3) \\ &\quad + 2(L_f - S_L)(L_l\sin\theta_1 - L_t\sin\theta_2 - L_s\sin\theta_3) - 2L_fS_L + S_L^2 \\ &= 0 \end{aligned} \tag{3.20}$$

If we consider the constraint $h(\theta_1, \theta_2, \theta_3) = 0$, the mathematical equation for the double-support phase can be written as equation(3.13). To obtain equation(3.13) we need to know ∇h (gradient of h) and $\mathbf{H} = \nabla \cdot \nabla^T h$ (Hessian matrix of h), where ∇h is defined as

$$\nabla h = \begin{bmatrix} \dfrac{\partial h}{\partial \theta_1} & \dfrac{\partial h}{\partial \theta_2} & \dfrac{\partial h}{\partial \theta_3} \end{bmatrix}$$

and

$$\begin{aligned} \frac{\partial h}{\partial \theta_1} &= h_1 = 2LL_t\sin(\theta_1-\theta_2) + 2LL_s\sin(\theta_1-\theta_3) + 2(d-S_L)L\cos\theta_1 \\ \frac{\partial h}{\partial \theta_2} &= h_2 = -2LL_t\sin(\theta_1-\theta_2) - 2L_tL_s\sin(\theta_2-\theta_3) - 2(d-S_L)L_t\cos\theta_2 \\ \frac{\partial h}{\partial \theta_3} &= h_3 = -2LL_s\sin(\theta_1-\theta_3) + 2L_tL_s\sin(\theta_2-\theta_3) - 2(d-S_L)L_s\cos\theta_3 \end{aligned} \tag{3.21}$$

H can be written as

$$\mathbf{H} = \nabla \cdot \nabla^T h$$

$$= \begin{bmatrix} \frac{\partial}{\partial\theta_1}(\frac{\partial h}{\partial\theta_1}) & \frac{\partial}{\partial\theta_1}(\frac{\partial h}{\partial\theta_2}) & \frac{\partial}{\partial\theta_1}(\frac{\partial h}{\partial\theta_3}) \\ \frac{\partial}{\partial\theta_2}(\frac{\partial h}{\partial\theta_1}) & \frac{\partial}{\partial\theta_2}(\frac{\partial h}{\partial\theta_2}) & \frac{\partial}{\partial\theta_2}(\frac{\partial h}{\partial\theta_3}) \\ \frac{\partial}{\partial\theta_3}(\frac{\partial h}{\partial\theta_1}) & \frac{\partial}{\partial\theta_3}(\frac{\partial h}{\partial\theta_2}) & \frac{\partial}{\partial\theta_3}(\frac{\partial h}{\partial\theta_3}) \end{bmatrix}$$

$$= \begin{bmatrix} h_{11} & h_{12} & h_{13} \\ h_{21} & h_{22} & h_{23} \\ h_{31} & h_{32} & h_{33} \end{bmatrix}$$

where

$$\begin{bmatrix} h_{11} \\ h_{21} \\ h_{31} \end{bmatrix} = \begin{bmatrix} 2L_l L_t \cos(\theta_1 - \theta_2) + 2L_l L_s \cos(\theta_1 - \theta_3) - 2(d - S_L) \cdot L_l \sin\theta_1 \\ -2L_l L_t \cos(\theta_1 - \theta_2) \\ -2L_l L_s \cos(\theta_1 - \theta_3) \end{bmatrix}$$

$$\begin{bmatrix} h_{12} \\ h_{22} \\ h_{32} \end{bmatrix} = \begin{bmatrix} -2L_l L_t \cos(\theta_1 - \theta_2) \\ 2L_l L_t \cos(\theta_1 - \theta_2) - 2L_t L_s \cos(\theta_2 - \theta_3) + 2(d - S_L) \cdot L_t \sin\theta_2 \\ 2L_t L_s \cos(\theta_2 - \theta_3) \end{bmatrix}$$

$$\begin{bmatrix} h_{13} \\ h_{23} \\ h_{33} \end{bmatrix} = \begin{bmatrix} -2L_l L_s \cos(\theta_1 - \theta_3) \\ 2L_t L_s \cos(\theta_2 - \theta_3) \\ 2L_l L_s \cos(\theta_1 - \theta_3) - 2L_t L_s \cos(\theta_2 - \theta_3) + 2(d - S_L) \cdot L_s \sin\theta_3 \end{bmatrix}$$

Therefore,

$$\underline{\dot{\theta}}^T \cdot \mathbf{H} \cdot \underline{\dot{\theta}} = \begin{bmatrix} \dot{\theta}_1 & \dot{\theta}_2 & \dot{\theta}_3 \end{bmatrix} \begin{bmatrix} h_{11} & h_{12} & h_{13} \\ h_{21} & h_{22} & h_{23} \\ h_{31} & h_{32} & h_{33} \end{bmatrix} \begin{bmatrix} \dot{\theta}_1 \\ \dot{\theta}_2 \\ \dot{\theta}_3 \end{bmatrix}$$

$$= \dot{\theta}_1(h_{11}\dot{\theta}_1 + h_{12}\dot{\theta}_2 + h_{13}\dot{\theta}_3) + \dot{\theta}_2(h_{21}\dot{\theta}_1 + h_{22}\dot{\theta}_2 + h_{23}\dot{\theta}_3)$$

$$+ \dot{\theta}_3(h_{31}\dot{\theta}_1 + h_{32}\dot{\theta}_2 + h_{33}\dot{\theta}_3)$$

$$\begin{aligned}\underline{\dot{\theta}}^T \cdot \mathbf{H} \cdot \underline{\dot{\theta}} = {} & 2L_l L_t \cos(\theta_1 - \theta_2)\cdot(\dot{\theta}_1^2 - \dot{\theta}_1\dot{\theta}_2 - \dot{\theta}_2\dot{\theta}_1 + \dot{\theta}_2^2) \\ & + 2L_l L_s \cos(\theta_1 - \theta_3)\cdot(\dot{\theta}_1^2 - \dot{\theta}_1\dot{\theta}_3 - \dot{\theta}_3\dot{\theta}_1 + \dot{\theta}_3^2) \\ & - 2L_t L_s \cos(\theta_2 - \theta_3)\cdot(\dot{\theta}_2^2 - \dot{\theta}_2\dot{\theta}_3 - \dot{\theta}_3\dot{\theta}_2 + \dot{\theta}_3^2) \\ & - 2(d - S_L)\cdot(L_l \sin\theta_1 \cdot \dot{\theta}_1^2 - L_t \sin\theta_2 \cdot \dot{\theta}_2^2 - L_s \sin\theta_3 \cdot \dot{\theta}_3^2)\end{aligned}$$

$$\begin{aligned}\therefore H = {} & -\underline{\dot{\theta}}^T \cdot \mathbf{H} \cdot \underline{\dot{\theta}} \\ = {} & -2L_l L_t \cos(\theta_1 - \theta_2)\cdot(\dot{\theta}_1 - \dot{\theta}_2)^2 \\ & - 2L_l L_s \cos(\theta_1 - \theta_3)\cdot(\dot{\theta}_1 - \dot{\theta}_3)^2 \\ & + 2L_t L_s \cos(\theta_2 - \theta_3)\cdot(\dot{\theta}_2 - \dot{\theta}_3)^2 \\ & + 2(d - S_L)\cdot(L_l \sin\theta_1 \cdot \dot{\theta}_1^2 - L_t \sin\theta_2 \cdot \dot{\theta}_2^2 - L_s \sin\theta_3 \cdot \dot{\theta}_3^2)\end{aligned} \tag{3.22}$$

When we compare equations(3.21) and (3.22) with equation(B.14) and (B.15), respectively, we can see that the derived dynamic equations using the generalized 2D walking model are identical with those derived using the Lagrangian. According to equation(3.13) the dynamic equations of a walking model for the double-support phase is:

$$\begin{bmatrix} c_{11}^* & c_{12}^* & c_{13}^* & -h_1 \\ c_{21}^* & c_{22}^* & c_{23}^* & -h_2 \\ c_{31}^* & c_{32}^* & c_{33}^* & -h_3 \\ h_1 & h_2 & h_3 & 0 \end{bmatrix} \begin{bmatrix} \ddot{\theta}_1 \\ \ddot{\theta}_2 \\ \ddot{\theta}_3 \\ \lambda \end{bmatrix} = \begin{bmatrix} -c_{12}^{**}\dot{\theta}_2^{\,2} - c_{13}^{**}\dot{\theta}_3^{\,2} - p_1\cos\theta_1 - b_1\dot{\theta}_1 - b_2(\dot{\theta}_1 - \dot{\theta}_2) \\ -c_{21}^{**}\dot{\theta}_1^{\,2} - c_{23}^{**}\dot{\theta}_3^{\,2} - p_2\cos\theta_2 - b_2(\dot{\theta}_2 - \dot{\theta}_1) - b_3(\dot{\theta}_2 - \dot{\theta}_3) \\ -c_{31}^{**}\dot{\theta}_1^{\,2} - c_{32}^{**}\dot{\theta}_2^{\,2} - p_3\cos\theta_3 - b_3(\dot{\theta}_3 - \dot{\theta}_2) \\ H \end{bmatrix}$$

When we take into account differences in Figure 3.1 and Figure B.1, the equation is the same as equation(B.18) in Appendix B.

3.4 Model Parameters

In our walking model there are 11 independent structural parameters, 4 independent gait parameters and 3 independent dynamic variables. These are described below. A complete assignment of these parameters determines a complete walking gait cycle.

3.4.1 Structural Parameters

The three length parameters are the lengths of the thigh(L_t), the shank(L_s) and the foot(L_f). The length of the leg is $L_l = L_t + L_s$. The three mass parameters are the masses of the thigh(m_t), shank(m_s) and upper body(m_u). The mass of the foot is considered to be included in the mass of the shank. The mass of the leg is $m_l = m_t + m_s$. The mass of the upper body is placed at the hip joint point(see Figure 3.1). The two independent mass center parameters are the mass centers of the thigh(z_t) and the shank(z_s). The mass center of the leg(z_l) is:

$$z_l = \frac{m_t z_t + m_s (L_t + z_s)}{m_l}$$

The three viscous parameters are the joint viscous coefficients of the ankle(a), knee(b) and hip(c) joints. Therefore, there are eleven independent structural parameters to be given to the mathematical equation of the model.

Of these eleven structural parameters, the lengths can be measured directly on each subject. However, the masses and mass centers of the thigh and shank cannot be measured. These parameters are obtained from Dempster's data(Veau 1977). The three viscous parameters can likewise not be measured directly. These parameters must be determined indirectly from experimental data by curve fitting. For a specific subject these structural parameters are assumed constant and indepenent of walking speed.

3.4.2 Independent Gait Parameters

There are four independent gait parameters. They are the toe-off angle(α), the step length(S_L), the duration of the swing phase(T_S) and the duration of the double-support phase(T_D). The walking speed(V) is $S_L/(T_S+T_D)$. With different gait parameters the mathematical model produces different gait solutions. Of all the possible gait solutions, the gait that consumes minimum energy is considered to be the optimum solution.

3.4.3 Independent Dynamic Variables

There are three independent dynamic variables in our model. Those variables are the angles for the stance leg(θ_1), and the thigh(θ_2) and shank(θ_3) of the swing leg(Figure 3.1). Once they are determined, the stick figure of the gait can be generated using length parameters. Once the mathematical equations of the model are solved, model output yields the numerical values of (θ_1, θ_2, θ_3, θ_1', θ_2', θ_3', θ_1'', θ_2'', θ_3'') as a function of time. With these model data, the energy dissipation as a function of time can be calculated.

3.5 Numerical Method

3.5.1 Two-Point Boundary Value Problem

The problem of finding gait trajectories can be mathematically regarded as solving a two-point boundary value problem. The two boundary points are the initial and final configurations of the walking phase(i.e. swing and double-support phases). If the step-length and the toe-off angle are known, these two boundary configurations can be determined. If, in addition to these 2 boundary points, the duration of the walking phases(T_S and T_D) are also specified, then enough information is prescribed to solve the equations of motion for the model (i.e. for the complete dynamics of the gait phase). The solution is obtained numerically using the shooting method(Press 1992).

The shooting method solves the two-point boundary problem by iteration. Each iteration is a solution of the initial value problem in which the initial configuration and a tentative guess for the initial velocity are given (4th order Runge-Kutta method). The initial value problem is solved up to the time T_S for the swing phase, and to the time T_D for the double-support phase. The configuration of the model at this time is compared to the specified final configuration. The difference between them ($||d||$) is used to find the next new guess for the initial velocity using a multidimensional root-finding algorithm. The iteration process continues until $||d||$ is less than a preselected value. The iteration process is explained in Appendix D.

3.5.2 Structural Parameter Identification

Of the structural parameters, the weights and mass centers of limbs, and the joint viscous coefficients can not be measured. The weights and mass centers of limbs are obtained from Dempster's data(Appendix A), but there are no data for joint viscous coefficients. To estimate these parameters the downhill simplex method(Jacoby 1972) is used. It is a multidimensional minimization method, that is, it finds local minima of a function of more than one independent variable. The advantage of this method is that it is simple to implement because it requires only function evaluations, and not derivatives.

During the process of the downhill simplex method, theoretical gait trajectories with different joint viscous coefficients are compared with the experimental gait trajectory, and the joint viscous coefficients which produce the minimum error between the theoretical gait data and the experimental gait data are the selected values. These joint viscous coefficients are picked as the true joint viscous coefficients. The down-hill simplex method is explained in Appendix E.

3.6 Calculation of Consumed Energy

During the swing phase, knee-lock, heel-strike and viscous mechanical energy losses are considered, and during the double-support phase only the viscous mechanical energy loss is considered. It is the sum of these mechanical energy losses that need to be resupplied by the muscles(equation(3.24)).

$$E(loss) = loss(knee\text{-}lock) + loss(heel\text{-}strike) + loss(viscosity). \tag{3.24}$$

If E(loss) is known, the energy loss per minute during walking is:

$$Ew = E(loss)\cdot 60/(T_S+T_D). \tag{3.25}$$

The energy loss per unit walking distance can also be obtained as

$$Em = E(loss) / Step\text{-}length\ . \tag{3.26}$$

In the gait space, containning all the possible model gait trajectories with different gait parameter values, that trajectory which consumes the minimum energy per unit walking

distance is hypothesized to be the optimum trajectory selected by the central nervous system.

The mechanical energy in this model at any instant is:

$$\begin{aligned} E(\underline{\theta}, \dot{\underline{\theta}}, t) &= \text{Kinetic Energy} + \text{Potential Energy} \\ &= \frac{1}{2}\dot{\underline{\theta}}^T \cdot \mathbf{C}^* \cdot \dot{\underline{\theta}} + \sum_{i=1}^{S} p_i \sin\theta_i \end{aligned} \tag{3.27}$$

Kinetic energy and potential energy are derived in Appendix C, and $\mathbf{C}^*$ and p_i are defined in equations (3.15) and (3.17), respectively. Each energy loss term is explained below.

3.6.1 Knee-Lock Energy Loss

Before the swing leg hits the ground, the thigh and shank of the swing leg become rigid at full knee extension. This joint impact at full knee extension consumes mechanical energy. It is assumed that knee-lock occurs just before the heel-strike of the swing leg. In Appendix F the change of limb velocities after knee-lock is shown. With this result, the energy loss due to knee-lock can be calculated:

$$\text{loss(knee-lock)} = E(\underline{\theta}, \dot{\underline{\theta}}, T_{bk}) - E(\underline{\theta}, \dot{\underline{\theta}}, T_{ak}) \tag{3.28}$$

where T_{bk} and T_{ak} are the times before and after knee-lock, respectively.

3.6.2 Heel-Strike Energy Loss

Heel-strike marks the end of the swing phase. At heel-strike the velocities of the limbs are suddenly changed because of ground impact. In Appendix G the change of limb velocities at heel-strike is derived. The heel-strike energy loss is:

$$\text{loss(heel-strike)} = E(\underline{\theta}, \dot{\underline{\theta}}, T_{sf}) - E(\underline{\theta}, \dot{\underline{\theta}}, T_{di}) \tag{3.29}$$

where T_{sf} and T_{di} are the times at the end of the swing phase, and at the beginning of the double-support phase, respectively.

3.6.3 Energy Loss Due to Viscosity

Our walking model is assumed to move under gravity without any energy input during the swing and double-support phases. (Energy input can occur in the model only at the beginning of each phase.) Viscous forces represent the only non-conservative forces in equations of motion that are satisfied during both of these phases. Therefore, if we know the energy at the beginning and at the end of each phase, then the mechanical energy loss from viscous terms is calculated to be the difference between the mechanical energy at the beginning and the mechanical energy at the end of each phase. If starting times of the swing and the double support phases are T_{si} and T_{di}, respectively, and the final time of the swing and double support phases are T_{sf} and T_{df}, then the viscous energy loss is:

$$\begin{aligned} \text{loss(viscosity)} &= \text{loss(swing phase)} + \text{loss(double - support phase)} \\ &= \{E(\underline{\theta}, \dot{\underline{\theta}}, T_{si}) - E(\underline{\theta}, \dot{\underline{\theta}}, T_{sf})\} + \{E(\underline{\theta}, \dot{\underline{\theta}}, T_{di}) - E(\underline{\theta}, \dot{\underline{\theta}}, T_{df})\} \end{aligned} \tag{3.30}$$

3.6.4 Basic Metabolic Energy Consumption

Basal Energy Expenditure(BEE) is the energy consumed at rest; this energy differs from person to person. The consumed energy in men is higher than in women, is higher in younger people than in older people, and is higher in a sitting position than when prone or supine. The Basal Energy Expenditure is estimated to be around 25~32 cal/min/kg. In equation(2.4) the BEE is assumed as 32 cal/min/kg. In comparing the theoretical results with the with the experimental ones, 32 cal/min/kg of BEE are added to the energy losses that was calculated theoretically.

CHAPTER 4

PREPARATION OF EXPERIMENTAL DATA

4.1 Raw Data

The experimental data were taken in the Motion Analysis Laboratory of the Kessler Institute for Rehabilitation in West Orange, NJ using the VICON 370 Movement Analysis System. The VICON system generates the three dimensional coordinates of markers attached to critical points on the walking subject. The data have information about x-, y- and z- coordinates of markers which are attached to the subject. The markers are attached to the Anterior Superior Iliac Spine(ASIS), hip, thigh, knee, tibia, ankle, heel and toe on left and right sides and an additional maker is at the sacrum. They are shown in Figure 4.1. For this model only the hip, knee, ankle, heel and toe markers are recorded and utilized. These are represented by open circles in Figure 4.1.

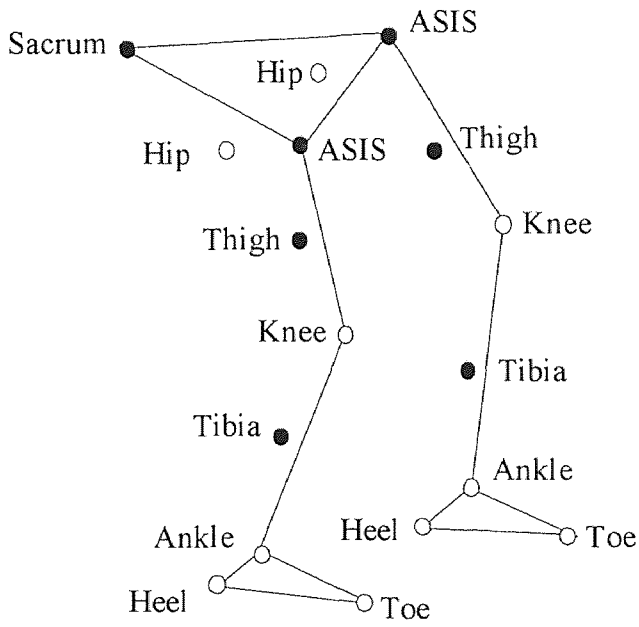

Figure 4.1 Positions of markers to get raw data

4.2 Projection on the Sagittal Plane

The walking model is a two dimensional one. Therefore, it is necessary to convert data collected in a three-dimensional coordinate system into a two-dimensional sytem. To this end the raw data are projected onto the sagittal plane of the body. If an arbitrary unit vector on the sagittal plane is given by $\mathbf{u} = (x_u, y_u, 0)$ with $x_u^2 + y_u^2 = 1$, then the projected vector $\mathbf{P}(x_p, y_p, z_p)$ of a vector $\mathbf{V}(x, y, z)$ in 3D coordinate space is :

$$\mathbf{P} = \begin{bmatrix} x_p \\ y_p \\ z_p \end{bmatrix} = \begin{bmatrix} x_u^2 & x_u y_u & 0 \\ x_u y_u & y_u^2 & 0 \\ 0 & 0 & 1 \end{bmatrix} \cdot \begin{bmatrix} x \\ y \\ z \end{bmatrix} \tag{4.1}$$

The process of obtaining the projected vector is explained in Appendix G.

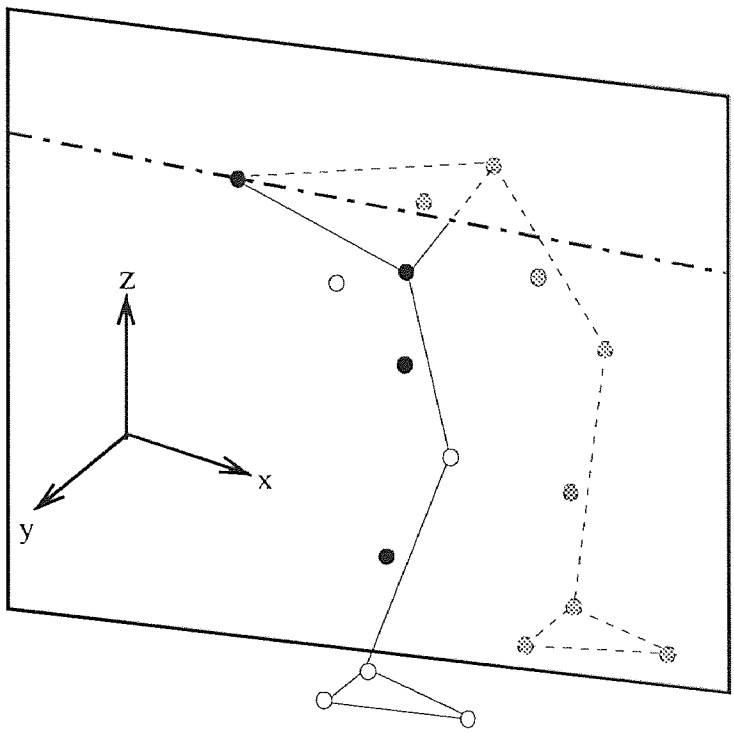

Figure 4.2 The sagittal plane on which the three dimensional data are projected.

The laboratory frame coordinate system is such that x-direction is in floor plane and parallel to walkway, y-direction in floor plane and perpendicular to walkway, and z-direction orthogonal to floor plane and up. The experimental layout was such that the sagittal plane was almost parallel with the x-z plane because the walking direction was in the x-direction. Therefore, the projected x- and z-coordinates are very similar to the x- and z-coordinates derived from the three dimensional raw data, and in normal gait there is little difference in the two dimensional data whether or not the projection is applied. Here, the process of projection is included for the general case when the sagittal plane is not parallel with the x-z plane. This may occur with significant gait pathology such as in stroke and amputees.

4.3 Angles of the Thigh and Shank of the Swing Leg

From the projected two dimensional coordinate data of markers, the angles of the thigh and shank of the left and right legs are calculated. For the thigh a line is drawn from the hip marker to the knee marker, and another line is drawn from the knee marker to the heel marker for the shank as shown in Figure 4.3. Angles are measured with respect to the vertical:

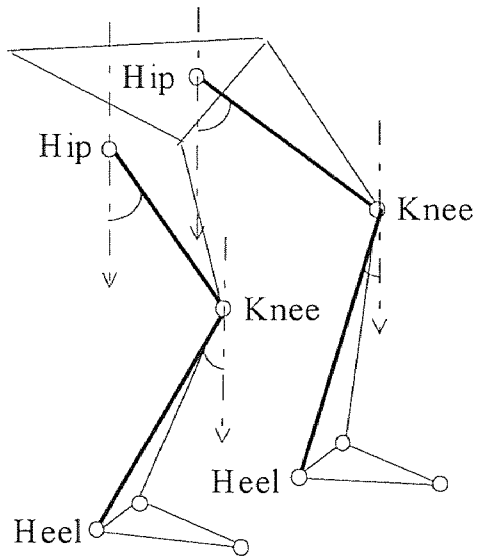

Figure 4.3 The thigh and shank lines of the left and right legs

$$\theta_{\text{Thigh}} = \frac{x_{p,Knee} - x_{p,Hip}}{\left|x_{p,Knee} - x_{p,Hip}\right|} \tan^{-1} \frac{\sqrt{(x_{p,Knee} - x_{p,Hip})^2 + (y_{p,Knee} - y_{p,Hip})^2}}{\left|z_{p,Knee} - z_{p,Hip}\right|} \qquad (4.2)$$

$$\theta_{\text{Shank}} = \frac{x_{p,Heel} - x_{p,Knee}}{\left|x_{p,Heel} - x_{p,Knee}\right|} \tan^{-1} \frac{\sqrt{(x_{p,Heel} - x_{p,Knee})^2 + (y_{p,Heel} - y_{p,Knee})^2}}{\left|z_{p,Heel} - z_{p,Knee}\right|}.$$

The calculated angles as a function of time are shown in Figure 4.4. The time axis is measured in times of frame number; the Vicon 370 system collects data at a 120 frames/sec. For the shank a line can be drawn from the knee to the ankle instead of the heel. But, if a line is drawn from the knee to the ankle for the shank, the knee of the swing leg appears hyper-extended before heel-strike. In normal walking the swing leg does not hyper-extend. Hyper-extending in experimental data occurs due to mispositioning of the markers. It is for this reason that the line is drawn from the knee to the heel instead of the ankle. Hyper-extended data are shown in Figure 4.5, with the hyper-extension highlighted by a dotted circle.

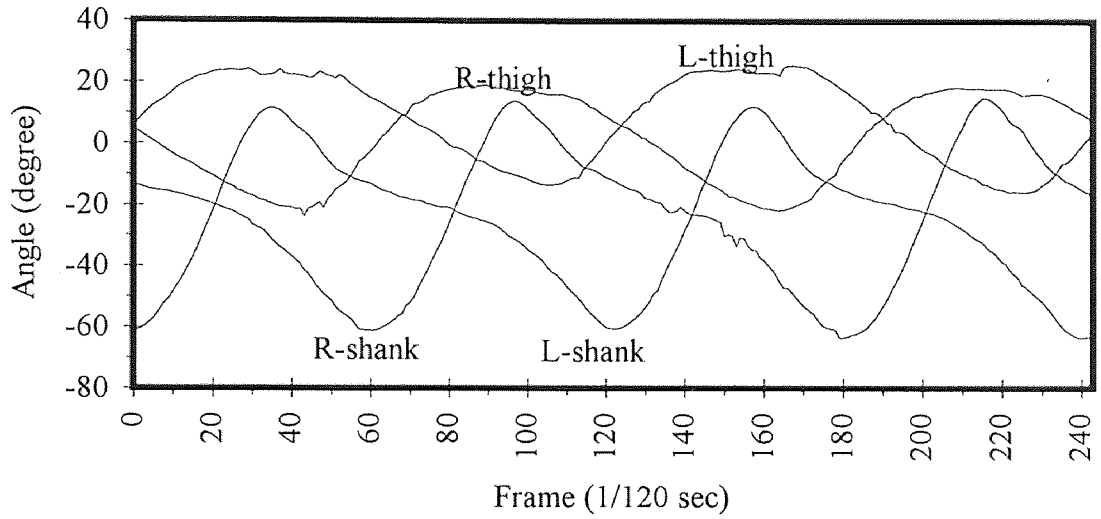

Figure 4.4 Measured angles of the thigh and shank of the left and right legs measured with respect to the vertical.

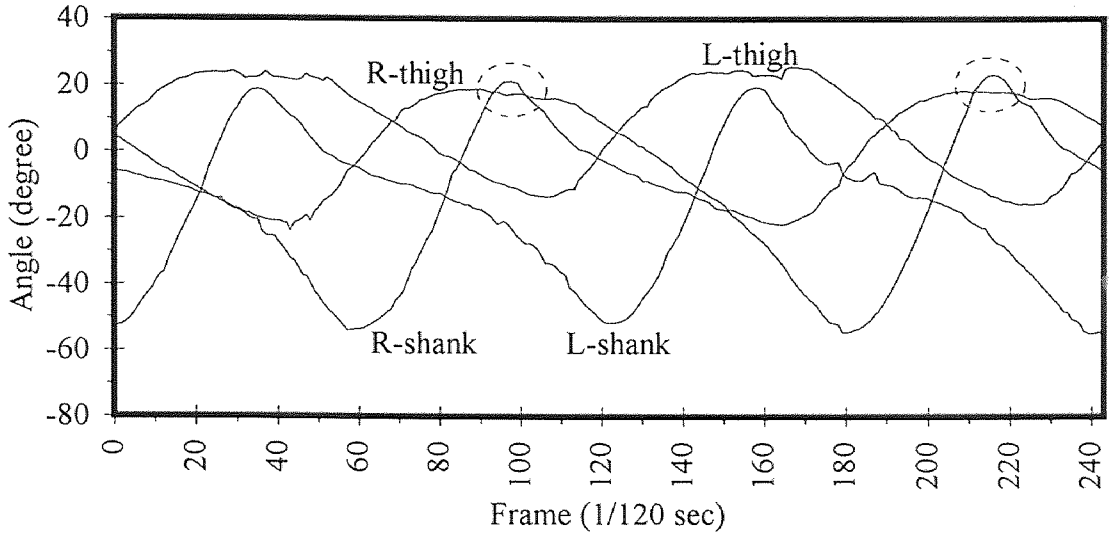

Figure 4.5 Measured angles of the thigh and shank of the left and right legs measured with respect to the vertical: hyper-extended knee area is highlighted with a dotted circle.

In Figure 4.4 the difference between the thigh and shank curves of the same leg is the angle which the knee of a leg bends while walking. Careful examination of Figure 4.4 reveals that in this subject the right leg bends less than the left leg while walking. The right and left leg experimental curves in this subject are not symmetric. Because the mathematical model is a symmetrical one, it is necessary to select either the right or left leg's measured data to compare to the output from the mathematical model. The model dictates that the swing leg becomes a straight line at heel-strike; therefore it is the right leg data that is selected because the angle between the right thigh and right shank at heel-strike is smaller than that of the left leg.

4.4 Angle of the Stance Leg

The stance leg of the model is represented by one segment, and the thigh and shank of the stance leg form a straight line during the entire walking cycle. Because the right leg is selected as the swing leg in section 4.3, it is the left leg that is selected as the stance leg.

To determine the angle of the stance leg, a line is drawn from the left hip to the left ankle as shown in Figure 4.6, and measured with respect to the vertical.

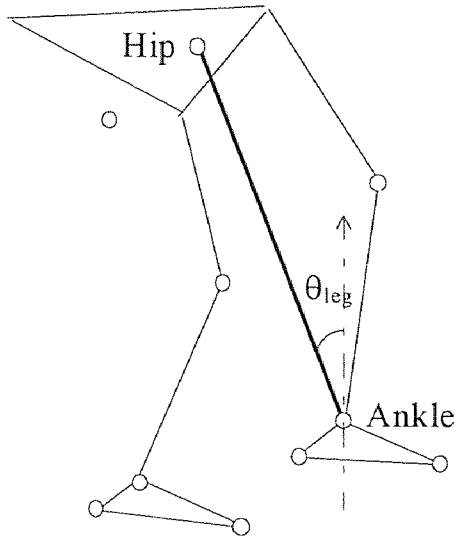

Figure 4.6 The stance leg

The angle of the stance leg is measured with respect to the vertical:

$$\theta_{\text{Stance Leg}} = \frac{x_{p,Ankle} - x_{p,Hip}}{\left|x_{p,Ankle} - x_{p,Hip}\right|} \tan^{-1} \frac{\sqrt{(x_{p,Ankle} - x_{p,Hip})^2 + (y_{p,Ankle} - y_{p,Hip})^2}}{\left|z_{p,Ankle} - z_{p,Hip}\right|}. \quad (4.3)$$

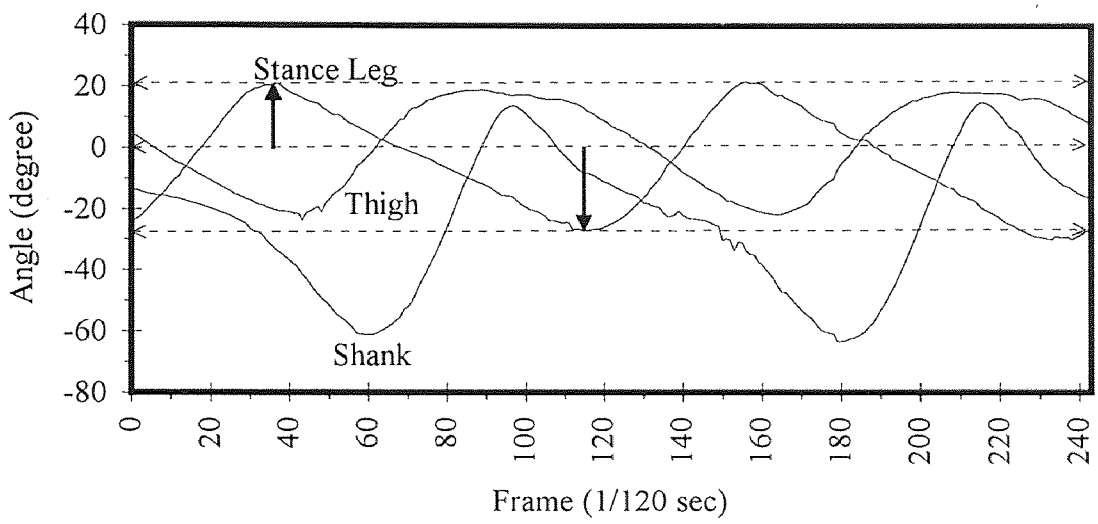

Figure 4.7 The angle of the stance leg when a line is drawn from the hip to the *ankle*, and the angles of the thigh and shank of the swing leg.

The calculated angle of the stance leg, and angles of the thigh and shank of the swing leg, as calculated from the measured data are shown together in Figure 4.7. The arrows indicate the maximum positive and negative values of the angle of the stance leg.

We can draw a line from the hip to the heel instead of the ankle. For this case the result is shown in Figure 4.8.

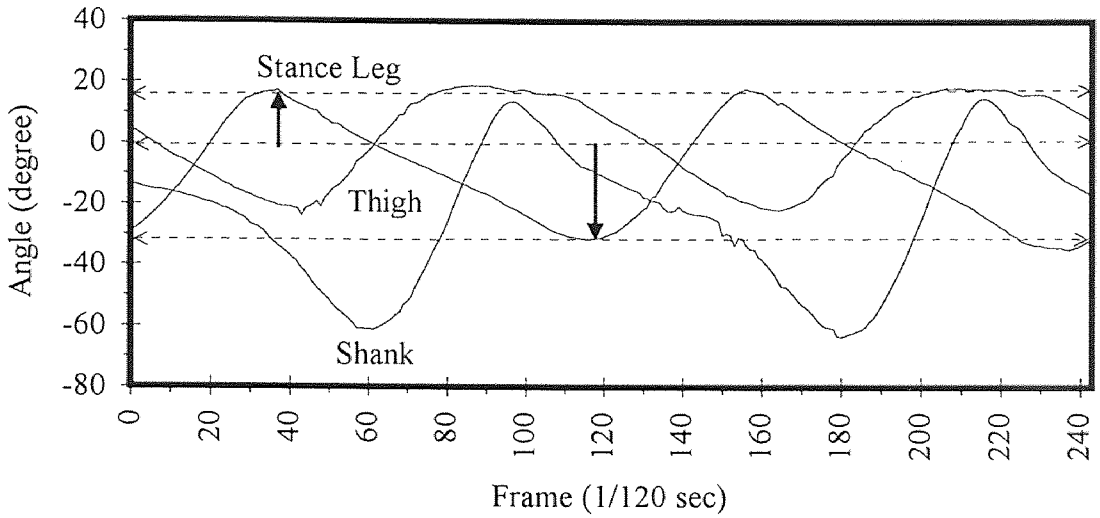

Figure 4.8 The angle of the stance leg when a line is drawn from the hip to the *heel*, and the angles of the thigh and shank of the swing leg.

The curves in Figure 4.7 and Figure 4.8 look similar, but, in Figure 4.7, the difference between the maximum positive and negative values of the stance leg's angle is smaller than in Figure 4.8. In the mathematical walking model the maximum positive and negative values of the stance leg's angle are equal. Therefore, it seems more appropriate to represent the stance leg with a straight line between the hip and ankle markers than between the hip and heel markers.

4.5 Smoothing the Data

There are small fluctuations in experimental data as can be seen in Figure 4.7. Fluctuations are adequately smoothed by averaging 7 consecutive data points. Data points are collected at the rate of 120 per second. This smoothing process does not have much effect on the theoretical results, but was necessary because of the flexibility of the wooden platform over which the subject was required to walk. The averaged data is:

$$\theta_i = \frac{1}{7}\sum_{j=i-3}^{i+3}\theta_j \,. \tag{4.4}$$

The smoothed data is shown in Figure 4.9.

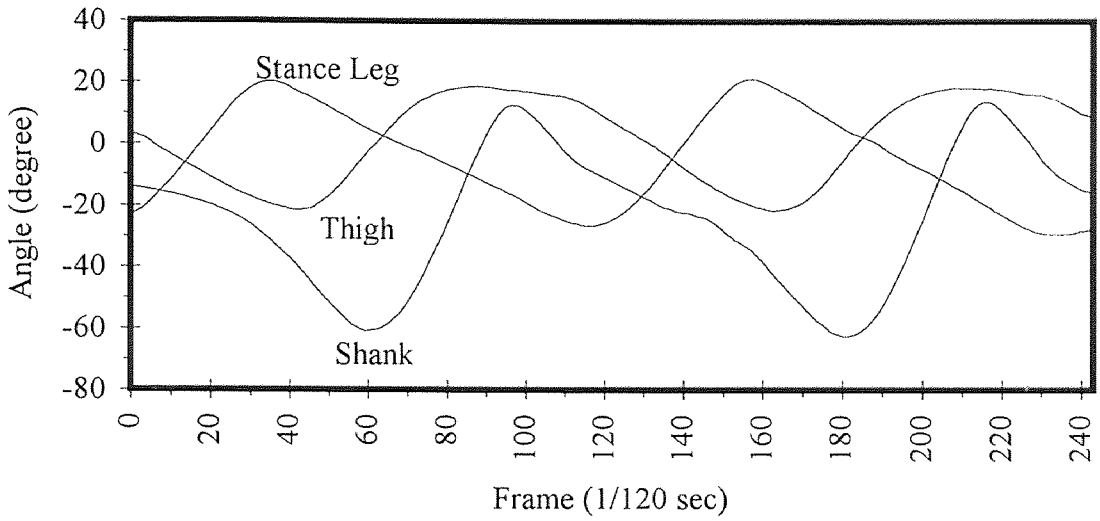

Figure 4.9 Smoothed angle data

4.6 Experimental Data of a Walking Cycle

The experimental data is collected over several walking cycles; it is necessary to select of one walking cycle - double-support and swing phases. The left leg is selected as the stance leg, and the right leg is selected as the swing leg. Therefore, the double-support phase begins when the left heel hits the ground(heel-strike), and ends when the right toe takes off from the ground(toe-off). When the double-support phase ends, the swing phase

begins, and that ends when the right heel hits the ground. From z-coordinates of the heel and toe of the left and right legs, the durations of the double-support and swing phases are determined. The z-coordinates of the heel and toe of the left and right legs are shown in Figure 4.10. The double-support phase is marked as 'D', and the swing phase is marked as 'S'. The duration of the double-support phase is 10 frames(10 x 1/120 sec), and the duration of the swing phase is 51 frames(51 x 1/120 sec). The line 'a' marks the time when the left-heel hits ground, the line 'b' when the right-toe lifts off ground and the line 'c' when the right-heel hits ground.

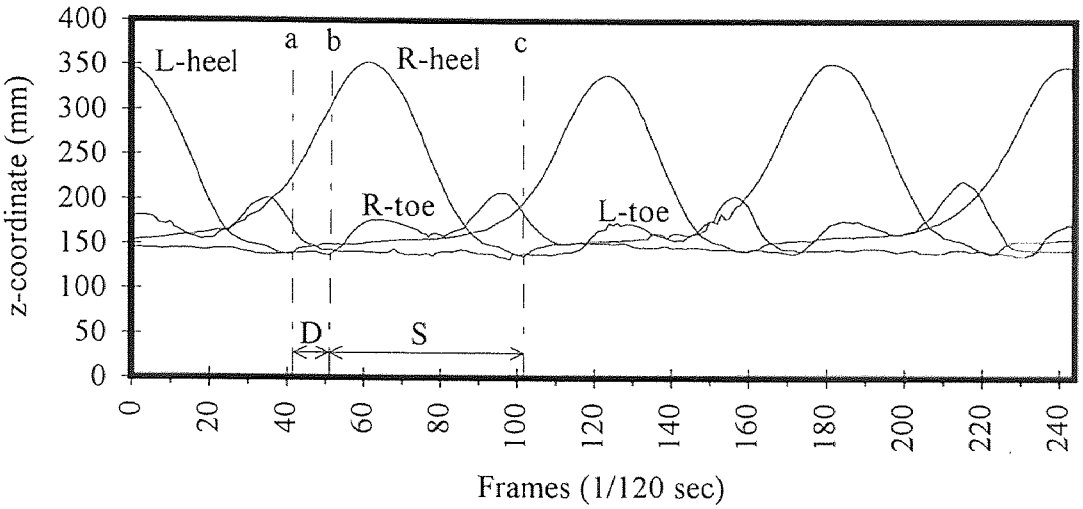

Figure 4.10 The measured z-coordinates of the heel and toe of the left and right legs

For the subject of our research 10 trials of data were collected at a self-selected walking speed in the range of normal walking speeds, with each trial comprising three or four steps. However, the durations of the double-support and swing phases are different for each step. Therefore, the duration of the double-support phase, and the duration of the swing phase were averaged for all steps. The averaged duration of the double-support phase is 9.71 frames, and the swing phase 50 frames. Unfortunately, there is no experimental data of one step whose double-support duration is 10 frames, and swing

duration 50 frames. One step whose double-support duration is 10 frames, and swing duration 51 frames is selected as the sample experimental data. Finally, the experimental angle data of the double-support and swing phases of the sample walking cycle are obtained and shown in Figure 4.11. This data will be used to determine the joint viscous coefficients of the mathematical walking model by curve fitting in the next chapter.

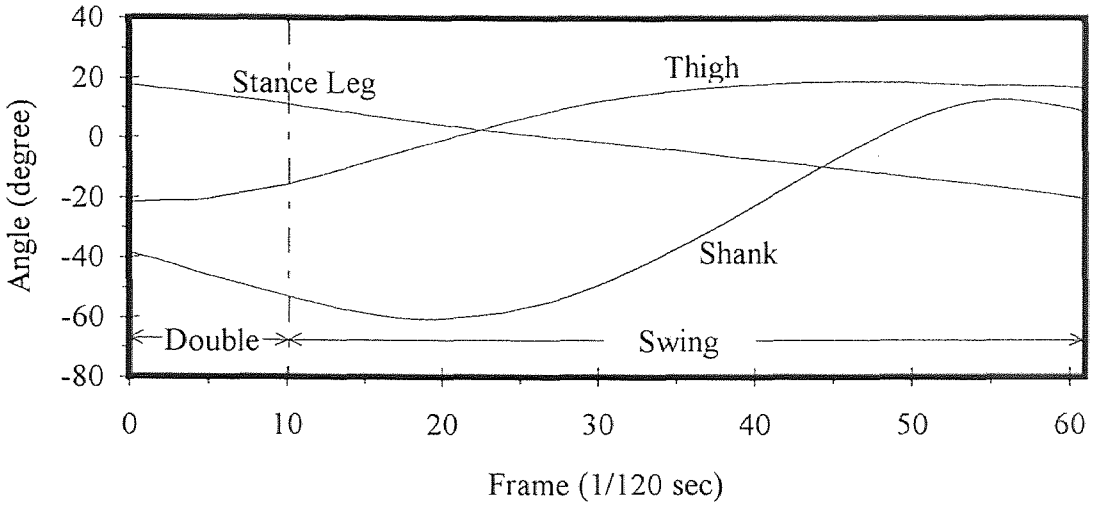

Figure 4.11 Experimental data of a single complete walking cycle: double and swing phases

4.7 Experimental Values of Structural and Gait Parameters

To compare the theoretical and experimental data, the theoretical data should be obtained with the same numerical values for the structural parameters and independent gait parameters as experimental data. The experimental data is the source of the limb lengths, step-length and toe-off angle that is applied to the mathematical model for ultimate curve fitting. Limb lengths are:

$$
\begin{aligned}
L_{Foot} &= \sqrt{(x_{p,Heel} - x_{p,Toe})^2 + (y_{p,Heel} - y_{p,Toe})^2 + (z_{p,Heel} - z_{p,Toe})^2} \\
L_{Thigh} &= \sqrt{(x_{p,Knee} - x_{p,Hip})^2 + (y_{p,Knee} - y_{p,Hip})^2 + (z_{p,Knee} - z_{p,Hip})^2} \\
L_{Shank} &= \sqrt{(x_{p,Heel} - x_{p,Knee})^2 + (y_{p,Heel} - y_{p,Knee})^2 + (z_{p,Heel} - z_{p,Knee})^2} \\
L_{Leg} &= L_{Thigh} + L_{Shank}.
\end{aligned}
\tag{4.5}
$$

The calculated limb lengths from the experimental data are shown in Table 4.1. As the limb lengths of the left and right legs are not equal, the averaged limb lengths are used for the mathematical equations.

Table 4.1 Lengths of limbs for model input

	Left	Right	Average
Foot (mm)	191.81	189.92	190.86
Thigh (mm)	359.83	390.83	375.33
Shank (mm)	385.58	353.19	369.38
Leg (mm)	745.41	744.02	744.71

If the x-, y- and z-coordinates of the left leg's heel at the beginning of the double-support phase are given as $H_{Left}(x_L, y_L, z_L)$, and the x-, y- and z-coordinates of the right leg's heel at the end of the swing phase are given as $H_{Right}(x_R, y_R, z_R)$, then the step-length is:

$$
S_L = \sqrt{(x_L - x_R)^2 + (y_L - y_R)^2 + (z_L - z_R)^2}\,. \tag{4.6}
$$

The toe-off angle is the shank's angle at the beginning of swing phase, and it is -53.1° from the experimental data. The measured independent gait parameters are summarized in Table 4.2. These are model inputs for curve fitting procedure to identify viscous parameters of the experimental subject.

Table 4.2 Independent gait parameters

Step-length	579.16 mm
Toe-off angle	-53.1°
Swing Duration	51 x (1/120) sec
Double-support duration	10 x (1/120) sec

CHAPTER 5

THEORETICAL RESULTS FROM THE MATHEMATICAL MODEL

The theoretical output from the mathematical model will yield the angles(θ_1, θ_2 θ_3), velocities(θ_1', θ_2' θ_3') and accelerations (θ_1'', θ_2'', θ_3'') of the three limbs as a function of time. The stick figures of the theoretical walking gait can be drawn with the angles(θ_1, θ_2, θ_3). The system energy at any instant can be calculated with the angles(θ_1, θ_2, θ_3) and velocities(θ_1', θ_2', θ_3') from equation(3.27), and the energy loss per unit walking distance can be calculated from equation(3.26). Using equation(3.26) the optimum gait of minimum energy consumption for a specific walking speed can be determined. With these results the relationships between the basic variables of walking - step length(S_L), step rate(steps/min), swing duration(T_S), double-support duration(T_D), toe-off angle(α) and energy expenditure(E) as a function of walking speed(V) - can also be determined.

5.1 Joint Viscous Coefficients

To obtain theoretical results from the dynamic equations of the mathematical walking model, it is necessary to first define the values of the structural parameters of the dynamic equations. The values of lengths of limbs can be measured directly.(Table 2.1) For the values of mass and mass center of limbs, Dempster's data can be used.(Table 2.2 and 2.3) However, to deduce the joint viscous coefficients, the Down-hill Simplex method is used as explained in section 3.4.2 because these data are not provided in Dempster's tables. The outputs of the down-hill simplex method are shown in Table 5.1 and Figure 4.1. Figure 5.1 shows the best fit curves between the theoretical and experimental data of the angles of the leg, thigh and shank when the joint viscous coefficients are 0.012379 N·m·sec.

Table 5.1 Joint viscous coefficient values

joint	ankle	hip	knee
joint viscous coefficient(N·m·sec)	0.012379	0.012379	0.012379

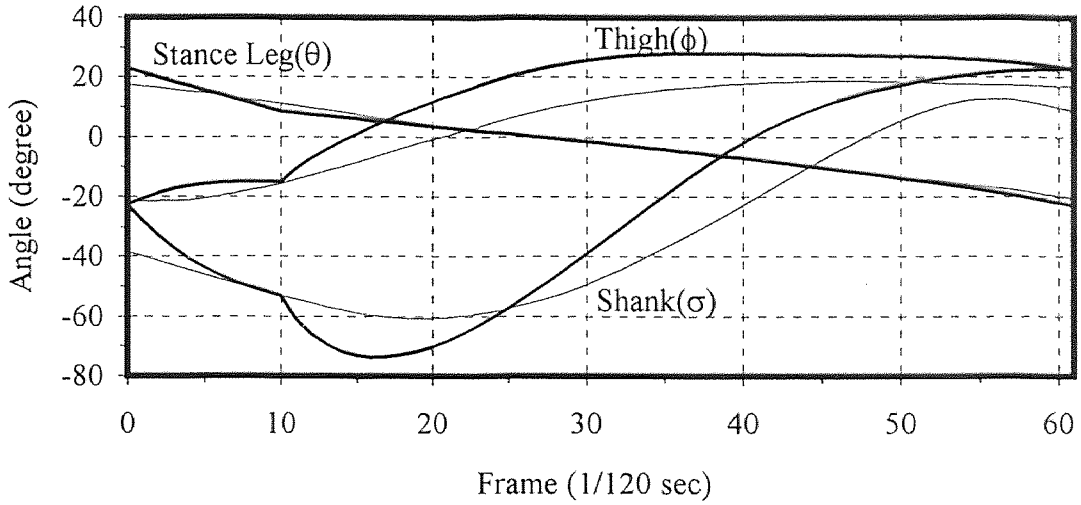

Figure 5.1 The best fit curves comparing the theoretical and experimental data of the angles of the leg, thigh and shank angles when the values of the joint viscous coefficients are 0.012379 (N·m·sec); solid lines represent the theoretical data, and regular lines represent the experimental data.

In the development of this model each joint was at first assigned its own specific viscous coefficients; Figure 5.2 demonstrates the comparison between the measured and theoretical curves when the Down-hill Simplex method was used to deduce a specific viscous coefficient for each joint. The curves in Figure 5.2 demonstrate a better correspondence than those in Figure 5.1. However, when a stick figure of the walking gait is developed from the data in Figure 5.2, the toe of the swing leg penetrates the ground, and this is considered to be physically unrealizable. The reason for this phenomenon is because the foot of the swing leg is assumed to be rigidly attached to the swing leg by a right angle. The Downhill-Simplex method does not take into consideration the position of the swing leg's toe. To keep the toe above the ground, a

different set of the joint viscous coefficient values must be assigned. Either, or both of the joint viscous coefficients of the knee and ankle can be decreased. The joint viscous coefficient of the hip, though its effect is smaller than that of the other two, can also be changed. There is no systematic way to find the best set of joint viscous coefficients which keep the toe above the ground. Consequently, the joint viscous coefficients for all three joints are assigned the same value, and Figure 5.1 is the result of the best fit curve.

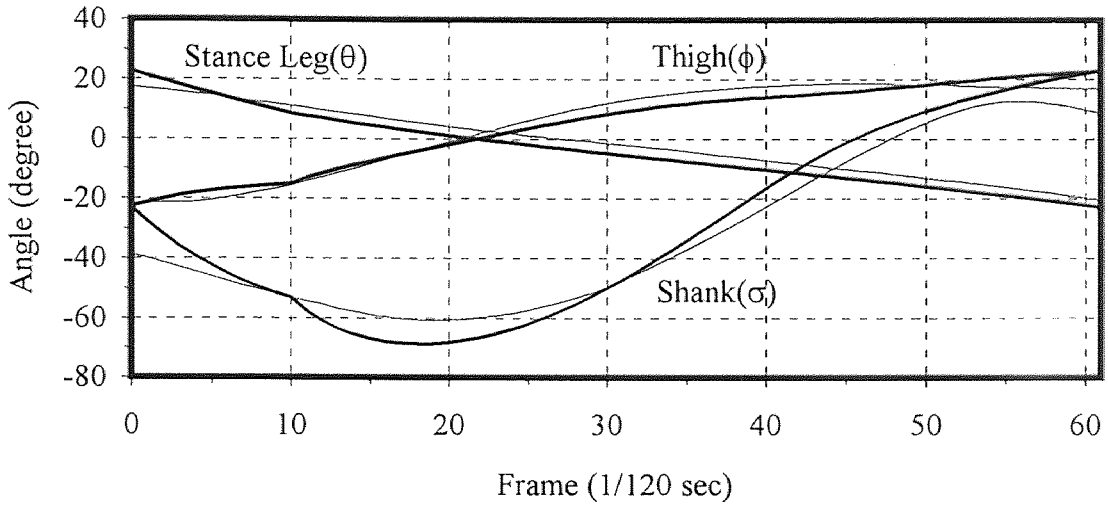

Figure 5.2 The best fit curves comparing the theoretical and experimental data of the angles of the leg, thigh and shank angles when the values of the joint viscous coefficients are 1.08607, 0.0 and 0.11(N·m·sec) for the ankle, hip and shank, respectively; solid lines represent the theoretical data, and regular lines represent the experimental data.

5.2 Survey in the Gait Space

Figure 2.3 displays data only of the swing phase, but Figure 5.1 displays data of the entire walking cycle - swing and double-support phases. With this entire walking cycle data, it is now possible to survey the gait space to find the optimum gait that consumes minimum mechanical energy per unit walking distance. In this walking model there are 4 independent gait parameters - step length(S_L), swing duration(T_S), double-support

duration(T_D), and toe-off angle(α). The effect these parameters have on the gait dynamics and energetics are examined below.

To determine the optimum gait of minimum mechanical energy consumption per unit walking distance it is necessary to calculate the energy losses of every gait for all different values of the gait parameters. This task can be accomplished with a suitable software program. However, to simplify the problem, the range of parameters are limited to those values that are physically realizable. For example, the toe-off angle is limited to the range:

$$\alpha_{min} < \alpha < \alpha_{max} \tag{5.1}$$

The minimum and maximum toe-off angles are calculated in Appendix H. The walking speed is also limited to 40 (m/min) < V < 120 (m/min) by the theoretical model. Gait speeds outside this range cannot be considered as normal gaits as explained in section 5.5. The step-length(S_L), the swing duration(T_S) and the double-support duration(T_L) are then constrained by:

$$\frac{40}{60} < \frac{S_L}{T_S + T_D} < \frac{120}{60} \tag{5.2}$$

The number 60 sec/min is necessary because S_L is expressed in units of 'm', T_S and T_D in units of 'sec', and V is in m/min. For a specific walking speed, the consumed energy for every possible gait is calculated for all different values of gait parameters, and the gait with the minimum mechanical energy consumption per unit walking distance is considered as the optimum gait for that walking speed.

5.2.1 Gaits for Different Swing and Double-Support Times

From equation(5.2), the step-length(S_L), the swing duration(T_S) and the double-support duration(T_D) are not independent for a specific walking speed(V). At a specific walking speed, the sum of swing duration and double-support duration is given by $T_S + T_D = V/S_L$. This value is constant as long as V and S_L are constant; if T_S is increased, T_D must be decreased and vice versa. To determine the effects of T_S and T_D, a step of length 57.92

cm, and toe-off angle of 53.1° with the walking speed 68.36 m/min are selected because these are close to normal walking step-length, toe-off angle and walking speed of the experimental data. The results can, however, be applied to any other step-lengths and toe-off angles.

With the step-length and the toe-off angle constant, the gait solutions for different values of T_S and T_D are shown in Figure 5.3 ~ 5.5. In Figure 5.3, where T_S is too small, the toe of the swing leg penetrates into the ground. If T_S is gradually increased, there is a specific value of T_S when the toe just clears the ground; this value of T_S is 0.425 sec, and the gait for this case is depicted in Figure 5.4. If T_S is increased further, then the toe clears the ground by several millimeters, but the shank kicks high in the air, This is shown in Figure 5.5. However, the energy consumption of walking is increased as the swing duration increases for a specific walking speed keeping the step-length and the toe-off angle constant. This is shown in Table 5.2 and Figure 5.6. Therefore, it can be said that, at a specific walking speed, there is only one specific T_S, which satisfies both the conditions that the toe does not penetrate into the ground, and that the consumed mechanical energy per unit walking distance is a minimum.

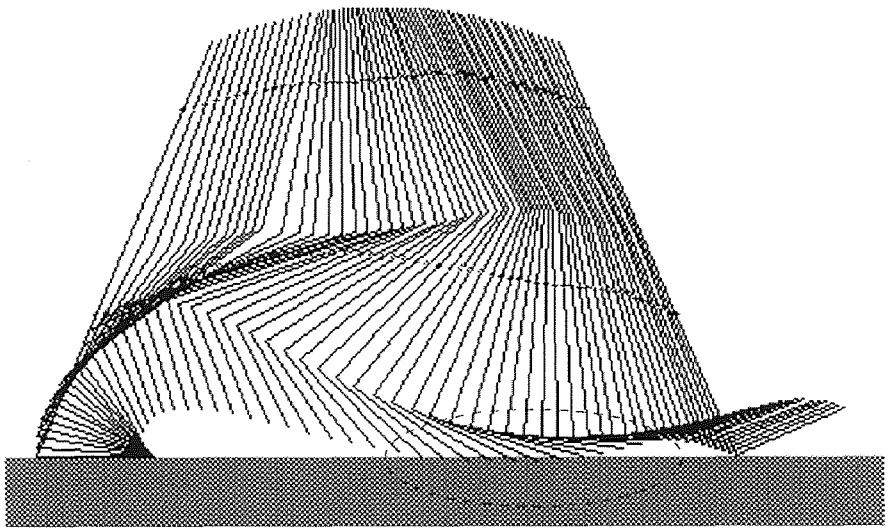

Figure 5.3 The stick figure of the gait with S_L = 57.92 cm, T_S = 0.408 sec, and T_D = 0.100 sec. The toe penetrates the ground in the dotted ellipse.

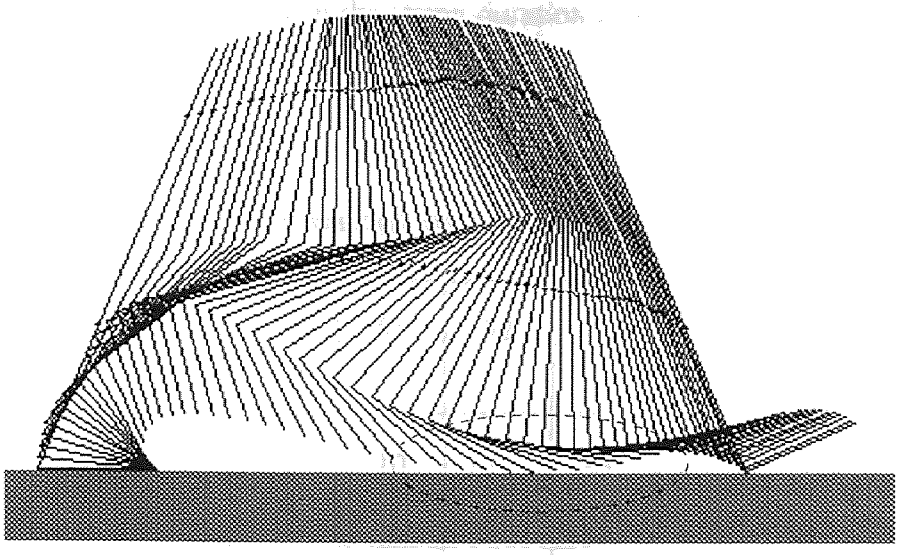

Figure 5.4 The stick figure of the gait with S_L = 57.92 cm, T_S = 0.425 sec, and T_D = 0.083 sec. The toe just clears the ground in the dotted ellipse.

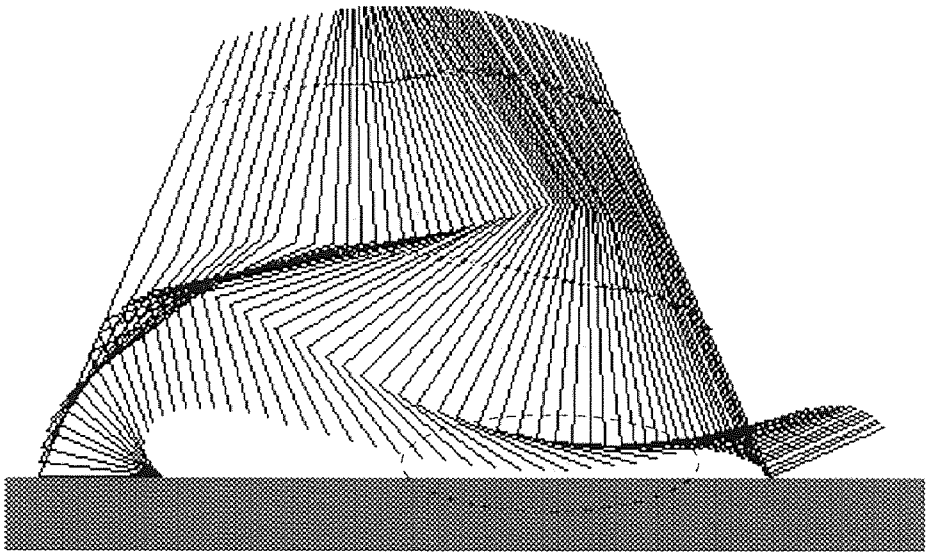

Figure 5.5 The stick figure of the gait with S_L = 57.92 cm, T_S = 0.442 sec, and T_D = 0.067 sec. The toe clears the ground by several millimeters in the dotted ellipse.

Table 5.2 demonstrates that the consumed energy decreases as the swing duration decreases at a constant walking speed. If the swing duration decreases more than a

specific value, the toe penetrate into the ground and the gait is considered to be physically unrealizable. This is the case when the swing duration is 49 x (1/120) sec and shown as shaded area in Table 5.2.

Table 5.2 Consumed energy per walking cycle when the swing duration is increased at a constant walking speed of 68.36 m/min.

Swing Time (1/120 sec)	(49)	***50***	51	52	53	54	55	56
Double-support Time (1/120 sec)	12	***11***	10	9	8	7	6	5
Consumed Energy (cal/min/kg)	26.47	***26.93***	27.50	28.20	29.05	30.08	31.37	33.03

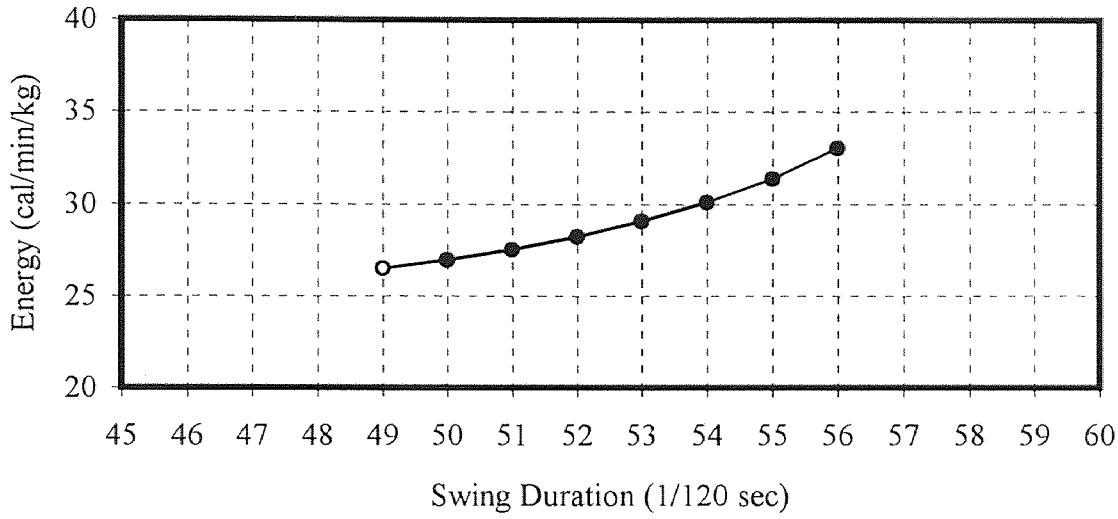

Figure 5.6 Consumed energy vs. swing time when the walking speed is 68.36 m/min.

5.2.2 Gaits for Different Step-Lengths

To demonstrate the effect of the step-length for a specific walking speed(V), the step-length is altered by changing $T = T_S + T_D$. The step-length is defined as $S_L = V \cdot T$. For

each step-length the consumed energy is calculated under the constraint that the toe does not penetrate into the ground. The result is shown in Table 5.3 and Figure 5.7. These results demonstrate that there is an optimum step-length of minimum mechanical energy consumption per unit walking distance for a specific walking speed. The optimum step-length satisfies both conditions that the toe does not penetrate into the ground and that the consumed energy is minimum. In Table 5.3 that optimum step-length is 0.551 m, and the consumed minimum energy is 25.69 cal/m/kg.

Table 5.3 Consumed energy when the step-length is increased at a constant walking speed of 68.36 m/min

Step-length (m)	0.522	0.532	0.541	***0.551***	0.560	0.570	0.579	0.589
Consumed Energy (cal/min/kg)	27.23	26.33	25.87	***25.69***	25.73	25.92	26.22	26.62

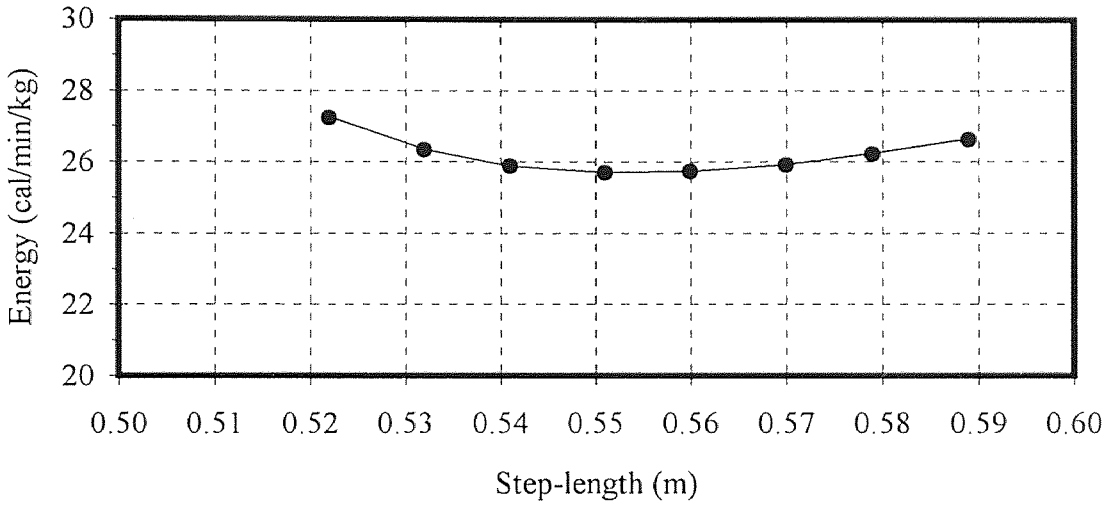

Figure 5.7 Consumed energy vs. step-length at a constant walking speed of 68.36 m/min.

5.2.3 Gaits for Different Toe-Off Angles

To observe the effect of the toe-off angle for a specific walking speed, the step length, swing duration and double-support duration are kept constant. For different toe-off angles consumed energy is calculated when the toe of the swing leg is constrained to remain above ground. The algorithm reveals that there is a specific toe-off angle which yields the minimum energy consumption. Table 5.4 and Figure 5.8 demonstrate the relationship between the consumed energy and different toe-off angles. The optimum toe-off angle satisfies both conditions that the toe of the swing leg does not penetrate into the ground and that the consumed energy is minimum. From Table 5.4 the minimum consumed energy is 27.26 cal/min/kg when the toe-off angle is -55°.

Table 5.4 Consumed energy for different toe-off angles at a constant walking speed of 68.36 m/min

toe-off angle (degree)	-52	-53	-54	***-55***	-56	57	-58	-59
consumed energy (cal/min/kg)	27.78	27.53	27.35	***27.26***	27.28	27.43	27.73	28.24

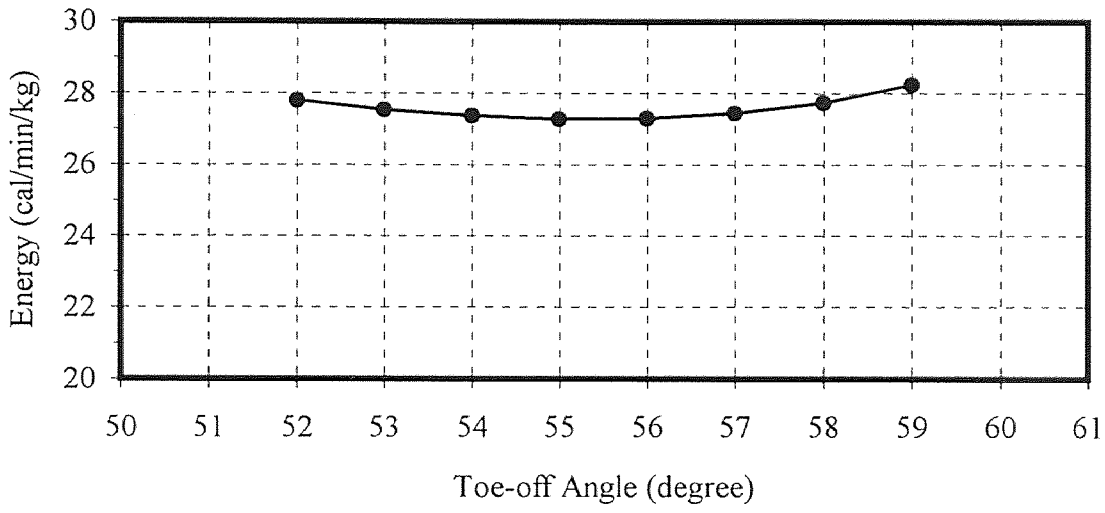

Figure 5.8 Consumed energy vs. toe-off angle at a constant walking speed of 68.36 m/min

5.3 Optimum Gait for a Specific Walking Speed

From the above results it can be calculated that, when the walking speed is given, there is only one set of independent gait parameters - swing duration(T_S), double-support duration(T_D), step-length(S_L) and toe-off angle(α) - which satisfy both the conditions that the toe of the swing leg does not penetrate into the ground and that the consumed energy is minimum. These specific values of independent gait parameters determine the optimum gait for a specific walking speed. The theoretical data of independent gait parameters and consumed energy of the optimum gait for different walking speeds are tabulated in Table 5.5. The theoretical data shows that the global optimum walking speed is 69 m/min.

Table 5.5 Basic walking variables of the optimum gait for different walking speeds

V (m/min)	T_S (sec) 1/120	T_D (sec) 1/120	S_L (m)	α (degree)	Ew (cal/min /kg)	Em (cal/m /kg)	n (steps /min)	S_L/n (m/steps /min)
40.0	52	27	0.43889	54	42.38	1.0596	91.1	0.00482
50.0	50	16	0.45833	55	45.81	0.9163	109.1	0.00420
60.0	50	13	0.52500	57	52.39	0.8731	114.3	0.00459
69.0	***49***	***9***	***0.55583***	***56***	***55.81***	***0.81***	***124.1***	***0.00448***
70.0	49	9	0.56389	56	59.08	0.8440	124.1	0.00454
80.0	50	7	0.63333	58	70.38	0.8798	126.3	0.00501
90.0	51	5	0.70000	55	83.53	0.9281	128.6	0.00544
100.0	51	4	0.76389	59	99.48	0.9948	130.9	0.00584
110.0	52	3	0.84028	58	118.89	1.0808	130.9	0.00642
120.0	54	3	0.95000	61	142.70	1.1892	126.3	0.00752

Figure 5.9 shows the graph of the consumed energy of the optimum gait for different walking speeds. Ew is the consumed energy per minute per kg(cal/min/kg), and Em is the consumed energy per unit walking distance per kg(cal/m/kg).

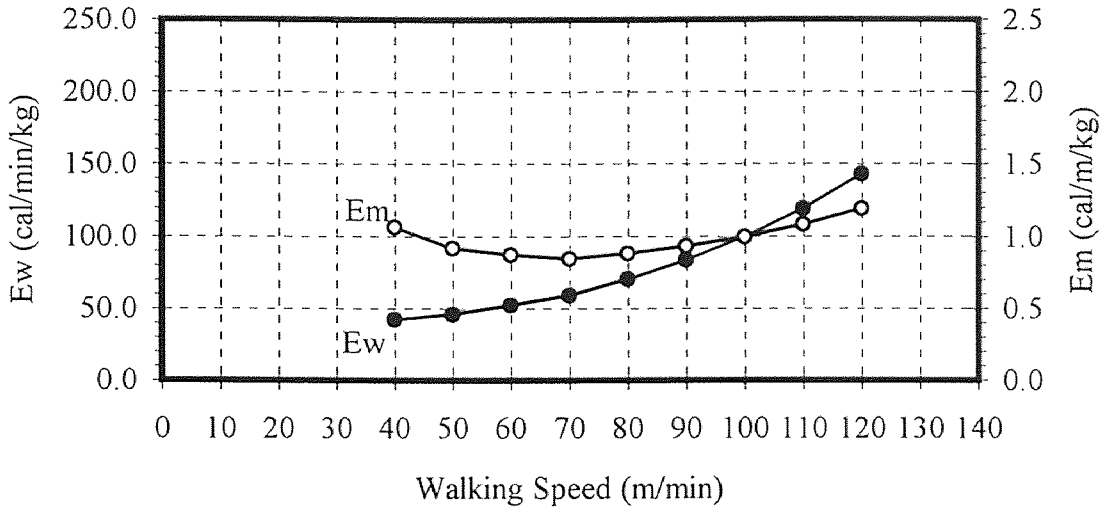

Figure 5.9 Theoretical consumed energy of the optimum gait for different walking speeds

5.4 Other Variables vs. Walking Speed

The above results suggest that there is an optimum gait for a given walking speed. Other variables such as the step-length, step-rate, step-length/step-rate, swing duration, double-support duration and toe-off angle at different walking speeds are shown in Figures 5.10-5.15.

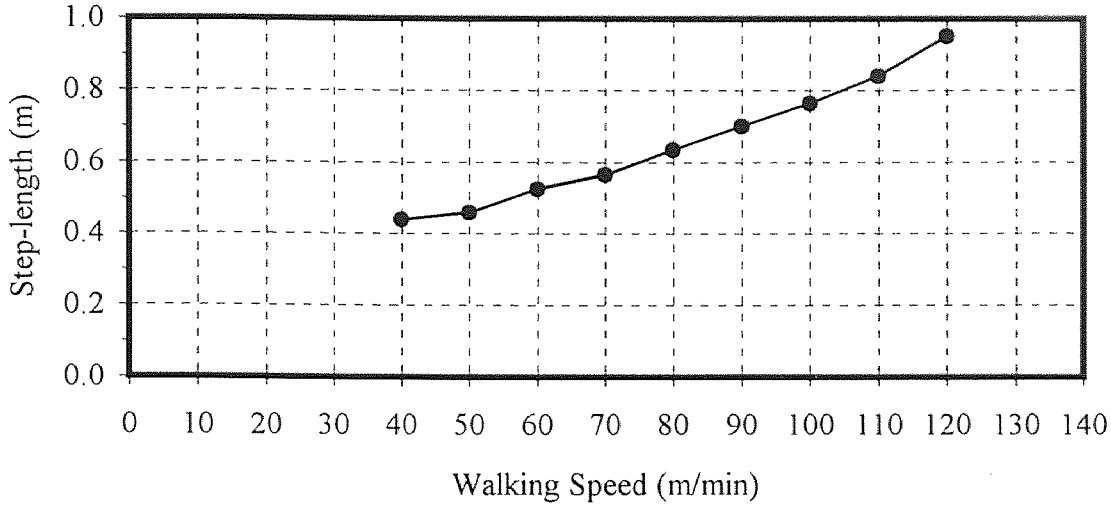

Figure 5.10 Theoretical predictions of step-length vs. walking speed assuming optimum mechanical efficiency

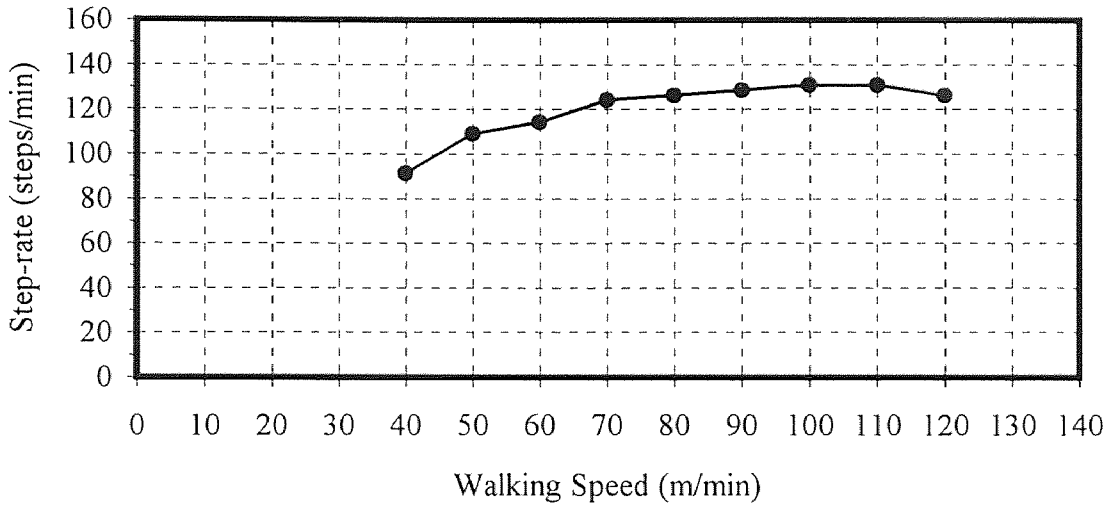

Figure 5.11 Theoretical predictions of step-rate vs. walking speed assuming optimum mechanical efficiency

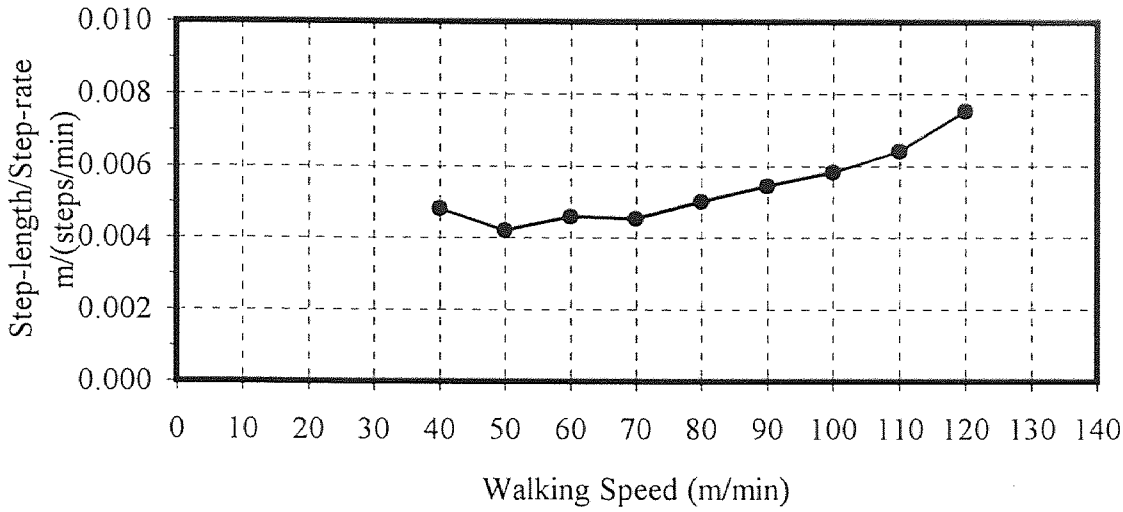

Figure 5.12 Theoretical predictions of step-length / Step-rate vs. walking speed assuming optimum mechanical efficiency

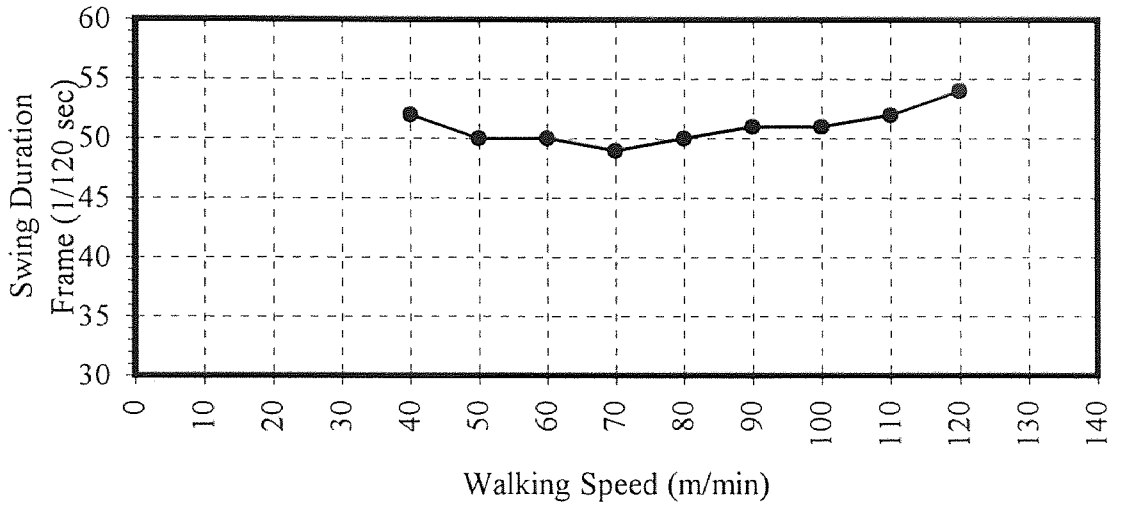

Figure 5.13 Theoretical predictions of swing duration vs. walking speed assuming optimum mechanical efficiency

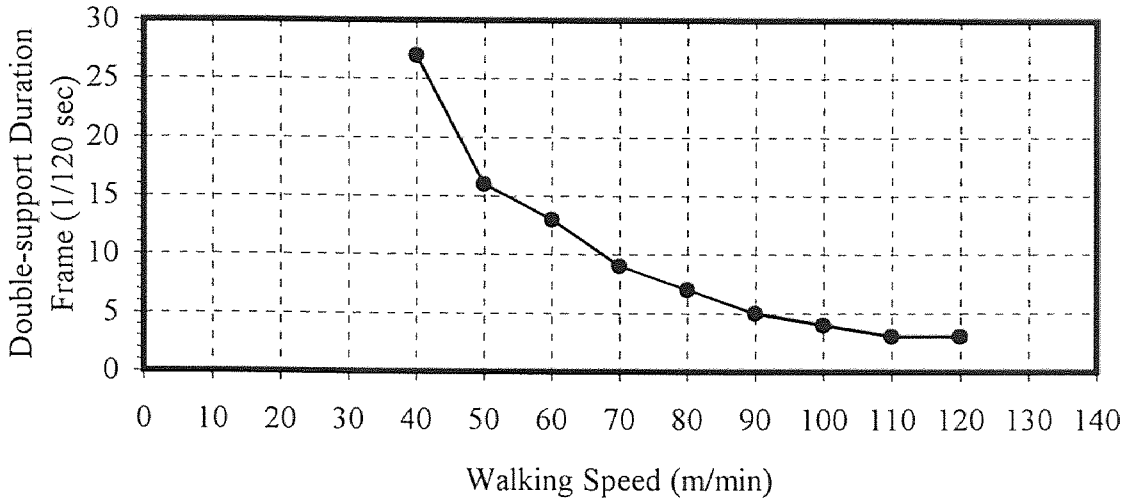

Figure 5.14 Theoretical predictions of double-support duration vs. walking speed assuming optimum mechanical efficiency

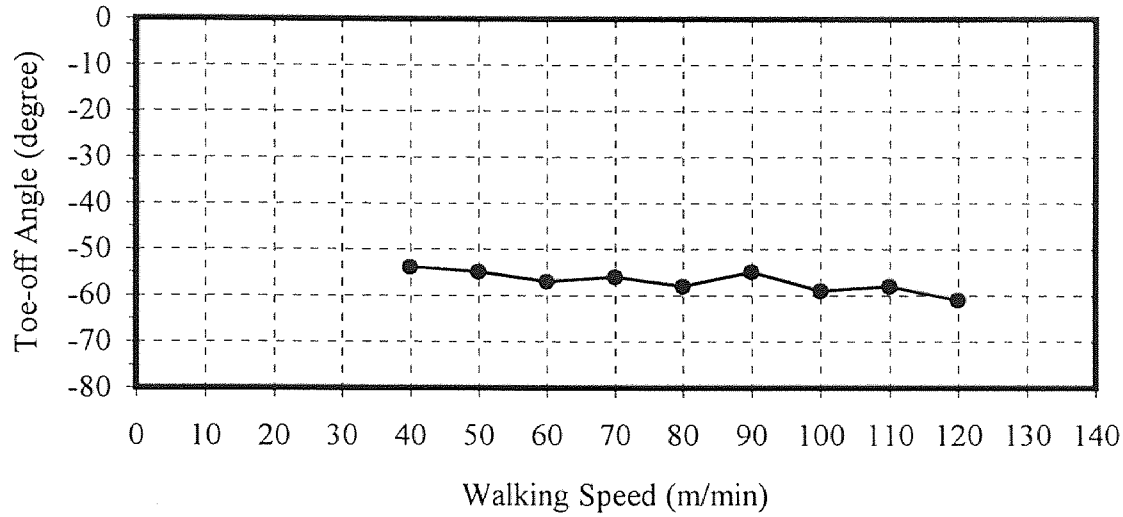

Figure 5.15 Theoretical predictions of toe-off angle vs. walking speed assuming optimum mechanical efficiency

5.5 Optimum Gaits for Low and High Walking Speeds

When the gait space is surveyed by changing independent gait parameters to obtain the optimum gait for different walking speeds, the solutions for low and high walking speeds deviate from that of the normal walking gait. The solution for a low walking speed(30 m/min) is shown in Figure 5.16; the flat area of the curve of the stance leg shows that the

stance leg remains immobile and even moves a little backward in the early stage of the swing phase. This region is circled by a dotted line in Figure 5.16. To demonstrate the backward movement, the dotted area in Figure 5.16 is expanded in Figure 5.17. The optimal solutions for other walking speeds less than 40 m/min have the same characteristics. These characteristics cannot be considered "normal" and it is concluded that this mathematical model is invalid at low walking speeds.

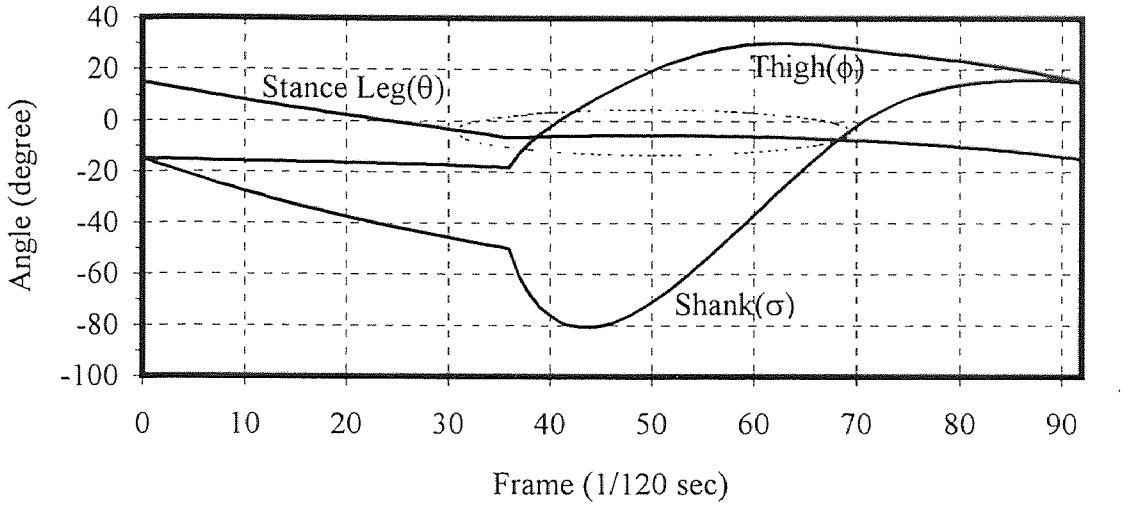

Figure 5.16 Theoretical results for a low walking speed of 30 m/min

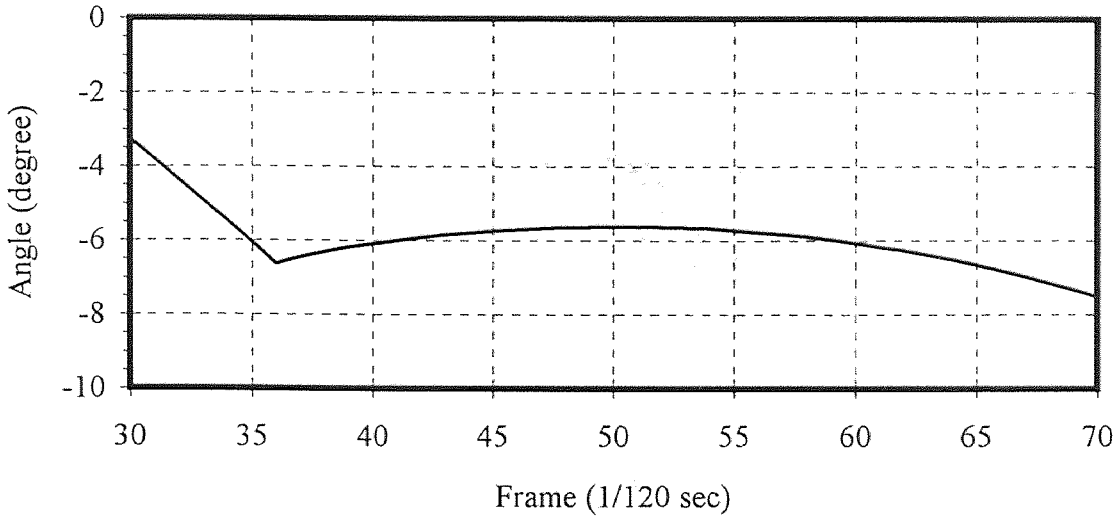

Figure 5.17 The expanded curve of the leg's angle of the dotted area in Figure 5.16

The theoretical optimum gait for a high walking speed of 120 m/min is shown in Figure 5.18. For clarity, the stance leg is displayed in bold only at the beginning of the double-support phase(line 'A') and at the end of the swing phase(line 'B'). The step-length seems to be large compared to the leg length. The gait does not appear stable and comfortable because of the long step-length. Any theoretical gait above this walking speed may not be acceptable as the normal gait. The gait might appear more normal if the step-length becomes smaller. Therefore, it is to be expected that the step-length becomes smaller. To compensate for the decreased step-length, it becomes necessary to increase the step-rate at a high walking speed. To increase the step-rate, the push-off of the stance leg starts earlier, before the swing leg contacts the ground, and the heel of the stance leg has left the ground even though the toe of the stance leg remains on the ground during the double-support phase. However, in this model, the heel of the stance leg remains on the ground until the heel of the swing leg contacts the ground as can be seen in Figure 5.18. This might be the reason why the theoretical output deviates from the normal gait for higher walking speeds.

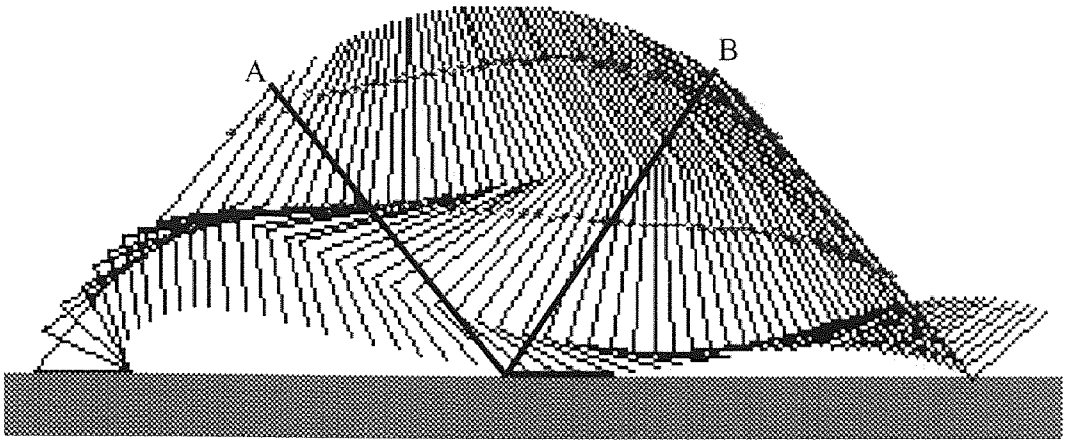

Figure 5.18 The theoretical gait for the high walking speed of 120 m/min

CHAPTER 6

COMPARISON WITH EXPERIMENTAL DATA

In order to validate the mathematical model the theoretical results will be compared with the results obtained from experimental measurements. Figure 5.1 demonstrates that the angles of limbs as calculated from the model can match experimental data relatively well. However, we are not satisfied with this alone. It is also necessary to compare consumed energy and other variables such as step-length, step-rate and step-length/step-rate. Experimental and empirical data of these variables are shown in Table 6.1.(Ralston 1974)

Table 6.1 Averaged values of Ew, Em, S_L, n and S_L/n for 4 different walking speeds(V) from 10 male, and 10 female subjects

	Speed (m/min)	Ew (cal/min/Kg)	Em (cal/m /Kg)	S_L (m)	n (steps/min)	S_L/n (m/steps/min)
Males	24.4	35.0	1.43	0.41	59.5	0.0069
	48.8	43.9	0.90	0.59	84.4	0.0070
	73.2	58.8	0.80	0.72	102.2	0.0072
	97.6	79.6	0.82	0.84	116.3	0.0070
Females	24.4	35.0	1.43	0.41	60.0	0.0068
	48.8	43.9	0.90	0.57	86.7	0.0066
	73.2	58.8	0.80	0.67	109.0	0.0061
	97.6	79.6	0.82	0.77	126.8	0.0064

In Table 6.1 Ew and Em are obtained from equations (2.4) and (2.5), respectively. Table 6.1 is the averaged data for 4 different walking speeds from 10 male and 10 female subjects. In this section these averaged data will be used for comparison with theoretical data from Table 5.5. The experimental and theoretical data of consumed energy, step-

length, step-rate and step-length/step-rate vs. walking speed are compared in Figures 6.1, 6.2, 6.3 and 6.4, respectively.

The theoretical and experimental data of consumed energy can be said to agree relatively well around normal walking speed range, but discrepancy between them increases as the walking speed increases.

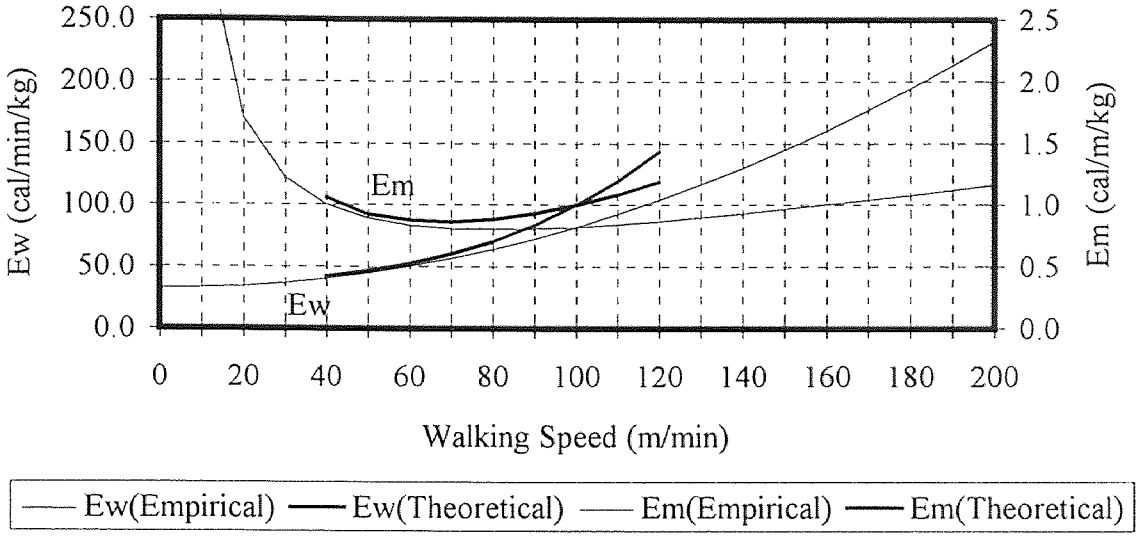

Figure 6.1 Comparison of consumed energy

The theoretical and experimental data of the step-length data show that they increase almost linearly as the walking speed increases, even though the theoretical data is a little concave and the experimental convex.

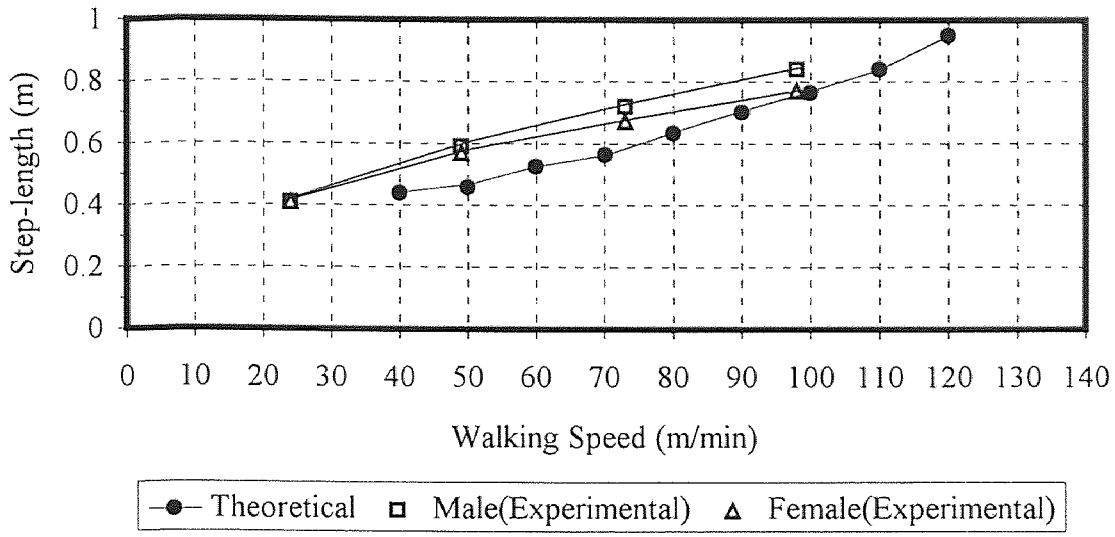

Figure 6.2 Step-length vs. walking speed

The experimental data of the step-rate increases almost linearly as the walking speed increases, but the theoretical data shows convex characteristic.

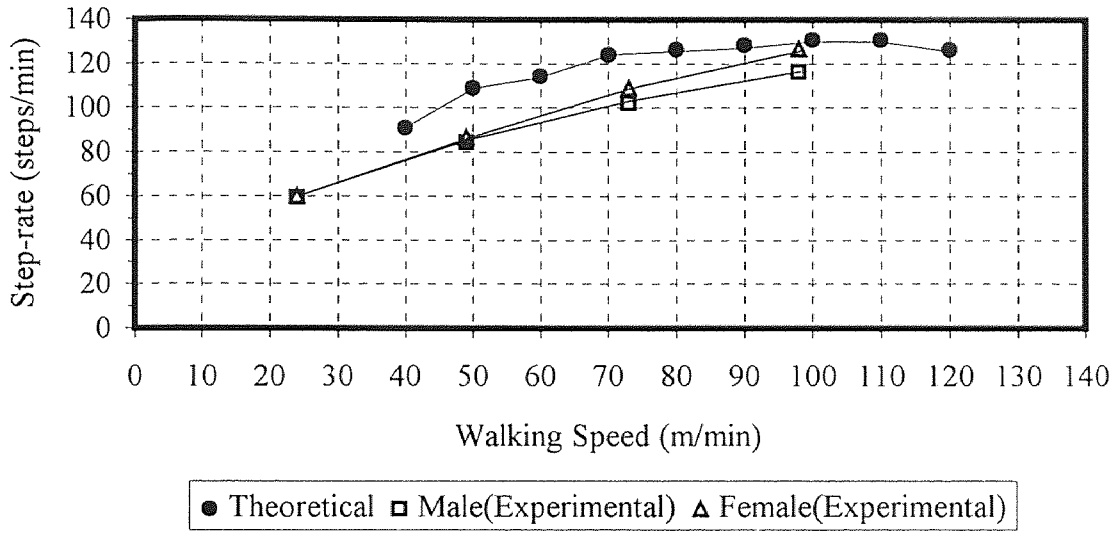

Figure 6.3 Step-rate vs. walking speed

It is generally known that the step-length/step-rate is almost constant as the walking speed increases. The experimental data of the step-length/step-rate seems to be constant as the walking speed increases. The theoretical data of the step-length/step-rate shows concave characteristic as the walking speed increases. It is because the step-rate shows convex characteristics as the walking speed increases.

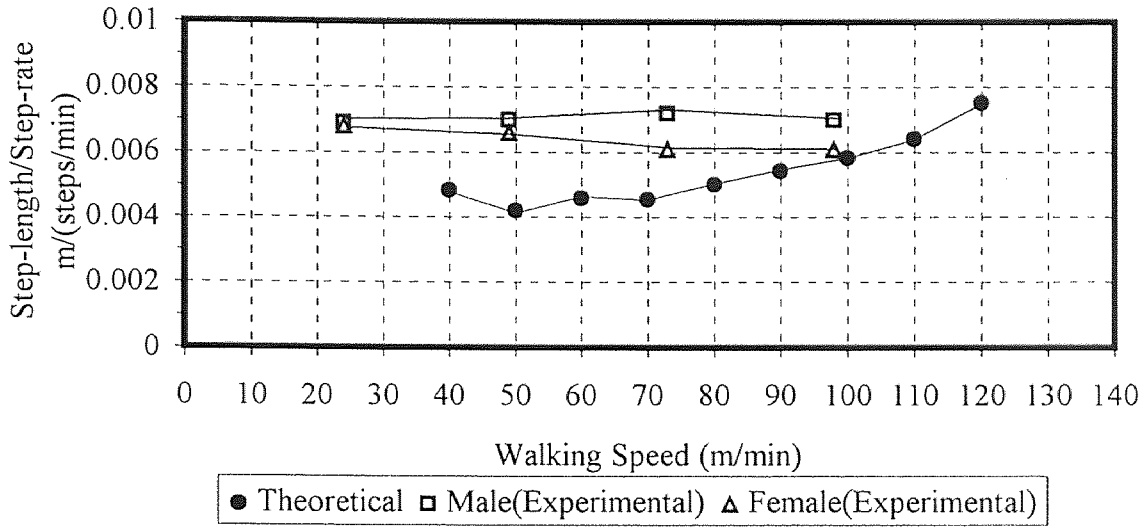

Figure 6.4 Step-length/Step-rate vs. walking speed

Table 6.2 Comparison of independent gait parameters between the theoretical global optimum and experimentally self-selected gaits

	Theoretical Global Optimum Gait	Experimentally Self-Selected gait
Swing Duration (x 1/120 sec)	49	51
Double-support Duration (x 1/120 sec)	9	10
Step-length (m)	0.55583	0.57916
Toe-off Angle (degree)	-56	-53.1
Walking Speed (m/min)	69.0	68.36

Table 6.2 shows comparison of independent gait parameters between the theoretical global optimum and experimentally self-selected gaits. The close agreements between them are quite interesting and encouraging considering how simple the model is.

CHAPTER 7

DISCUSSION

7.1 Gait for Normal Walking Speed

The relatively close agreement between theoretical and experimental data at normal walking speed(80 m/min) in Figure 6.1 suggests that this walking model is relatively good for the prediction of optimum gait. However, there are still discrepancies between theoretical and experimental data. When a person walks, the knee of the stance leg maintains a slight bend. At heel strike the knee of the swing leg bends a little as well. In this model the stance leg is a straight line, and the swing leg becomes a straight line at heel-strike. Therefore, its theoretical data cannot be expected to match the experimental data precisely. In an attempt to account for these bends, when preparing experimental data of the stance leg, a straight line is drawn from the hip to the ankle, and the angle which the line makes with the vertical line is calculated. However, it could be better to add one more segment to the mathematical model and allow the knee of the stance leg to bend; the stance leg should be separated into a thigh segment and a shank segment. This would create a four dynamic angle model, and it is expected that the theoretical data would more closely match the experimental data than the three angle model used in this dissertation.

7.2 Gait for Fast Walking Speed

The predicted energy consumption curve(Figure 6.1) shows that the discrepancy between the theoretical and experimental data becomes larger as the walking speed increases. In this model the heel of the stance leg remains on the ground until the heel of the swing leg contacts the ground. In human walking, when the walking speed increases, the heel of the stance leg has lifted off the ground, even though the toe of the stance leg remains on the ground, before the heel of the swing leg contacts the ground. This means that the push off

of the stance leg has already begun before the double-support phase has started that is, before the swing leg has made contact with the ground. This transient state between the swing and the double-support phases becomes larger in duration, and the double-support phase becomes shorter, as the walking speed increases. When the walking speed increases even further, the double-support phase eventually disappears and the walking gait changes into a running gait. Therefore, to expand the predictive utility of the model to higher walking speeds, it is necessary to incorporate a third walking phase between the start of swing and heel lift of the stance leg. To this end the origin of the stance leg needs to be shifted from the heel to the toe so that the segment from heel to the proximal end of the toe can function as an independent segment, thus adding a fifth segment and dynamic angle to the model.

7.3 Gait for Slow Walking Speed

For slow walking speed(< 40m/min) the model was unable to predict an optimal and realizable gait. At slow walking speed, at the theoretical optimum gait at which the energy consumption is minimum and the toe of the swing leg is constrained from penetrating into the ground, the stance leg moves back and forth during walking as demonstrated in Figure 5.17. This suggests that the body does not behave like a free pendulum at the slow walking speeds because the model is based on the assumption of a coupled free pendulum. In the model energy is supplied as an impulse to the body at the beginning of each walking phase, but physiologically energy is supplied as continuous input during the double-support phase. If the double-support duration becomes long as the walking speed decreases, the constrained free pendulum of our model is not a valid model for the double-support phase; it is necessary to improve the double-support phase by designing a new algorithm with provision for continuous energy input. Even in the swing phase, the hamstring and quadriceps muscle group are active and participate in

accelerating and decelerating the body. At slow walking speeds muscle activity is continuous in the swing phase in order to maintain balance.

7.4 Joint Viscous Coefficients

The model described here differs from other models reported in the literature by incorporating joint viscous coefficients of the ankle, hip and knee. Initially a specific viscous coefficient was defined for each joint. However, there was large discrepancy between theoretical and experimental data when each joint was assigned a specific viscous coefficient. With the joint viscous coefficients the same values, the theoretical energy consumption during walking matches the experimental data relatively well. The results of this research effort suggest that the joint viscous coefficients are important parameters in the development of a valid mathematical walking model; however, the coefficients cannot be measured directly. In this project the numerical values for the coefficients were deduced by curve-fitting the theoretical time history of the angles between the model components and the measured angles of the lower extremities. It ought to be possible to devise a more direct method for measuring the joint viscous coefficients, and therefore directly validating model predictions.

7.5 Experimental Data

The experimental data revealed that the limb lengths of the left and right legs are not exactly equal. This is probably due to actual physical assymetries in the experimental subject, imprecise placements of the reflective markers on the subject, or slight movements in the position of the markers as the subject walked back and forth within the calibration volume of the Vicon 370 Motion Analysis System. It is estimated that the measured angles may be in error by as much as 20%; thus the quantitative results derived for the joint viscous coefficients are unreliable, their qualitative contribution to the mathematical model is demonstrated.

7.6 Experimental Energy Consumption Curve

To validate our mathematical walking model the theoretical data about energy consumption during walking were compared with empirical data which obtained from oxigen consumption of the humal body. The empirical data are not results of direct measurement of consumed energy. Therefore, it is assumed that there is tight coupling between mechanical and metabolic energy consumption. This would be true for only well designed mechanical system in which chemical energy transforms to mechanical work.

CHAPTER 8

CONCLUSION

The mathematical walking model developed here is a highly idealized model of human walking with only three segments(stance leg, thigh and shank of the swing leg). It has been improved by adding velocity-dependent energy dissipation terms contributed by joint viscous coefficients, and an important kinetic energy loss that occurs as a result of the heel-strike impact at each step. It is a complete walking cycle model, with both of the swing and double-support phases being considered in the model. Thus the consumed energy of the entire walking cycle can be calculated from the model. It predicts, at each walking speed, an optimum gait and optimizes the parameters such as swing duration, double-support duration, step length and toe-off angle that minimize the mechanical energy loss per unit walking distance. These optimal walking solutions can be obtained using only the body structural parameters such as segment lengths, masses, mass centers and joint viscosities.

The theoretical output data are compared with experimental data to validate the model. The results show that the model is a relatively good one, and that it can be used to explore human gait. From the results it can be concluded that the hypothesis that gait selection is strongly correlated with mechanical energy efficiency in normal subjects is theoretically substantiated.

The three angle model is an adequate one for normal walking speeds. At higher-than-normal walking speeds($>$ 120 m/min), the model begins to fail because there is an uncertain period between the swing and double-support phases during which the heel of the stance leg has been off the ground and propelled the body before the heel of the swing leg contacts the ground. The model also fails at lower walking speeds($<$ 40 m/min). The reason might be because the human body does not move as a free pendulum at low walking speeds.

The gait that consumes the minimum energy occurs when the toe just clears the ground. When the toe is lifted above the ground-clearance level, the energy consumption increases.

The generalized 2-D mathematical walking model can be used for the expansion of the model to a model with any number of segments. The two-point boundary solution method can be extended to handle multiple phases of motion with muscle impulses at each inter-phase obtained as model output.

From the primitive, yet effective, model a more sophisticated model can be developed that is suitable for understanding and improving the gait in amputees and other gait-impaired individuals. This model should also be helpful in gait trainning and in the design of more effective prostheses.

The following steps are recommended to expand the capability of the model:

1. Allow the knee of the stance leg to bend in order to achieve a better correspondence between the theoretical and experimental data.
2. Uncouple the foot from the shank so as to allow the foot to flex and extend in order to improve the model at higher walking speeds. This will require the addition of an additional walking phase in which the foot of the stance leg pushes the body before the heel of the swing leg contacts the ground.
3. There is no proven theory that the body moves as a free pendulum during the double-support phase. If the double-support duration is relatively short, it might not make any difference whether the energy input during the double-support phase is an impulse or a distrbuted one. However, if the double-support duration is increased, it will be necessary to consider the fact that the body is controlled during the double-support phase. The quadriceps muscle group is used for acceleration, even in the swing phase, and the hamstring group is used for deceleration.
4. The upper body segments are assumed as one mass in our model. It is possible to extend our model by attaching trunk and arm segments.

5. The 2-D walking model can be expanded into a 3-D model.
6. Joint viscous coefficients are assumed equal in each joint in this research. Specific coefficients should be derived for each joint.

APPENDIX A

DEMPSTER'S DATA

Dempster's data(Veau 1977, 211-212) is shown below in Table A.1 and Table A.2. They are ratios of segment weight to body weight, and ratios of center of mass to segment length to proximal end.

Table A.1 Segmental Weight / Body Weight Ratios

Segment	Dempster's Data(%)	Adjusted Dempster's Data(%)
Head	7.9	8.1
Trunk	48.6	49.7
Upper arm	2.7	2.8
Forearm	1.6	1.6
Hand	0.6	0.6
Total arm	4.9	5.0
Forearm and hand	2.2	2.2
Thigh	9.7	9.9
Calf	4.5	4.6
Foot	1.4	1.4
Total leg	15.7	16.1
Calf and foot	6.0	6.1
Sum	97.7	100.0

The sum is calculated as Head + Trunk + 2*(Total arm + Total leg). As the sum is not exactly 100%, Dempster's data is slightly adjusted to make the sum 100%.

Table A.2 Center of Mass / Segment Length Ratios to Proximal End

Segment	Dempster's Data(%)
Head	43.3
Arm	43.6
Forearm	43.0
Hand	49.4
Forearm and hand	67.7
Thigh	43.3
Calf	43.3
Foot	42.9
Total leg	43.3
Calf and foot	43.7

APPENDIX B

MATHEMATICAL WALKING MODEL OF THREE ANGLES

B.1 Swing Phase

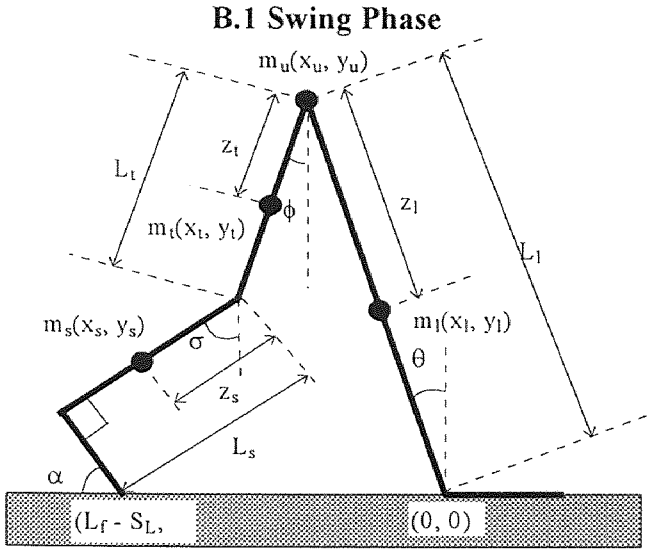

Figure B.1 Configuration of the leg, thigh and shank at toe-off

$$x_l = -(L_l - z_l)\sin\theta \qquad \dot{x}_l = -(L_l - z_l)\cos\theta\cdot\dot{\theta}$$

$$y_l = (L_l - z_l)\cos\theta \qquad \dot{y}_l = -(L_l - z_l)\sin\theta\cdot\dot{\theta}$$

$$x_u = -L_l\sin\theta \qquad \dot{x}_u = -L_l\cos\theta\cdot\dot{\theta}$$

$$y_u = L_l\cos\theta \qquad \dot{y}_u = -L_l\sin\theta\cdot\dot{\theta}$$

$$x_t = -L_l\sin\theta + z_t\sin\phi \qquad \dot{x}_t = -L_l\cos\theta\cdot\dot{\theta} + z_t\cos\phi\cdot\dot{\phi}$$

$$y_t = L_l\cos\theta - z_t\cos\phi \qquad \dot{y}_t = -L_l\sin\theta\cdot\dot{\theta} + z_t\sin\phi\cdot\dot{\phi}$$

$$x_s = -L_l\sin\theta + L_t\sin\phi + z_s\sin\sigma \qquad \dot{x}_s = -L_l\cos\theta\cdot\dot{\theta} + L_t\cos\phi\cdot\dot{\phi} + z_s\cos\sigma\cdot\dot{\sigma}$$

$$y_s = L_l\cos\theta - L_t\cos\phi - z_s\cos\sigma \qquad \dot{y}_s = -L_l\sin\theta\cdot\dot{\theta} + L_t\sin\phi\cdot\dot{\phi} + z_s\sin\sigma\cdot\dot{\sigma}$$

where

L_l, L_t, L_s	Lengths of the leg, thigh and shank
z_l, z_t, z_s	Distances of the center of mass of the leg, thigh and shank
m_l, m_t, m_s	Masses of the leg, thigh and shank
m_u, m_T	Masses of the upper body and the total body
θ, ϕ, σ	Angles that the leg, thigh and shank make with the vertical line
$\dot{\theta}, \dot{\phi}, \dot{\sigma}$	Velocities of the leg, thigh and shank
L_f	Length of the foot
S_L	Step length

Potential energy is expressed as follows:

$$\begin{aligned} PE &= (m_l y_l + m_u y_u + m_t y_t + m_s y_s)g \\ &= (m_l L_l - m_l z_l + m_u L_l + m_t L_l + m_s L_l)g\cos\theta - (m_t z_t + m_s L_t)g\cos\phi \\ &\qquad - m_s z_s g\cos\sigma \\ &= (m_T L_l - m_l z_l)g\cos\theta - (m_t z_t + m_s L_t)g\cos\phi - m_s z_s g\cos\sigma \end{aligned}$$

$$\therefore PE = \sum_{i=1}^{3} p_i \cos\omega_i \tag{B.1}$$

where

$$\begin{aligned} (p_1,\ p_2,\ p_3) &= (m_T L_l g - m_l z_l g,\ -m_t z_t g - m_s L_t g,\ -m_s z_s g) \\ (\omega_1,\ \omega_2,\ \omega_3) &= (\theta,\ \phi,\ \sigma)\ . \end{aligned} \tag{B.2}$$

Kinetic energy is expressed as follows:

$$KE_l = \frac{1}{2} m_l (\dot{x}_l^2 + \dot{y}_l^2) = \frac{1}{2} m_l (L_l - Z_l)^2 \dot{\theta}^2$$

$$KE_u = \frac{1}{2} m_u (\dot{x}_u^2 + \dot{y}_u^2) = \frac{1}{2} m_u {L_l}^2 \dot{\theta}^2$$

$$KE_t = \frac{1}{2} m_t (\dot{x}_t^2 + \dot{y}_t^2) = \frac{1}{2} m_t \{{L_l}^2 \dot{\theta}^2 + z_t^2 \dot{\phi}^2 - 2L_l z_t \cos(\theta - \phi)\cdot\dot{\theta}\cdot\ \dot{\phi}\}$$

$$\begin{aligned} KE_s &= \frac{1}{2} m_s (\dot{x}_s^2 + \dot{y}_s^2) \\ &= \frac{1}{2} m_s (L_l^2 \dot{\theta}^2 + L_t^2 \dot{\phi}^2 + z_s^2 \dot{\sigma}^2) \\ &\quad + m_s \{-L_l L_t \cos(\theta - \phi)\cdot\dot{\theta}\cdot\dot{\phi} - L_l z_s \cos(\theta - \sigma)\cdot\dot{\theta}\cdot\dot{\sigma} + L_l z_s \cos(\phi - \sigma)\cdot\dot{\phi}\cdot\dot{\sigma}\} \end{aligned}$$

$$\begin{aligned} KE &= KE_l + KE_u + KE_t + KE_s \\ &= \frac{1}{2}(m_T {L_l}^2 - 2m_l L_l z_l + m_l {z_l}^2)\dot{\theta}^2 + \frac{1}{2}(m_t {z_t}^2 + m_s {L_t}^2)\dot{\phi}^2 + \frac{1}{2} m_s {z_s}^2 \dot{\sigma}^2 \\ &\quad - (m_t L_l z_t + m_s L_l L_t)\cos(\theta - \phi)\cdot\dot{\theta}\cdot\dot{\phi} - m_s L_l z_s \cos(\theta - \sigma)\cdot\dot{\theta}\cdot\dot{\sigma} \\ &\quad + m_s L_t z_s \cos(\phi - \sigma)\cdot\dot{\phi}\cdot\dot{\sigma} \end{aligned}$$

$$\therefore KE = \frac{1}{2}\sum_{i,j=1}^{3} c_{ij}^{*}\dot{\omega}_i\dot{\omega}_j \tag{B.3}$$

where

$$\begin{bmatrix} c_{11} & c_{12} & c_{13} \\ c_{21} & c_{22} & c_{23} \\ c_{31} & c_{32} & c_{33} \end{bmatrix} = \begin{bmatrix} m_T {L_l}^2 - 2m_l L_l z_l + m_l {z_l}^2 & -m_l L_l z_t - m_s L_l L_t & -m_s L_l z_s \\ -m_t L_l z_t - m_s L_l L_t & m_t {z_t}^2 + m_s {L_t}^2 & m_s L_t z_s \\ -m_s L_l z_s & m_s L_l z_s & m_s {z_s}^2 \end{bmatrix} . \tag{B.4}$$

$$c_{ij}^{*} = c_{ij}\cos(\omega_i - \omega_j) \tag{B.5}$$

Lagrange's equations of motion can be derived as follows:

$$L = KE - PE$$
$$= \frac{1}{2}\sum_{i,j=1}^{3} c_{ij}^{*}\dot{\omega}_i\dot{\omega}_j - \sum_{i=1}^{3} p_i \cos\omega_i$$

First, we find $\frac{d}{dt}(\frac{\partial L}{\partial \dot{\omega}_k})$.

$$\frac{\partial L}{\partial \dot{\omega}_k} = \frac{1}{2}\sum_{\substack{i=1 \\ i\neq k}}^{3} c_{ik}^{*}\dot{\omega}_i + \frac{1}{2}\sum_{\substack{j=1 \\ j\neq k}}^{3} c_{kj}^{*}\dot{\omega}_j + c_{kk}^{*}\dot{\omega}_k$$
$$= \sum_{\substack{i=1 \\ i\neq k}}^{3} c_{ik}^{*}\dot{\omega}_i + c_{kk}^{*}\dot{\omega}_k \ (\because c_{ik}^{*} = c_{kj}^{*})$$
$$= \sum_{i=1}^{3} c_{ik}^{*}\dot{\omega}_i$$
$$\frac{d}{dt}(\frac{\partial L}{\partial \dot{\omega}_k}) = \sum_{i=1}^{3}\frac{d}{dt}(c_{ik}^{*})\dot{\omega}_i + \sum_{i=1}^{3} c_{ik}^{*}\ddot{\omega}_i$$
$$= -\sum_{i=1}^{3} c_{ik}^{**}(\dot{\omega}_i - \dot{\omega}_k)\dot{\omega}_i + \sum_{i=1}^{3} c_{ik}^{*}\ddot{\omega}_i$$

where

$$c_{ik}^{**} = c_{ik}\sin(\omega_i - \omega_k). \qquad \text{(B.6)}$$

Second, we find $\frac{\partial L}{\partial \omega_k}$.

$$\frac{\partial L}{\partial \omega_k} = -\frac{1}{2}\sum_{i,j=1}^{3} c_{ij}^{**}\dot{\omega}_i\dot{\omega}_j\frac{d}{d\omega_k}(\omega_i - \omega_j) + p_k\sin\omega_k$$
$$= -\frac{1}{2}\sum_{j=1}^{3} c_{kj}^{**}\dot{\omega}_k\dot{\omega}_j + \frac{1}{2}\sum_{i=1}^{3} c_{ik}^{**}\dot{\omega}_i\dot{\omega}_k + p_k\sin\omega_k$$
$$= \sum_{i=1}^{3} c_{ik}^{**}\dot{\omega}_i\dot{\omega}_k + p_k\sin\omega_k \ (\because c_{ik}^{**} = -c_{kj}^{**})$$

Then, Lagrange's equations are obtained as follows:

$$\therefore \frac{d}{dt}(\frac{\partial L}{\partial \dot{\omega}_k}) - \frac{\partial L}{\partial \omega_k} = \sum_{i=1}^{3} c_{ik}^{*}\ddot{\omega}_i - \sum_{i=1}^{3} c_{ik}^{**}\dot{\omega}_i^{\,2} - p_k\sin\omega_k = 0.$$

The mathematical equations of the three angle model for the swing phase are given as

$$\sum_{i=1}^{3} c_{ki}^{*}\ddot{\omega}_i + \sum_{i=1}^{3} c_{ki}^{**}\dot{\omega}_i^{\,2} = p_k\sin\omega_k (k = 1,2,3)$$

or

$$\begin{aligned} c_{11}^{*}\ddot{\theta} + c_{12}^{*}\ddot{\phi} + c_{13}^{*}\ddot{\sigma} + c_{12}^{**}\dot{\phi}^2 + c_{13}^{**}\dot{\sigma}^2 &= p_1 \sin\theta \\ c_{21}^{*}\ddot{\theta} + c_{22}^{*}\ddot{\phi} + c_{23}^{*}\ddot{\sigma} + c_{21}^{**}\dot{\theta}^2 + c_{23}^{**}\dot{\sigma}^2 &= p_2 \sin\phi \\ c_{31}^{*}\ddot{\theta} + c_{32}^{*}\ddot{\phi} + c_{33}^{*}\ddot{\sigma} + c_{31}^{**}\dot{\theta}^2 + c_{32}^{**}\dot{\phi}^2 &= p_3 \sin\sigma \ . \end{aligned} \tag{B.7}$$

We can rewrite as follows:

$$\begin{aligned} c_{11}^{*}\ddot{\theta} + c_{12}^{*}\ddot{\phi} + c_{13}^{*}\ddot{\sigma} &= -c_{12}^{**}\dot{\phi}^2 - c_{13}^{**}\dot{\sigma}^2 + p_1 \sin\theta \\ c_{21}^{*}\ddot{\theta} + c_{22}^{*}\ddot{\phi} + c_{23}^{*}\ddot{\sigma} &= -c_{21}^{**}\dot{\theta}^2 - c_{23}^{**}\dot{\sigma}^2 + p_2 \sin\phi \\ c_{31}^{*}\ddot{\theta} + c_{32}^{*}\ddot{\phi} + c_{33}^{*}\ddot{\sigma} &= -c_{31}^{**}\dot{\theta}^2 - c_{32}^{**}\dot{\phi}^2 + p_3 \sin\sigma \ . \end{aligned} \tag{B.8}$$

B.2 Joint Viscous Effects

There are three joints in the system. They are ankle, hip and knee joints, of which the joint viscous coefficients are a, b and c, respectively. The joint viscous forces can be found (Wells 1967, 61), and the dynamic equations are obtained as follows:

$$\begin{aligned} c_{11}^{*}\ddot{\theta} + c_{12}^{*}\ddot{\phi} + c_{13}^{*}\ddot{\sigma} &= -c_{12}^{**}\dot{\phi}^2 - c_{13}^{**}\dot{\sigma}^2 + p_1 \sin\theta - a\dot{\theta} - b(\dot{\theta} - \dot{\phi}) \\ c_{21}^{*}\ddot{\theta} + c_{22}^{*}\ddot{\phi} + c_{23}^{*}\ddot{\sigma} &= -c_{21}^{**}\dot{\theta}^2 - c_{23}^{**}\dot{\sigma}^2 + p_2 \sin\phi - b(\dot{\phi} - \dot{\theta}) - c(\dot{\phi} - \dot{\sigma}) \\ c_{31}^{*}\ddot{\theta} + c_{32}^{*}\ddot{\phi} + c_{33}^{*}\ddot{\sigma} &= -c_{31}^{**}\dot{\theta}^2 - c_{32}^{**}\dot{\phi}^2 + p_3 \sin\sigma - c(\dot{\sigma} - \dot{\phi}) \ . \end{aligned} \tag{B.9}$$

B.3 Double-Support Phase

There is a constraint that the toe of the swing leg is fixed on the ground during the double-support phase. This constraint gives one more independent in the dynamic variables(θ, ϕ, σ) equation of the mathematical model for the double-support. The constraint can be expressed as follows:

$$\begin{aligned} L_f - S_L &= -L_l \sin\theta + L_t \sin\phi + L_s \sin\sigma + L_f \cos\alpha \quad &&\text{:(x - coordinate of the toe)} \\ 0 &= L_l \cos\theta - L_t \cos\phi - L_s \cos\sigma + L_f \sin\alpha \quad &&\text{:(y - coordinate of the toe)} \end{aligned}$$

where L_f is the foot length, S_L is the step length, and α is defined as in Figure B.1.

After rearranging equations, we get

$$\begin{aligned} L_f \cos\alpha &= L_l \sin\theta - L_t \sin\phi - L_s \sin\sigma + L_f - S_L \\ L_f \sin\alpha &= -L_l \cos\theta + L_t \cos\phi + L_s \cos\sigma \ . \end{aligned}$$

Squaring and adding both equations, we get

$$\begin{aligned} L_f^2 &= (L_l \sin\theta - L_t \sin\phi - L_s \sin\sigma + L_f - S_L)^2 + (-L_l \cos\theta + L_t \cos\phi + L_s \cos\sigma)^2 \\ &= L_l^2 + L_t^2 + L_s^2 - 2L_l L_t \cos(\theta-\phi) - 2L_l L_s \cos(\theta-\sigma) + 2L_t L_s \cos(\phi-\sigma) \\ &\quad + 2(L_f - S_L)(L_l \sin\theta - L_t \sin\phi - L_s \sin\sigma) + L_f^2 - 2L_f S_L + S_L^2 \end{aligned}$$

Removing $L_f{}^2$ from both sides, we get

$$\begin{aligned} h(\theta,\phi,\sigma) &= L_l^2 + L_t^2 + L_s^2 \\ &\quad - 2L_l L_t \cos(\theta-\phi) - 2L_l L_s \cos(\theta-\sigma) + 2L_t L_s \cos(\phi-\sigma) \\ &\quad + 2(L_f - S_L)(L_l \sin\theta - L_t \sin\phi - L_s \sin\sigma) - 2L_f S_L + S_L^2 \\ &= 0 \end{aligned} \tag{B.10}$$

If we consider the constraint $h(\theta, \phi, \sigma) = 0$, the mathematical equation for the double-support phase can be derived as follows:

$$\begin{aligned} c_{11}^*\ddot{\theta} + c_{12}^*\ddot{\phi} + c_{13}^*\ddot{\sigma} &= -c_{12}^{**}\dot{\phi}^2 - c_{13}^{**}\dot{\sigma}^2 + \lambda\frac{\partial h}{\partial\theta} + p_1 \sin\theta - a\dot{\theta} - b(\dot{\theta}-\dot{\phi}) \\ c_{21}^*\ddot{\theta} + c_{22}^*\ddot{\phi} + c_{23}^*\ddot{\sigma} &= -c_{21}^{**}\dot{\theta}^2 - c_{23}^{**}\dot{\sigma}^2 + \lambda\frac{\partial h}{\partial\phi} + p_2 \sin\phi - b(\dot{\phi}-\dot{\theta}) - c(\dot{\phi}-\dot{\sigma}) \\ c_{31}^*\ddot{\theta} + c_{32}^*\ddot{\phi} + c_{33}^*\ddot{\sigma} &= -c_{31}^{**}\dot{\theta}^2 - c_{32}^{**}\dot{\phi}^2 + \lambda\frac{\partial h}{\partial\sigma} + p_3 \sin\sigma - c(\dot{\sigma}-\dot{\phi}) \end{aligned} \tag{B.11}$$

where

$$\begin{aligned} \frac{\partial h}{\partial\theta} &= 2L_l L_t \sin(\theta-\phi) + 2L_l L_s \sin(\theta-\sigma) + 2(L_f - S_L)L_l \cos\theta \\ \frac{\partial h}{\partial\phi} &= -2L_l L_t \sin(\theta-\phi) - 2L_t L_s \sin(\phi-\sigma) - 2(L_f - S_L)L_t \cos\phi \\ \frac{\partial h}{\partial\sigma} &= -2L_l L_s \sin(\theta-\sigma) + 2L_t L_s \sin(\phi-\sigma) - 2(L_f - S_L)L_s \cos\sigma \end{aligned} \tag{B.12}$$

and λ is the Lagrange multiplier(Greenwood 1977, 55). We need one more equation to solve the system with a constraint because one more variable λ is introduced into the system. To find the necessary equation we differentiate the constraint $h(\theta, \phi, \sigma) = 0$ twice.

$$\begin{aligned} \dot{h}(\theta,\phi,\sigma,\dot{\theta},\dot{\phi},\dot{\sigma}) &= 2L_l L_t \sin(\theta-\phi)\cdot(\dot{\theta}-\dot{\phi}) + 2L_l L_s \sin(\theta-\sigma)\cdot(\dot{\theta}-\dot{\sigma}) \\ &\quad - 2L_t L_s \sin(\phi-\sigma)\cdot(\dot{\phi}-\dot{\sigma}) \\ &\quad + 2(L_f - S_L)(L_l \cos\theta\cdot\dot{\theta} - L_t \cos\phi\cdot\dot{\phi} - L_s \cos\sigma\cdot\dot{\sigma}) \end{aligned}$$

$$\begin{aligned}\ddot{h}(\theta,\phi,\sigma,\dot{\theta},\dot{\phi},\dot{\sigma},\ddot{\theta},\ddot{\phi},\ddot{\sigma}) &= 2L_lL_t\cos(\theta-\phi)\cdot(\dot{\theta}-\dot{\phi})^2 + 2L_lL_t\sin(\theta-\phi)\cdot(\ddot{\theta}-\ddot{\phi}) \\ &\quad + 2L_lL_s\cos(\theta-\sigma)\cdot(\dot{\theta}-\dot{\sigma})^2 + 2L_lL_s\sin(\theta-\sigma)\cdot(\ddot{\theta}-\ddot{\sigma}) \\ &\quad - 2L_tL_s\cos(\phi-\sigma)\cdot(\dot{\phi}-\dot{\sigma})^2 - 2L_tL_s\sin(\phi-\sigma)\cdot(\ddot{\phi}-\ddot{\sigma}) \\ &\quad + 2(L_f-S_L)(-L_l\sin\theta\cdot\dot{\theta}^2 + L_t\sin\phi\cdot\dot{\phi}^2 + L_s\sin\sigma\cdot\dot{\sigma}^2) \\ &\quad + 2(L_f-S_L)(L_l\cos\theta\cdot\ddot{\theta} - L_t\cos\phi\cdot\ddot{\phi} - L_s\cos\sigma\cdot\ddot{\sigma}) \\ &= 0\end{aligned}$$

Rearranging terms, we get

$$\begin{aligned}&\{2L_lL_t\sin(\theta-\phi) + 2L_lL_s\sin(\theta-\sigma) + 2(L_f-S_L)L_l\cos\theta\}\ddot{\theta} \\ &+\{-2L_lL_t\sin(\theta-\phi) - 2L_tL_s\sin(\phi-\sigma) - 2(L_f-S_L)L_t\cos\phi\}\ddot{\phi} \\ &+\{-2L_lL_s\sin(\theta-\sigma) + 2L_tL_s\sin(\phi-\sigma) - 2(L_f-S_L)L_s\cos\sigma\}\ddot{\sigma} \\ &= -2L_lL_t\cos(\theta-\phi)\cdot(\dot{\theta}-\dot{\phi})^2 - 2L_lL_s\cos(\theta-\sigma)\cdot(\dot{\theta}-\dot{\sigma})^2 \\ &+ 2L_tL_s\cos(\phi-\sigma)\cdot(\dot{\phi}-\dot{\sigma})^2 \\ &- 2(L_f-S_L)(-L_l\sin\theta\cdot\dot{\theta}^2 + L_t\sin\phi\cdot\dot{\phi}^2 + L_s\sin\sigma\cdot\dot{\sigma}^2)\,.\end{aligned} \tag{B.13}$$

Let

$$\begin{aligned}h_1 &= 2L_lL_t\sin(\theta-\phi) + 2L_lL_s\sin(\theta-\sigma) + 2(L_f-S_L)L_l\cos\theta \\ h_2 &= -2L_lL_t\sin(\theta-\phi) - 2L_tL_s\sin(\phi-\sigma) - 2(L_f-S_L)L_t\cos\phi \\ h_3 &= -2L_lL_s\sin(\theta-\sigma) + 2L_tL_s\sin(\phi-\sigma) - 2(L_f-S_L)L_s\cos\sigma\end{aligned} \tag{B.14}$$

$$\begin{aligned}H &= -2L_lL_t\cos(\theta-\phi)\cdot(\dot{\theta}-\dot{\phi})^2 - 2L_lL_s\cos(\theta-\sigma)\cdot(\dot{\theta}-\dot{\sigma})^2 \\ &\quad + 2L_tL_s\cos(\phi-\sigma)\cdot(\dot{\phi}-\dot{\sigma})^2 \\ &\quad - 2(L_f-S_L)(-L_l\sin\theta\cdot\dot{\theta}^2 + L_t\sin\phi\cdot\dot{\phi}^2 + L_s\sin\sigma\cdot\dot{\sigma}^2)\,.\end{aligned} \tag{B.15}$$

Then, equation(B.13) can be written as follows:

$$h_1\ddot{\theta} + h_2\ddot{\phi} + h_3\ddot{\sigma} = H\,. \tag{B.16}$$

After comparing equations(B.12) and (B.14), we can find

$$\begin{aligned}\nabla h &= \begin{bmatrix}\dfrac{\partial h}{\partial\theta_1} & \dfrac{\partial h}{\partial\theta_2} & \dfrac{\partial h}{\partial\theta_3}\end{bmatrix} \\ &= \begin{bmatrix}h_1 & h_2 & h_3\end{bmatrix}.\end{aligned} \tag{B.17}$$

If we put together equations(B.11) and (B.16) in matrix form, and use the property of equation(B.17), the mathematical equations for the double-support phase can be obtained as follows:

$$\begin{bmatrix} c_{11}^{*} & c_{12}^{*} & c_{13}^{*} & -h_1 \\ c_{21}^{*} & c_{22}^{*} & c_{23}^{*} & -h_2 \\ c_{31}^{*} & c_{32}^{*} & c_{33}^{*} & -h_3 \\ h_1 & h_2 & h_3 & 0 \end{bmatrix} \begin{bmatrix} \ddot{\theta} \\ \ddot{\phi} \\ \ddot{\sigma} \\ \lambda \end{bmatrix} = \begin{bmatrix} -c_{12}^{**}\dot{\phi}^2 - c_{13}^{**}\dot{\sigma}^2 + p_1 \sin\theta - a\dot{\theta} - b(\dot{\theta} - \dot{\phi}) \\ -c_{21}^{**}\dot{\theta}^2 - c_{23}^{**}\dot{\sigma}^2 + p_2 \sin\phi - b(\dot{\phi} - \dot{\theta}) - c(\dot{\phi} - \dot{\sigma}) \\ -c_{31}^{**}\dot{\theta}^2 - c_{32}^{**}\dot{\phi}^2 + p_3 \sin\sigma - c(\dot{\sigma} - \dot{\phi}) \\ H \end{bmatrix} \quad \text{(B.18)}$$

APPENDIX C

GENERALIZED 2-D MATHEMATICAL WALKING MODEL

C.1 Relation Matrix

Let us assume that a system consists of many connected segments and point masses on segments. The relation matrix **R** shows the relationship of connection between segments of the system. Each row of **R** represents a point mass of the system, and has the information about the path from the origin of the system to the point mass. Each column represents a segment, and has the information about the usage of the segment for every path to point masses. For a system with S segments and P point masses, the relation matrix **R** has the form as

$$\mathbf{R} = \begin{bmatrix} r_{11} & r_{12} & \cdots & r_{1S} \\ r_{21} & r_{22} & \cdots & r_{2S} \\ \vdots & \vdots & \ddots & \vdots \\ r_{P1} & r_{P2} & \cdots & r_{PS} \end{bmatrix}.$$

The path from the origin to the p-th point mass may consist of many segments. Let us assume that the p-th point mass is on the i-th segment of the system. Then, the i-th segment is the last segment of the path, and all other segments of the path are called as forefather segments of the i-th segment. Using the above information each element r_{ps} of **R** can be determined as follows:

$$r_{ps} = \begin{cases} z_p & \text{if } s = i, \\ L_s & \text{if the } s\text{-th segment is a forefather segment of the } i\text{-th segment,} \\ 0 & \text{otherwise.} \end{cases} \quad \text{(C.1)}$$

where

z_p : mass center of the p-th particle from the joint with its forefather segment

L_s : length of the s-th segment

p = 1, 2, ... P (P : total number of particles)

s = 1, 2, ... S (S : total number of segments).

After the relation matrix **R** is determined, x- and y-coordinates of point masses can be written as follows:

$$\mathbf{x} = \begin{bmatrix} x_1 & x_2 & \cdots & x_P \end{bmatrix}^T = \mathbf{R} \cdot \begin{bmatrix} \cos\theta_1 & \cos\theta_2 & \cdots & \cos\theta_S \end{bmatrix}^T \qquad \text{(C.2)}$$

$$\mathbf{y} = \begin{bmatrix} y_1 & y_2 & \cdots & y_P \end{bmatrix}^T = \mathbf{R} \cdot \begin{bmatrix} \sin\theta_1 & \sin\theta_2 & \cdots & \sin\theta_S \end{bmatrix}^T \qquad \text{(C.3)}$$

where

θ_s : angle of the s-th segment with respect to the horizontal right direction (counterclockwise).

An example is given to show the method to obtain a relation matrix. There are four segments and five point masses in the example as shown in Figure C.1. Each segment has one mass, but the 4-th segment has two masses. The mass centers of two point masses on the 4-th segment are expressed as $m_{4,1}$ and $m_{4,2}$, and center of masses are expressed as $z_{4,1}$ and $z_{4,2}$.

For the below diagram, the relation matrix can be obtained according to equation(C.1). It is given as follows:

$$\mathbf{R} = \begin{bmatrix} z_1 & 0 & 0 & 0 & 0 \\ L_1 & z_2 & 0 & 0 & 0 \\ L_1 & L_2 & z_3 & 0 & 0 \\ L_1 & 0 & 0 & z_{4,1} & 0 \\ L_1 & 0 & 0 & z_{4,2} & 0 \\ L_1 & 0 & 0 & L_4 & z_5 \end{bmatrix}.$$

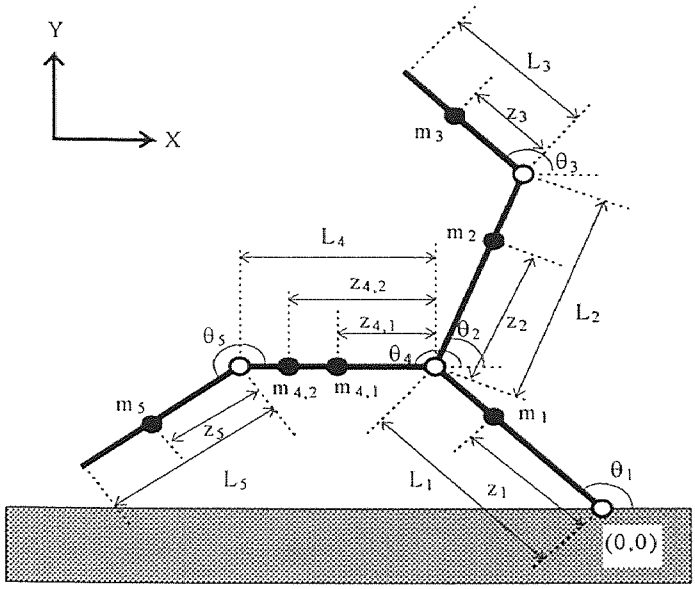

Figure C.1 A generalized 2-D system with 6 point masses and 5 segments

From equation(C.2) and (C.3), x- and y-component of the velocity of point masses can be determined as follows:

$$\dot{\mathbf{x}} = \begin{bmatrix} \dot{x}_1 & \dot{x}_2 & \cdots & \dot{x}_P \end{bmatrix}^T = -\mathbf{R} \cdot \underline{\sin\Theta} \cdot \dot{\underline{\theta}} \tag{C.4}$$

$$\dot{\mathbf{y}} = \begin{bmatrix} \dot{y}_1 & \dot{y}_2 & \cdots & \dot{y}_P \end{bmatrix}^T = \mathbf{R} \cdot \underline{\cos\Theta} \cdot \dot{\underline{\theta}} \tag{C.5}$$

where

$$\underline{\cos\Theta} = \begin{bmatrix} \cos\theta_1 & 0 & \cdots & 0 \\ 0 & \cos\theta_2 & \cdots & 0 \\ \vdots & \vdots & \ddots & \vdots \\ 0 & 0 & \cdots & \cos\theta_S \end{bmatrix}$$

$$\underline{\sin\Theta} = \begin{bmatrix} \sin\theta_1 & 0 & \cdots & 0 \\ 0 & \sin\theta_2 & \cdots & 0 \\ \vdots & \vdots & \ddots & \vdots \\ 0 & 0 & \cdots & \sin\theta_S \end{bmatrix}$$

$$\underline{\dot{\theta}} = \begin{bmatrix} \dot{\theta}_1 & \dot{\theta}_2 & \cdots & \dot{\theta}_S \end{bmatrix}^T .$$

C.2 Potential Energy

The total potential energy of a system can be calculated by adding up potential energies of all the point masses of the system.

$$\begin{aligned} P &= \sum_{p=1}^{P} g m_p y_p \\ &= g \mathbf{y}^T \mathbf{M} \begin{bmatrix} 1 & \cdots & 1 \end{bmatrix}_{1xP}^T \\ &= g \begin{bmatrix} \sin\theta_1 & \cdots & \sin\theta_S \end{bmatrix} \cdot \mathbf{R}^T \cdot \mathbf{M} \cdot \begin{bmatrix} 1 & \cdots & 1 \end{bmatrix}_{1xP}^T \\ &= \begin{bmatrix} \sin\theta_1 & \cdots & \sin\theta_S \end{bmatrix} \cdot \begin{bmatrix} p_i \end{bmatrix}_{Sx1} \end{aligned}$$

$$\therefore P = \sum_{i=1}^{S} p_i \sin\theta_i \qquad \text{(C.6)}$$

where

$$\mathbf{M} = \begin{bmatrix} m_1 & 0 & \cdots & 0 \\ 0 & m_2 & \cdots & 0 \\ \vdots & \vdots & \ddots & \\ 0 & 0 & \cdots & m_P \end{bmatrix} .$$

C.3 Kinetic Energy

The total kinetic energy of a system can be calculated by adding up kinetic energies of all the point masses of the system. When the mass and the velocity of the p-th point mass are m_p and v_p, respectively, the kinetic energy of the point mass is given as $e_p = (1/2)\, m_p v_p^2$. If

v_p^2 is substituted by $\dot{x}_p^2 + \dot{y}_p^2$, the total kinetic energy K of a system with P point masses can be written as follows:

$$\begin{aligned} K &= \frac{1}{2}\sum_{p=1}^{P} m_p(\dot{x}_p^2 + \dot{y}_p^2) \\ &= \frac{1}{2}(\dot{\mathbf{x}}^T \cdot \mathbf{M} \cdot \dot{\mathbf{x}} + \dot{\mathbf{y}}^T \cdot \mathbf{M} \cdot \dot{\mathbf{y}}) \end{aligned} \tag{C.6}$$

Substitute equation(C.4) and (C.5) into equation(C.6).

$$\begin{aligned} K &= \frac{1}{2}(\dot{\underline{\theta}}^T \cdot \underline{\sin\Theta}^T \cdot \mathbf{R}^T \cdot \mathbf{M} \cdot \mathbf{R} \cdot \underline{\sin\Theta} \cdot \dot{\underline{\theta}} + \dot{\underline{\theta}}^T \cdot \underline{\cos\Theta}^T \cdot \mathbf{R}^T \cdot \mathbf{M} \cdot \mathbf{R} \cdot \underline{\cos\Theta} \cdot \dot{\underline{\theta}}) \\ &= \frac{1}{2}(\dot{\underline{\theta}}^T \cdot \underline{\sin\Theta}^T \cdot \mathbf{C} \cdot \underline{\sin\Theta} \cdot \dot{\underline{\theta}} + \dot{\underline{\theta}}^T \cdot \underline{\cos\Theta}^T \cdot \mathbf{C} \cdot \underline{\cos\Theta} \cdot \dot{\underline{\theta}}) \\ &= \frac{1}{2}\dot{\underline{\theta}}^T \cdot (\underline{\sin\Theta}^T \cdot \mathbf{C} \cdot \underline{\sin\Theta} + \underline{\cos\Theta}^T \cdot \mathbf{C} \cdot \underline{\cos\Theta}) \cdot \dot{\underline{\theta}} \end{aligned}$$

where

$$\begin{aligned} \mathbf{C} &= \mathbf{R}^T \cdot \mathbf{M} \cdot \mathbf{R} \\ &= [c_{ij}]_{S \times S} \end{aligned}$$

$$c_{ij} = \sum_{p=1}^{P} m_p r_{pi} r_{pj} \quad .$$

Then, the total kinetic energy can be written in a compact form as

$$\therefore K = \frac{1}{2}\dot{\underline{\theta}}^T \cdot \mathbf{C}^* \cdot \dot{\underline{\theta}} \tag{C.7}$$

where

$$\begin{aligned} \mathbf{C}^* &= \underline{\sin\Theta}^T \cdot \mathbf{C} \cdot \underline{\sin\Theta} + \underline{\cos\Theta}^T \cdot \mathbf{C} \cdot \underline{\cos\Theta} \\ &= [c_{ij}\cos(\theta_i - \theta_j)]_{S \times S} \\ &= [c_{ij}^*]_{S \times S} \end{aligned}$$

$$c_{ij}^* = c_{ij}\cos(\theta_i - \theta_j) \quad .$$

C.4 Lagrangian Equations

For a system of S indenpendent variables, the Lagrangian equations take the form(Wells 1967, 60)

$$\frac{d}{dt}\left(\frac{\partial K}{\partial \dot{\theta}_s}\right) - \frac{\partial K}{\partial \theta_s} = F_{\theta_s} \tag{C.8}$$

where $s = 1, 2, \ldots, S$, and generalized forces F_{θ_s} are given for two dimensional space as

$$F_{\theta_s} = \sum_{p=1}^{P}\left(F_{x_p}\frac{\partial x_p}{\partial \theta_s} + F_{y_p}\frac{\partial y_p}{\partial \theta_s}\right) \tag{C.9}$$

Apply equation(C.7) to equation(C.8).

$$\frac{\partial K}{\partial \dot{\theta}_s} = \frac{1}{2}\sum_{i=1}^{S}\left\{c^*_{si}\dot{\theta}_i + c^*_{is}\dot{\theta}_i\right\}$$

$$= \sum_{i=1}^{S} c^*_{si}\dot{\theta}_i \qquad (\because c^*_{si} = c^*_{is})$$

$$\therefore \frac{d}{dt}\left(\frac{\partial K}{\partial \dot{\theta}_s}\right) = \sum_{i=1}^{S}\left\{-c_{si}\sin(\theta_s - \theta_i)\cdot(\dot{\theta}_s - \dot{\theta}_i)\cdot\dot{\theta}_i + c^*_{si}\ddot{\theta}_i\right\}$$

$$\frac{\partial K}{\partial \theta_s} = \frac{1}{2}\sum_{i=1}^{S}\left\{-c_{si}\sin(\theta_s - \theta_i)\cdot\dot{\theta}_s\cdot\dot{\theta}_i + c_{is}\sin(\theta_i - \theta_s)\cdot\dot{\theta}_i\cdot\dot{\theta}_s\right\}$$

$$= -\sum_{i=1}^{S} c_{si}\sin(\theta_s - \theta_i)\cdot\dot{\theta}_s\cdot\dot{\theta}_i$$

$$(\because c_{si} = c_{is})$$

Using the above results, re-write the equation(C.8) as

$$\sum_{i=1}^{S}\left\{-c_{si}\sin(\theta_s - \theta_i)\cdot(\dot{\theta}_s - \dot{\theta}_i)\cdot\dot{\theta}_i + c^*_{si}\ddot{\theta}_i\right\} - \left\{-\sum_{i=1}^{S} c_{si}\sin(\theta_s - \theta_i)\cdot\dot{\theta}_s\cdot\dot{\theta}_i\right\} = F_{\theta_s}$$

$$\therefore \sum_{i=1}^{S}\left\{c^*_{si}\ddot{\theta}_i + c_{si}\sin(\theta_s - \theta_i)\cdot\dot{\theta}_i^2\right\} = F_{\theta_s} \tag{C.10}$$

Equation(C.10) can be re-written in matrix form as

$$\mathbf{C}^{*}\ddot{\underline{\theta}} + \mathbf{C}^{**}\dot{\underline{\theta}}^{2} = \mathbf{F} \tag{C.11}$$

where

$$\mathbf{C}^{**} = \left[c_{ij}\sin(\theta_i - \theta_j)\right]_{S\times S} = \left[c_{ij}^{**}\right]_{S\times S}$$

$$\mathbf{F} = \begin{bmatrix} F_{\theta_1} & F_{\theta_2} & \cdots & F_{\theta_S} \end{bmatrix}^T$$

$$\dot{\underline{\theta}} = \begin{bmatrix} \dot{\theta}_1 & \dot{\theta}_2 & \cdots & \dot{\theta}_S \end{bmatrix}^T$$

$$\ddot{\underline{\theta}} = \begin{bmatrix} \ddot{\theta}_1 & \ddot{\theta}_2 & \cdots & \ddot{\theta}_S \end{bmatrix}^T .$$

C.4.1 Generalized Forces

It is assumed that there are two generalized forces in the walking system. They are gravitational and joint viscous forces. Therefore, generalized forces of the system can be written as

$$\mathbf{F} = \mathbf{F}_{grv} + \mathbf{F}_{vis}$$

where

$$\mathbf{F}_{grv} = \begin{bmatrix} F_{grv,\theta_1} & F_{grv,\theta_2} & \cdots & F_{grv,\theta_S} \end{bmatrix}^T$$

$$\mathbf{F}_{vis} = \begin{bmatrix} F_{vis,\theta_1} & F_{vis,\theta_2} & \cdots & F_{vis,\theta_S} \end{bmatrix}^T .$$

C.4.1.1 Generalized Gravitational Forces According to equation(C.9) the generalized gravitational forces can be written as

$$F_{grv,\theta_s} = \sum_{p=1}^{P}(F_{x_p}\frac{\partial x_p}{\partial \theta_s} + F_{y_p}\frac{\partial y_p}{\partial \theta_s})$$

$$= -g\sum_{p=1}^{P} m_p \frac{\partial y_p}{\partial \theta_s}$$

$$(\because F_{x_p} = 0,\ F_{y_p} = -gm_p)$$

$$= -g\sum_{p=1}^{P} m_p r_{ps}\cos\theta_s$$

$$(\because \text{from equation(C.3)},\ \frac{\partial y_p}{\partial \theta_s} = r_{ps}\cos\theta_s)\ .$$

Therefore, the generalized gravitational forces can be written in matrix form as

$$\therefore \mathbf{F}_{grv} = \left[F_{grv,\theta_1} \quad F_{grv,\theta_2} \quad \cdots \quad F_{grv,\theta_S}\right]^T$$

$$= -g\left[\sum_{p=1}^{P} m_p r_{p1}\cos\theta_1 \quad \sum_{p=1}^{P} m_p r_{p2}\cos\theta_2 \quad \cdots \quad \sum_{p=1}^{P} m_p r_{pS}\cos\theta_S\right]^T$$

$$= -g\cdot\underline{\cos\Theta}^T\cdot\left[\sum_{p=1}^{P} m_p r_{p1} \quad \sum_{p=1}^{P} m_p r_{p2} \quad \cdots \quad \sum_{p=1}^{P} m_p r_{pS}\right]^T$$

$$= -g\cdot\underline{\cos\Theta}\cdot\mathbf{R}^T\cdot\left[m_1 \quad m_2 \quad \cdots \quad m_P\right]^T$$

$$(\because \underline{\cos\Theta}^T = \underline{\cos\Theta})$$

$$= -g\cdot\underline{\cos\Theta}\cdot\mathbf{R}^T\cdot\mathbf{M}\cdot\left[1 \quad 1 \quad \cdots \quad 1\right]^T$$

$$\therefore \mathbf{F}_{grv} = -\underline{\cos\Theta}\cdot\mathbf{P} \tag{C.12}$$

where

$$\mathbf{P} = g\cdot\mathbf{R}^T\cdot\mathbf{M}\cdot\left[1 \quad 1 \quad \cdots \quad 1\right]^T_{1\times P}$$

$$= [p_i]_{S\times 1}\ .$$

C.4.1.2 Generalized Joint Viscous Forces A simple diagram of segments is drawn in Figure C.2 to explain the method how to get the generalized joint viscous forces(Wells 1967, 61).

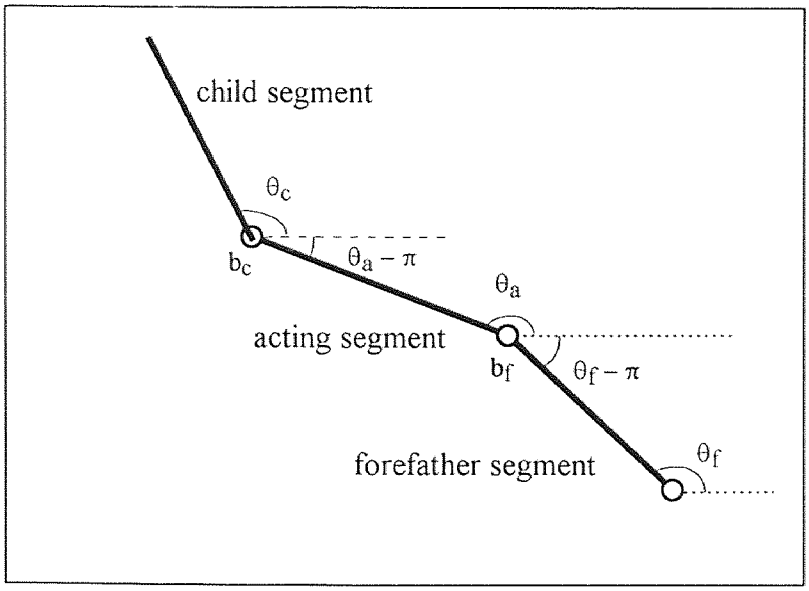

Figure C.2 Connection diagram of child, acting and forefather segments

b_f : joint viscous coefficient between the acting and the forefather segments
b_c : joint viscous coefficient between the acting and the child segments
θ_s : angle of the acting segment from the horizontal line
θ_f : angle of the forefather segment from the horizontal line
θ_c : angle of the child segment from the horizontal line

When all coordinates of a system are varied simultaneously, the total work δW_{total} can be written in the form

$$\delta W_{total} = \left[\cdots\right]_1 \delta\theta_1 + \left[\cdots\right]_2 \delta\theta_2 + \cdots + \left[\cdots\right]_S \delta\theta_S$$

and the bracket $[\ldots]_i$, which is the coefficient of $\delta\theta_i$, is the generalized joint viscous force F_{vis,θ_i}. The angle between the acting and forefather segments can be found as $(\theta_a - \theta_f + \pi)$ in Figure C.2. Therefore, the work δW_{af} done by the joint viscous force between the acting and forefather segments is

$$\delta W_{af} = -b_f(\dot{\theta}_a - \dot{\theta}_f)(\delta\theta_a - \delta\theta_f) \quad . \tag{C.13}$$

There is a negative sign because the joint viscous force is dissipative. Similarly, the work δW_{ac} done by the joint viscous force between the acting and child segments can be obtaind as

$$\delta W_{ac} = -b_c(\dot{\theta}_c - \dot{\theta}_a)(\delta\theta_c - \delta\theta_a) \ . \tag{C.14}$$

Adding the equations (C.13) and (C.14), we get, after collecting terms,

$$\begin{aligned}
\delta W_a &= \delta W_{af} + \delta W_{ac} \\
&= -b_f(\dot{\theta}_a - \dot{\theta}_f)(\delta\theta_a - \delta\theta_f) - b_c(\dot{\theta}_c - \dot{\theta}_a)(\delta\theta_c - \delta\theta_a) \\
&= \left(-b_f(\dot{\theta}_a - \dot{\theta}_f) + b_c(\dot{\theta}_c - \dot{\theta}_a)\right)\delta\theta_a + b_f(\dot{\theta}_a - \dot{\theta}_f)\delta\theta_f - b_c(\dot{\theta}_c - \dot{\theta}_a)\delta\theta_c \\
&= \left(-(b_f + b_c)\dot{\theta}_a + b_f\dot{\theta}_f + b_c\dot{\theta}_c\right)\delta\theta_a + b_f(\dot{\theta}_a - \dot{\theta}_f)\delta\theta_f + b_c(\dot{\theta}_a - \dot{\theta}_c)\delta\theta_c \ .
\end{aligned} \tag{C.15}$$

The coefficient of $\delta\theta_a$ in equation(C.15) is the generalized joint viscous force F_{vis,θ_a} . That is,

$$F_{vis,\theta_a} = -(b_f + b_c)\dot{\theta}_a + b_f\dot{\theta}_f + b_c\dot{\theta}_c \ . \tag{C.16}$$

Many segments may be connected to each joint of the acting segment. Let us assume that n forefather segments are connected to one joint, and m child segments are connected to another joint. Then, the work done by joint viscous forces can be written as

$$\delta W_a = (\delta W_{af1} + \delta W_{af2} + \cdots + \delta W_{afn}) + (\delta W_{ac1} + \delta W_{ac2} + \cdots + \delta W_{acm}) \tag{C.17}$$

where

δW_{af_i}: work done by the joint viscous force between acting and i-th forefather segments
δW_{af_j}: work done by the joint viscous force between acting and j-th child segments .

After applying equations (C.13) and (C.14) into (C.17), and collecting terms, take the coefficient of $\delta\theta_a$. Then, an equation similar to equation (C.16) can be obtained as

$$\begin{aligned} F_{vis,\theta_a} = &-\left\{(b_{f1}+b_{f2}+\cdots+b_{fn})+(b_{c1}+b_{c2}+\cdots+b_{cm})\right\}\dot{\theta}_a \\ &+b_{f1}\dot{\theta}_{f1}+b_{f2}\dot{\theta}_{f2}+\cdots+b_{fn}\dot{\theta}_{fn} \\ &+b_{c1}\dot{\theta}_{c1}+b_{c1}\dot{\theta}_{c1}+\cdots+b_{c1}\dot{\theta}_{c1} \end{aligned} \tag{C.18}$$

where

b_{fi}: joint viscous coefficient between the acting and i-th forefather segments

b_{cj}: joint viscous coefficient between the acting and j-th child segments .

If the acting segment is the s-th segment of the system, of which the total number of segments are S, equation (C.18) can be re-written as

$$F_{vis,\theta_s} = \begin{bmatrix} b_{s1} & b_{s2} & \cdots & b_{sS} \end{bmatrix} \underline{\dot{\theta}}$$

where b_{si} is the viscous coefficient between s-th and i-th segments. From equation(C.18), the following property can be found about b_{si}.

$$b_{ss} = -\sum_{i=0,\, i\neq s}^{S} b_{si} \tag{C.19}$$

where b_{i0} is the joint viscous coefficient between the i-th segment and the origin, and $b_{si=0}$ when there is no joint viscous coupling between s-th and i-th segments.

Then the generalized joint viscous forces can be written as

$$\begin{aligned} \mathbf{F}_{vis} &= \begin{bmatrix} F_{vis,\theta_1} & F_{vis,\theta_2} & \cdots & F_{vis,\theta_S} \end{bmatrix}^T \\ &= \mathbf{B}\cdot\underline{\dot{\theta}} \end{aligned} \tag{C.20}$$

and viscous coefficient matrix **B** is defined as

$$\mathbf{B} = \begin{bmatrix} b_{11} & b_{12} & \cdots & b_{1S} \\ b_{21} & b_{22} & \cdots & b_{2S} \\ \vdots & \vdots & \cdots & \vdots \\ b_{S1} & b_{S2} & \cdots & b_{SS} \end{bmatrix}$$

where b_{ij} satisfies equation(C.19).

C.4.2 Lagrange Equations without Constraints

If equation (C.12) and equation (C.20) are substituted into equation (C.11), the dynamic equations of a non-constrained system can be written as

$$\mathbf{C}^{*} \cdot \underline{\ddot{\theta}} + \mathbf{C}^{**} \cdot \underline{\dot{\theta}}^{2} = -\underline{\cos\Theta} \cdot \mathbf{P} + \mathbf{B} \cdot \underline{\dot{\theta}} \quad . \tag{C.21}$$

Equation (C.21) is used as the mathematical model for the swing phase of a walking cycle.

C.4.3 Lagrange Equations with Constraints

If n constraints are expressed in the form

$$\mathbf{h}(\underline{\theta}) = \mathbf{0} \tag{C.22}$$

where

$$\mathbf{h}(\underline{\theta}) = \begin{bmatrix} h_1(\underline{\theta}) & h_2(\underline{\theta}) & \cdots & h_n(\underline{\theta}) \end{bmatrix}^T$$

$$\mathbf{0} = \underbrace{\begin{bmatrix} 0 & 0 & \cdots & 0 \end{bmatrix}^T}_{n}$$

, the dynamic equations of a constrained system can be written as

$$\mathbf{C}^{*} \cdot \underline{\ddot{\theta}} + \mathbf{C}^{**} \cdot \underline{\dot{\theta}}^{2} = (\nabla \mathbf{h})^{T} \cdot \underline{\lambda} - \underline{\cos\Theta} \cdot \mathbf{P} + \mathbf{B} \cdot \underline{\dot{\theta}} \tag{C.23}$$

where

$$\underline{\lambda} = \begin{bmatrix} \lambda_1 & \lambda_2 & \cdots & \lambda_n \end{bmatrix}^T$$

$$\nabla = \begin{bmatrix} \dfrac{\partial}{\partial \theta_1} & \dfrac{\partial}{\partial \theta_2} & \cdots & \dfrac{\partial}{\partial \theta_S} \end{bmatrix} .$$

Here, λ's are Lagrange multipliers(Greenwood 1977, 55). Because of constraints, n new variables(λ's) are introduced into the system. To solve equation (C.23), n more equations are necessary. For this purpose differentiate equation(C.22).

$$\begin{aligned}\mathbf{h}'(\underline{\theta}) &= \frac{\partial \mathbf{h}}{\partial \theta_1}\dot{\theta}_1 + \frac{\partial \mathbf{h}}{\partial \theta_2}\dot{\theta}_2 + \cdots + \frac{\partial \mathbf{h}}{\partial \theta_S}\dot{\theta}_S \\ &= \nabla \mathbf{h} \cdot \underline{\dot{\theta}} \\ &= \mathbf{0}\end{aligned} \tag{C.24}$$

Differentiate equation(C.24) one more time.

$$\begin{aligned}\mathbf{h}''(\underline{\theta}) &= \frac{d}{dt}(\nabla \mathbf{h}) \cdot \underline{\dot{\theta}} + \nabla \mathbf{h} \cdot \underline{\ddot{\theta}} \\ &= \mathbf{0}\end{aligned} \tag{C.25}$$

$$\begin{aligned}\frac{d}{dt}(\nabla \mathbf{h}) \cdot \underline{\dot{\theta}} &= \left\{ \frac{\partial}{\partial \theta_1}(\nabla \mathbf{h}) \cdot \dot{\theta}_1 + \frac{\partial}{\partial \theta_2}(\nabla \mathbf{h}) \cdot \dot{\theta}_2 + \cdots + \frac{\partial}{\partial \theta_S}(\nabla \mathbf{h}) \cdot \dot{\theta}_S \right\} \cdot \underline{\dot{\theta}} \\ &= \underline{\dot{\theta}}^T \cdot (\nabla^T \cdot \nabla \mathbf{h}) \cdot \underline{\dot{\theta}} \\ &= \underline{\dot{\theta}}^T \cdot \mathbf{H} \cdot \underline{\dot{\theta}}\end{aligned}$$

where

$$\mathbf{H} = \nabla^T \cdot \nabla \mathbf{h}$$

and

$$\nabla^T \cdot \nabla = \begin{bmatrix} \frac{\partial^2}{\partial \theta_1 \partial \theta_1} & \frac{\partial^2}{\partial \theta_1 \partial \theta_2} & \cdots & \frac{\partial^2}{\partial \theta_1 \partial \theta_S} \\ \frac{\partial^2}{\partial \theta_2 \partial \theta_1} & \frac{\partial^2}{\partial \theta_2 \partial \theta_2} & \cdots & \frac{\partial^2}{\partial \theta_2 \partial \theta_S} \\ \vdots & \vdots & \ddots & \vdots \\ \frac{\partial^2}{\partial \theta_S \partial \theta_1} & \frac{\partial^2}{\partial \theta_S \partial \theta_2} & \cdots & \frac{\partial^2}{\partial \theta_S \partial \theta_S} \end{bmatrix}.$$

$\therefore$ From equation(C.25),

$$\nabla \mathbf{h} \cdot \underline{\ddot{\theta}} = -\underline{\dot{\theta}}^T \cdot \mathbf{H} \cdot \underline{\dot{\theta}} \quad . \tag{C.26}$$

Rearrange equation(C.23) and put equations (C.23) and (C.26) together. The dynamic equations of a constrained system can be written as

$$\begin{bmatrix} \mathbf{C}^{*} & -(\nabla \mathbf{h})^{T} \\ \nabla \mathbf{h} & \mathbf{0} \end{bmatrix} \begin{bmatrix} \underline{\ddot{\theta}} \\ \underline{\lambda} \end{bmatrix} = \begin{bmatrix} -\mathbf{C}^{**} \cdot \underline{\dot{\theta}}^{2} - \underline{\cos\Theta} \cdot \mathbf{P} + \mathbf{B} \cdot \underline{\dot{\theta}} \\ -\underline{\dot{\theta}}^{T} \cdot \mathbf{H} \cdot \underline{\dot{\theta}} \end{bmatrix} . \qquad \text{(C.27)}$$

During the double-support phase of a walking cycle, the constraint is that the toe of a foot is on the ground. Because of this constraint, equation(C.27) can be used for the double-support phase. Equation(C.21) is a special case of equation(C.27). Therefore, equation(C.27) can be called as the generalized 2-D walking model.

APPENDIX D

SHOOTING METHOD

To solve the two-point boundary problem we used the shooting method. The flowchart of this method is shown in the figure D.1. Explanation for the flowchart is given below. First, we preapre boundary conditions, which are initial $\underline{\theta}^b(t=0)$ and final $\underline{\theta}^b(t=T)$ configurations of a walking phase. We guess reasonable initial velocities $\underline{\dot{\theta}}(t=0)$ where $\underline{\dot{\theta}}(t=0)$ means $(\dot{\theta}_1, \dot{\theta}_2, \dot{\theta}_3, t=0)$. We solve the problem as an initial value problem, and find $\underline{\theta}(t=T)$. We compute the discrepancy between $\underline{\theta}(t=T)$ and the boundary condition $\underline{\theta}^b(t=T)$. If every element of the discrepancy $\mathbf{e}_0 = \begin{bmatrix} e_{10} & e_{20} & e_{30} \end{bmatrix}^T$ are smaller than some reference value ε, the iteration stops. If the discrepancy is greater than ε, the iteration process continues. We find $\underline{\theta}(t=T)$'s with different initial velocities, which are $(\dot{\theta}_1 + \Delta\dot{\theta}_1, \dot{\theta}_2, \dot{\theta}_3, t=0)$, $(\dot{\theta}_1, \dot{\theta}_2 + \Delta\dot{\theta}_2, \dot{\theta}_3, t=0)$ and $(\dot{\theta}_1, \dot{\theta}_2, \dot{\theta}_3 + \Delta\dot{\theta}_3, t=0)$. From the results we can calculate discrepancy vectors $\mathbf{e}_1 = \begin{bmatrix} e_{11} & e_{21} & e_{31} \end{bmatrix}^T$, $\mathbf{e}_2 = \begin{bmatrix} e_{12} & e_{22} & e_{32} \end{bmatrix}^T$ and $\mathbf{e}_3 = \begin{bmatrix} e_{13} & e_{23} & e_{33} \end{bmatrix}^T$. From these discrepancy vectors we can calculate the sensitivity of the results with respect to initial velocities. The Jacobian matrix **J** has components given by $J_{ij} = \dfrac{\partial e_{ij}}{\partial \dot{\theta}_j} \approx \dfrac{e_{ij} - e_{i0}}{\Delta\dot{\theta}_j}$. From the Jacobian **J**, we predict the amount of change of initial velocities $\delta\underline{\dot{\theta}}$, which are necessary to make the discrepancy zero. With $\delta\underline{\dot{\theta}}$, we find the new guessed velocities $\underline{\dot{\theta}}^{new}(t=0)$ as given by $\underline{\dot{\theta}}^{new}(t=0) = \underline{\dot{\theta}}^{old}(t=0) + \delta\underline{\dot{\theta}}$. With this new initial velocities the iteration process start again. The iteration continues until the criterion are satisfied.

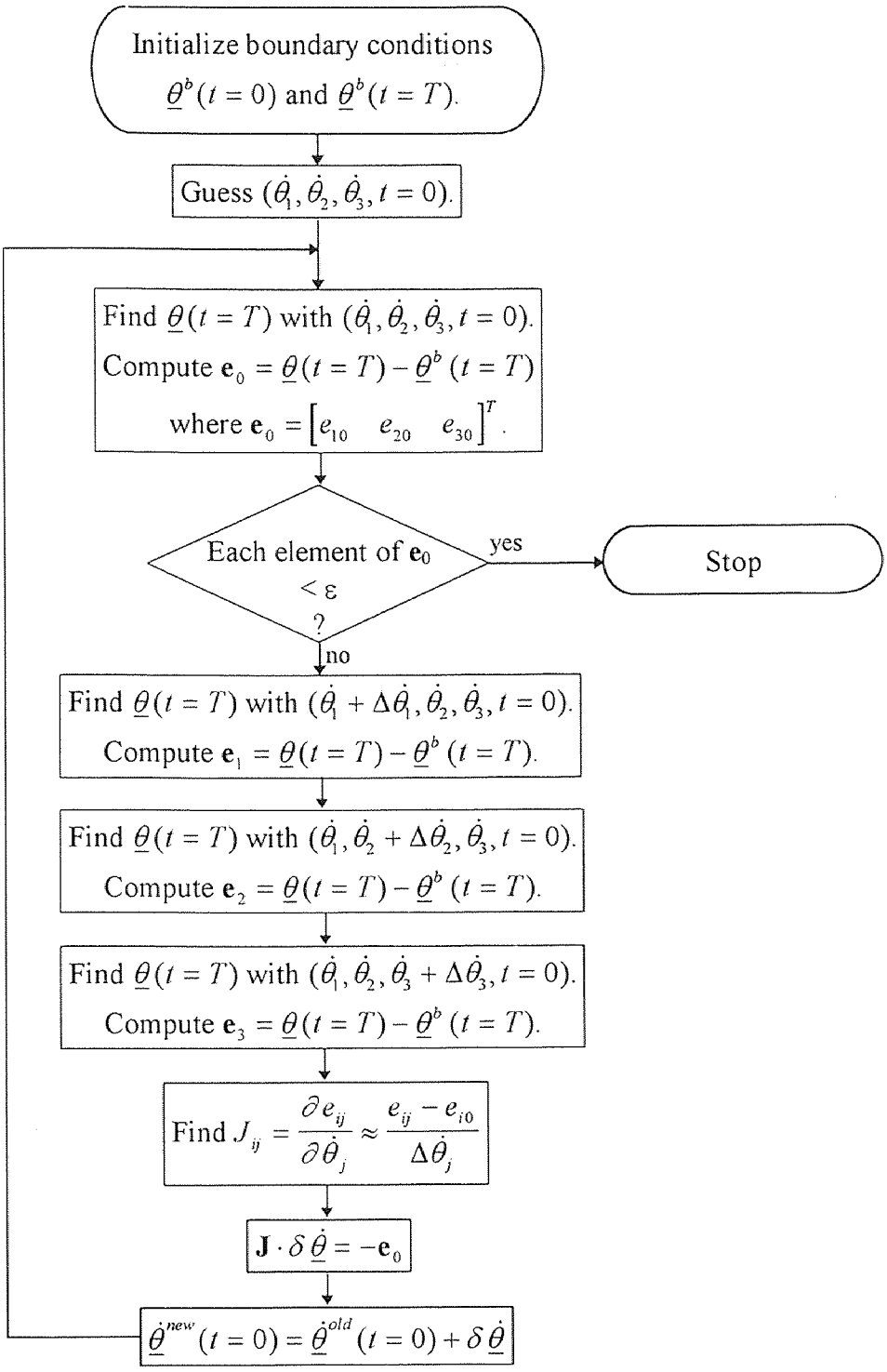

Figure D.1 Flowchart of the shooting method

APPENDIX E

DOWN-HILL SIMPLEX METHOD

The down-hill simplex method which was used to find joint viscous coefficients $\mathbf{b} = (b_1, b_2, b_3)$ is explained below. Here, b_1, b_2 and b_3 are viscous coefficients of the ankle, hip and knee joints, respectively. The simplex method is based on the comparison of the objective function values $E(\mathbf{b})$, which is the difference between the theoretical data and experimental data, at the (n+1) vertices of a general simplex and moving this simplex towards the optimum point. This movement is achieved by three basic operations: reflecton, expansion and contraction.

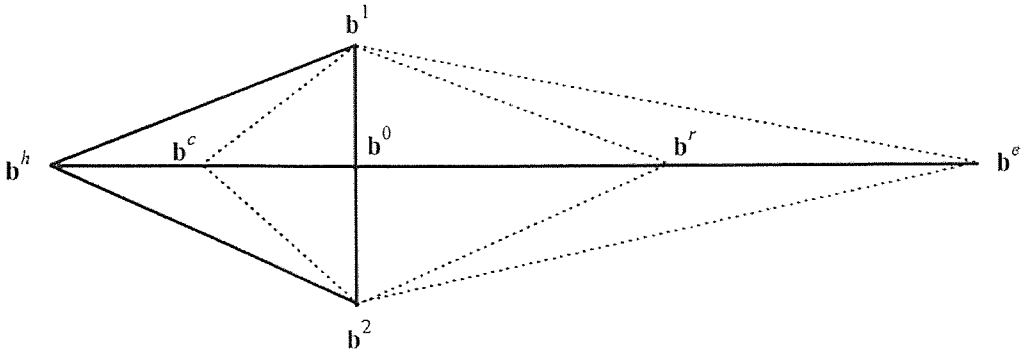

Figure E.1 The reflection($\mathbf{b}^r$), expansion($\mathbf{b}^e$), and contraction($\mathbf{b}^c$) operations in the simplex method

The operation of moving the point of the simplex where the function is largest through the opposite face of the simplex to a lower point is called reflection. In reflection $\mathbf{b}^h$ is replaced by $\mathbf{b}^r$, and $\mathbf{b}^r$ is given by

$$\mathbf{b}^r = \mathbf{b}^0 - \alpha(\mathbf{b}^h - \mathbf{b}^0) \qquad \alpha > 0. \tag{E.1}$$

The operation of expanding the simplex in the direction along which a further improvement of the function value than in reflection may be expected is called expansion.

$$\mathbf{b}^e = \mathbf{b}^0 + \gamma(\mathbf{b}^r - \mathbf{b}^0) \qquad \gamma > 1 \tag{E.2}$$

The simplex contracts itself in the transverse direction and tries to ooze down the valley. This operation is called contraction. In contraction $\mathbf{b}^h$ is replaced by $\mathbf{b}^c$, where $\mathbf{b}^c$ is given by

$$\mathbf{b}^c = \mathbf{b}^0 + \beta(\mathbf{b}^h - \mathbf{b}^0) \qquad 1 > \beta > 0 \tag{E.3}$$

Otherwise, if there is a situation where the simplex is trying to pass through the eye of a needle, it contracts itself in all directions, pulling itself in around its lowest(best) point. Every $\mathbf{b}^i$ is replaced by $0.5*(\mathbf{b}^i + \mathbf{b}^l)$. Suggested values are $\alpha = 1$, $\gamma = 2$ and $\beta = 0.5$(Nelder 1965, 308).

The iteration steps of the simplex method is shown in Figure E.2, and each step is explained as follows:

1. The initialization step to find the initial simplex which assures that its vertices span the full n-dimensional space. The initial simplex is given by as follows:

$$\begin{bmatrix} \mathbf{b}1 \\ \mathbf{b}2 \\ \mathbf{b}3 \\ \mathbf{b}4 \end{bmatrix} = \begin{bmatrix} b_1 & b_2 & b_3 \\ b_1 + \lambda & b_2 & b_3 \\ b_1 & b_2 + \lambda & b_3 \\ b_1 & b_2 & b_3 + \lambda \end{bmatrix}$$

where λ is a constant which is the guess of the problem's characteristic length scale.

2. The vertices $\mathbf{b}^h$, $\mathbf{b}^s$, $\mathbf{b}^l$ and the centroid of the simplex($\mathbf{b}^0$) are determined, and convergence test is performed. If the test is passed, the iteration process stops.

$$\begin{cases} \mathbf{b}^h : \text{the vertex corresponding to the highest E}(\mathbf{b}). \\ \mathbf{b}^s : \text{the vertex with the second highest value of E}(\mathbf{b}) \\ \mathbf{b}^l : \text{the vertex with the lowest value of E}(\mathbf{b}). \\ \mathbf{b}^0 : \text{the centroid of all } \mathbf{b}^i \text{ except } \mathbf{b}^h \end{cases}$$

$$\mathbf{b}^0 = \frac{1}{n} \sum_{\substack{i=1 \\ i \neq h}}^{n+1} \mathbf{b}^i$$

and the convergence criterion is

$$\frac{|E(b^h) - E(b^l)|}{|E(b^h)| + |E(b^l)|} < 0.001.$$

3. $\mathbf{b}^h$ is reflected and the value $E(\mathbf{b}^r)$ is computed.

4. If $E(\mathbf{b}^s) > E(\mathbf{b}^r) > E(\mathbf{b}^l)$ then $\mathbf{b}^h$ is replaced by $\mathbf{b}^r$, and the process is restarted from step 1.

5. If $E(\mathbf{b}^r) < E(\mathbf{b}^l)$, we expand the new simplex further in the direction $\mathbf{b}^r$-$\mathbf{b}^0$. The expansion is successful if $E(\mathbf{b}^e) < E(\mathbf{b}^l)$, and in this case $\mathbf{b}^h$ is replaced by $\mathbf{b}^e$. In the case of failure $\mathbf{b}^h$ is replaced by $\mathbf{b}^r$, and in either case we restart from step 1.

6. If the reflection (step 2) produces $\mathbf{b}^r$ such that $E(\mathbf{b}^h) > E(\mathbf{b}^r) > E(\mathbf{b}^s)$, we replace $\mathbf{b}^h$ by $\mathbf{b}^r$ and make the contraction move. The contraction is also applied if $E(\mathbf{b}^r) > E(\mathbf{b}^h)$.

7. If $E(\mathbf{b}^h) > E(\mathbf{b}^c)$, then $\mathbf{b}^h$ is replaced by $\mathbf{b}^c$ and the procedure is restarted from step 1. If $E(\mathbf{b}^h) < E(\mathbf{b}^c)$, the current simplex is shrunk about the point $\mathbf{b}^l$ as follows:

$$\mathbf{b}^i = \frac{1}{2}(\mathbf{b}^i + \mathbf{b}^l) \quad i = 1, \ldots, n+1$$

and we restart from step 1.

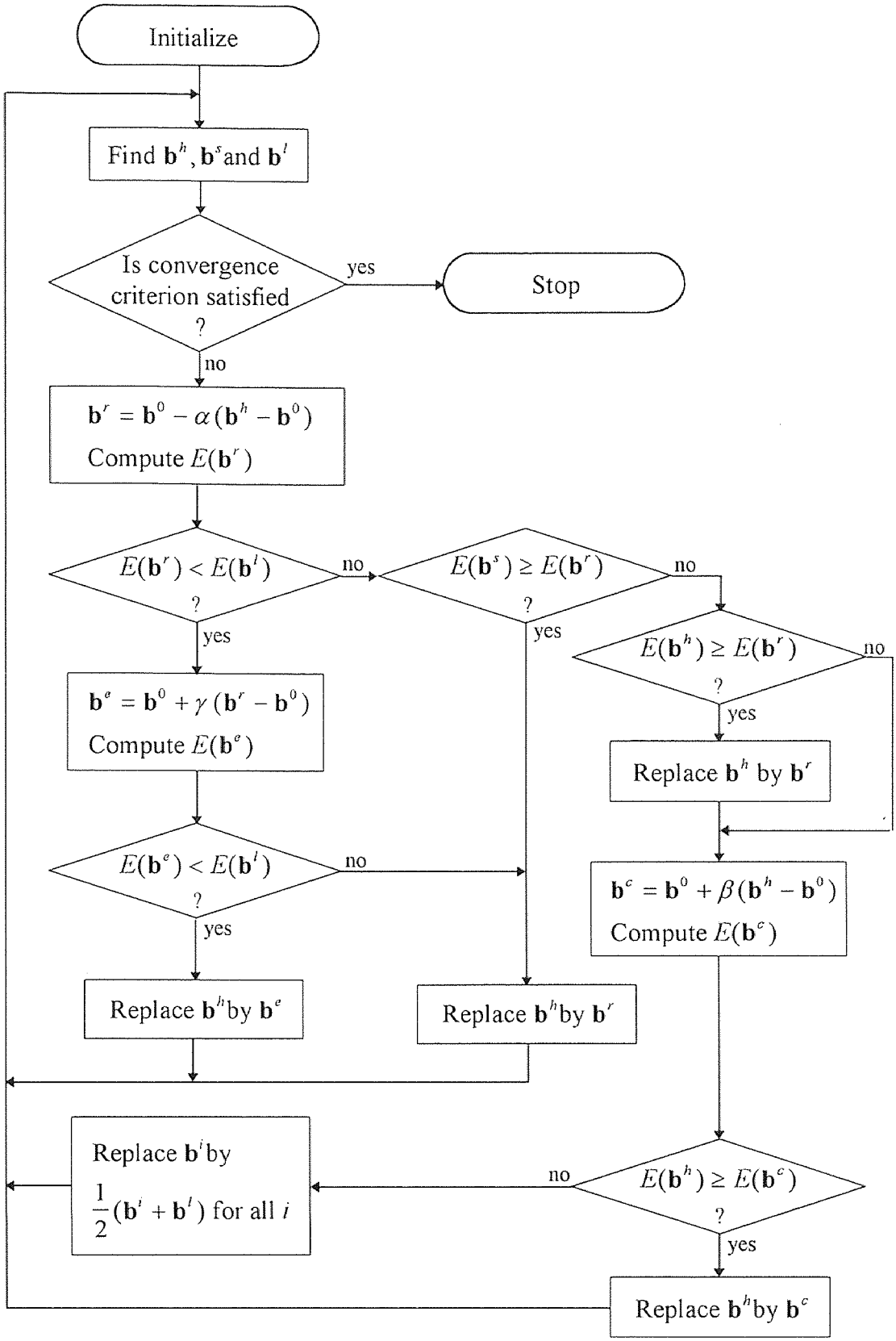

Figure E.2 Flowchart of the down-hill simplex method

APPENDIX F

ANGULAR VELOCITIES OF LIMBS AFTER KNEE-LOCK

Angular velocities of the thigh and shank of the swing leg after knee-lock are calculated from the conservation law of momentum. The definition of variables are in Appendix B. The calculation process is as follows:

The x-component of momentum of each mass at any instant is given by

$$\begin{aligned} m_h \dot{x}_h &= -m_h (L_h - z_h)\cos\theta \cdot \dot{\theta} \\ m_u \dot{x}_u &= -m_u L_h \cos\theta \cdot \dot{\theta} \\ m_t \dot{x}_t &= -m_t L_h \cos\theta \cdot \dot{\theta} + m_t z_t \cos\phi \cdot \dot{\phi} \\ m_s \dot{x}_s &= -m_s L_h \cos\theta \cdot \dot{\theta} + m_s L_t \cos\phi \cdot \dot{\phi} + m_s z_s \cos\sigma \cdot \dot{\sigma} \end{aligned} \tag{F.1}$$

The total x-component of momentum is biven by

$$\begin{aligned} M_x &= m_h \dot{x}_h + m_u \dot{x}_u + m_t \dot{x}_t + m_s \dot{x}_s \\ &= (-m_T L_h + m_h z_h)\cos\theta \cdot \dot{\theta} + (m_t z_t + m_s L_t)\cos\phi \cdot \dot{\phi} + m_s z_s \cos\sigma \cdot \dot{\sigma} \end{aligned} \tag{F.2}$$

The y-component of momentum of each mass at any instant is given by

$$\begin{aligned} m_h \dot{y}_h &= -m_h (L_h - z_h)\sin\theta \cdot \dot{\theta} \\ m_u \dot{y}_u &= -m_u L_h \sin\theta \cdot \dot{\theta} \\ m_t \dot{y}_t &= -m_t L_h \sin\theta \cdot \dot{\theta} + m_t z_t \sin\phi \cdot \dot{\phi} \\ m_s \dot{y}_s &= -m_s L_h \sin\theta \cdot \dot{\theta} + m_s L_t \sin\phi \cdot \dot{\phi} + m_s z_s \sin\sigma \cdot \dot{\sigma} \end{aligned} \tag{F.3}$$

The total y-component of momentum is biven by

$$\begin{aligned} M_y &= m_h \dot{y}_h + m_u \dot{y}_u + m_t \dot{y}_t + m_s \dot{y}_s \\ &= (-m_T L_h + m_h z_h)\sin\theta \cdot \dot{\theta} + (m_t z_t + m_s L_t)\sin\phi \cdot \dot{\phi} + m_s z_s \sin\sigma \cdot \dot{\sigma} \end{aligned} \tag{F.4}$$

Let angular variables after knee-lock as $(\bar{\theta}, \bar{\phi}, \bar{\sigma}, \dot{\bar{\theta}}, \dot{\bar{\phi}}, \dot{\bar{\sigma}})$.

The x-components of momentum before and after knee-lock must be same.

$$\begin{aligned} &(-m_T L_h + m_h z_h)\cos\theta \cdot \dot{\theta} + (m_t z_t + m_s L_t)\cos\phi \cdot \dot{\phi} + m_s z_s \cos\sigma \cdot \dot{\sigma} \\ &= (-m_T L_h + m_h z_h)\cos\bar{\theta} \cdot \dot{\bar{\theta}} + (m_t z_t + m_s L_t)\cos\bar{\phi} \cdot \dot{\bar{\phi}} + m_s z_s \cos\bar{\sigma} \cdot \dot{\bar{\sigma}} \end{aligned} \tag{F.5}$$

The y-components of momentum before and after knee-lock must be same.

$$\begin{aligned}&(-m_T L_l + m_l z_l)\sin\theta\cdot\dot{\theta} + (m_t z_t + m_s L_t)\sin\phi\cdot\dot{\phi} + m_s z_s \sin\sigma\cdot\dot{\sigma}\\ &= (-m_T L_l + m_l z_l)\sin\bar{\theta}\cdot\dot{\bar{\theta}} + (m_t z_t + m_s L_t)\sin\bar{\phi}\cdot\dot{\bar{\phi}} + m_s z_s \sin\bar{\sigma}\cdot\dot{\bar{\sigma}}\end{aligned} \tag{F.6}$$

We know the values of $(\theta, \phi, \sigma, \dot{\theta}, \dot{\phi}, \dot{\sigma})$ before knee-lock, and $\theta = \bar{\theta}$, $\phi = \bar{\phi}$, $\dot{\phi} = \bar{\sigma}$ and $\dot{\bar{\phi}} = \dot{\bar{\sigma}}$.

Let

$$\begin{aligned}p &= (-m_T L_l + m_l z_l)\cos\theta\cdot\dot{\theta} + (m_t z_t + m_s L_t)\cos\phi\cdot\dot{\phi} + m_s z_s \cos\sigma\cdot\dot{\sigma}\\ q &= (-m_T L_l + m_l z_l)\sin\theta\cdot\dot{\theta} + (m_t z_t + m_s L_t)\sin\phi\cdot\dot{\phi} + m_s z_s \sin\sigma\cdot\dot{\sigma}\end{aligned}$$

$$\begin{aligned}a &= (-m_T L_l + m_l z_l)\cos\bar{\theta}\\ b &= (m_t z_t + m_s L_t + m_s z_s \cos\bar{\phi}\end{aligned} \tag{F.7}$$

$$\begin{aligned}c &= (-m_T L_l + m_l z_l)\sin\bar{\theta}\\ d &= (m_t z_t + m_s L_t + m_s z_s)\sin\bar{\phi}\end{aligned}$$

Then, from the equations of x and y components of momentum, we get

$$\begin{cases}p = a\dot{\bar{\theta}} + b\dot{\bar{\phi}}\\ q = c\dot{\bar{\theta}} + d\dot{\bar{\phi}}\end{cases} \tag{F.9}$$

Therefore, after knee-lock, angular velocity of the stance leg is given by

$$\dot{\bar{\theta}} = \frac{dp - bq}{ad - bc} \tag{F.10}$$

and angular velocities of the thigh and shank of the swing leg are given by

$$\dot{\bar{\phi}} = \dot{\bar{\sigma}} = \frac{aq - cp}{ad - bc} \tag{F.11}$$

APPENDIX G

PROJECTION

We want to project a vector $\mathbf{V} = (x, y, z)$ on a plane of which one unit vector is given by $\mathbf{u} = (x_u, y_u, 0)$ where $x_u^2 + y_u^2 = 1$. First, we find a normal vector to the plane. the normal vector can be written as $\mathbf{n} = (y_u, -x_u, 0)$. Next, the vector $\mathbf{V}$ is projected on the normal vector $\mathbf{n}$, and we get a new vector $\mathbf{V}_n$. The magnitude of $\mathbf{V}_n$ is $\mathbf{V}\cdot\mathbf{n}$, and the direction of $\mathbf{V}_n$ is same as the normal vector $\mathbf{n}$. Therefore, $\mathbf{V}_n$ can be written as

$$\mathbf{V}_n = (\mathbf{V} \cdot \mathbf{n})\,\mathbf{n}$$

where $\mathbf{V}\cdot\mathbf{n} = y_u x - x_u y$.

$$\therefore\ \mathbf{V}_n = (y_u x - x_u y)\,(y_u, -x_u, 0) = (y_u^2 x - x_u y_u y,\ -x_u y_u x + x_u^2 y,\ 0)$$

If the vector $\mathbf{V}_n$ is substracted from the vector $\mathbf{V}$, the projected vector $\mathbf{P}$ can be obtained.

$$\begin{aligned}
\mathbf{P} &= \mathbf{V} - \mathbf{V}_n \\
&= (x, y, z) - (y_u^2 x - x_u y_u y, -x_u y_u x + x_u^2 y, 0) \\
&= (x_u^2 x + x_u y_u y, x_u y_u x + y_u^2 y, z) \\
&= \begin{bmatrix} x_u^2 & x_u y_u & 0 \\ x_u y_u & y_u^2 & 0 \\ 0 & 0 & 1 \end{bmatrix} \cdot \begin{bmatrix} x \\ y \\ z \end{bmatrix}
\end{aligned}$$

APPENDIX H

RANGE OF TOE-OFF ANGLE

The range of toe-off angle is limited by the configuration of the leg, thigh and shank. The configuration at toe-off is shown in the Figure H.1 and H.2. At toe-off the hip should be on the circle A. The knee of the stance leg should be on the circle B. The knee of the swing leg should be on the circle C. Equations of circles A, B and C are given by

$$x^2 + y^2 = L_t^2 \tag{H.1}$$

$$x^2 + y^2 = L_s^2 \tag{H.2}$$

$$(x + S_L - L_f)^2 + y^2 = L_s^2 + L_f^2 \tag{H.3}$$

The minimum toe-off angle is shown in the Figure H.1, and the maximum toe-off angle is shown in the figure H.2.

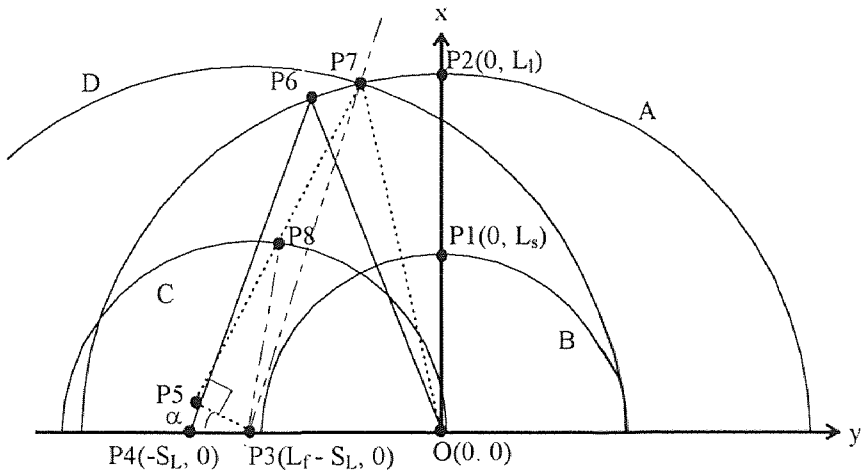

Figure H.1 The minimum toe-off angle

The knee of the swing leg is expressed as the point P8. If the point moves to the left, the swing leg bends backward. This is not the possible configuration. Therefore, the point moves to the left until the swing leg becomes a straight line. At this point the toe-off angle becomes minimum. To find the minimum toe-off angle we should know the

coordinate of point P7(x_7, y_7). The point P7(x_7, y_7) is the crossing point between the circles A and D. Equation of the circle D is given by

$$(x + S_L - L_f)^2 + y^2 = L_l^2 + L_f^2 \tag{H.3}$$

If we subtract equation(H.4) from equation(H.1), we get

$$2(S_L - L_f)x + (S_L - L_f)^2 = L_f^2$$

$$\therefore x_7 = -\frac{S_L^2 - 2S_L - L_f}{S_L - L_f} \tag{H.5}$$

If we substitute equation(H.5) into equation(H.1), we get

$$y_7 = \sqrt{L_L^2 - x_7^2} \tag{H.6}$$

The angle $\angle P_7P_3P_5$ can be obtained as

$$\angle P_7P_3O = \cos\left(\frac{L_f}{\sqrt{L_l^2 + L_f^2}}\right)$$

The angle $\angle P_7P_3O$ can be obtained as

$$\angle P_7P_3O = \cos\left(\frac{-S_L + L_f + x_7}{\sqrt{L_l^2 + L_f^2}}\right)$$

Therefore, the minimum toe-off angle can be obtained as

$$|\alpha| = 180^\circ - \angle P_7P_3P_5 - \angle P_7P_3O \tag{H.7}$$

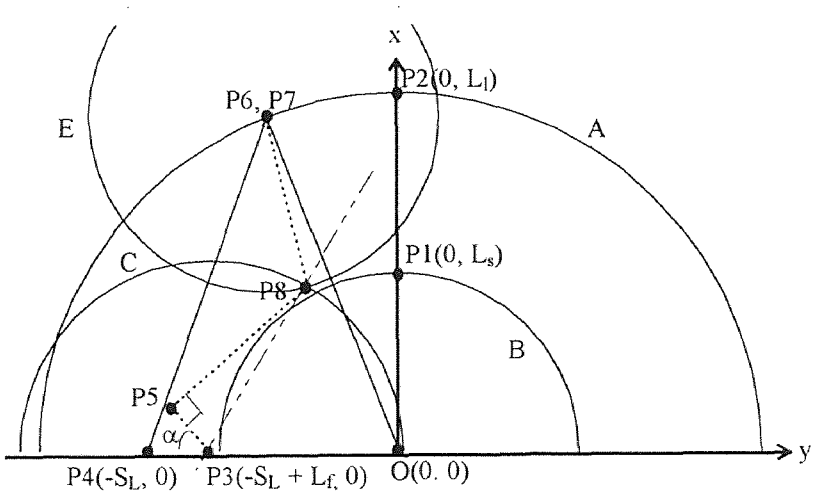

Figure H.2 The maximum toe-off angle

The point P6 is the position of the hip at heel-strike. At toe-off, if the hip point P7 is behind the point P6, it means that the body moves backward during the double-support phase. It is not an normal walking movement. Therefore, the point P7 can not be behind the point P6. When the points P6 and P7 coincide, the maximum toe-off angle is obtained. To find the maximum toe-off angle from the Figure H.2, we should know the coordinates of the points P6(x_6, y_6) and P8(x_8, y_8).

$$x_6 = -0.5S_L$$
$$y_6 = \sqrt{L_L^2 - (0.5S_L)^2}$$

The point P8 is the crossing point between the circles C and E. Equation of the circle E is given by

$$(x - x_6)^2 + (y - y_6)^2 = L_t^2 \tag{H.8}$$

To get the coordinate of point P8, we subract equation(H.8) from equation(H.3).

$$2(S_L - L_f)x + (S_L - L_f)^2 + 2x_6x - x_6^2 + 2y_6y - y_6^2 = L_s^2 + L_f^2 - L_t^2$$

After rearranging terms, we get

$$y_8 = -\frac{S_L - L_f + x_6}{y_6}x_8 + \frac{L_s^2 + L_f^2 - L_t^2 + x_6^2 + y_6^2 - (S_L - L_f)^2}{2y_6}$$

$$\therefore y_8 = ax_8 + b \tag{H.9}$$

where

$$a = -\frac{S_L - L_f + x_6}{y_6}$$
$$b = \frac{L_s^2 + L_f^2 - L_t^2 + x_6^2 + y_6^2 - (S_L - L_f)^2}{2y_6}$$

If we apply equation(H.9) into equation(H.8), we get

$$(x_8 - x_6)^2 + (ax_8 + b - y_6)^2 = L_t^2$$
$$(1 + a^2)x_8^2 + 2\{a(b - y_6) - x_6\}x_8 + x_6^2 + (b - y_6)^2 = L_t^2$$
$$x_8^2 + \frac{2\{a(b - y_6) - x_6\}}{(1 + a^2)}x_8 + \frac{x_6^2 + (b - y_6)^2 - L_t^2}{(1 + a^2)} = 0$$

$$x_8^2 + cx_8 + d = 0 \tag{H.10}$$

where

$$c = \frac{2\{a(b - y_6) - x_6\}}{(1 + a^2)}$$

$$d = \frac{x_6^2 + (b - y_6)^2 - L_t^2}{(1 + a^2)}$$

From equation(H.10), we can get

$$x_8 = \frac{-c \pm \sqrt{c^2 - 4d}}{2}$$

From the Figure H.2, we know x_8 is the greater number.

$$\therefore x_8 = \frac{-c + \sqrt{c^2 - 4d}}{2} \qquad \text{(H.11)}$$

If we substitute equation(H.11) into equation(H.9), we can get y_8.

The angle $\angle P_8P_3P_5$ can be obtained as

$$\angle P_8P_3P_5 = \cos\left(\frac{L_f}{\sqrt{L_s^2 + L_f^2}}\right)$$

Thw angle $\angle P_8P_3O$ can be obtained as

$$\angle P_8P_3O = \cos\left(\frac{-S_L + L_f + x_8}{\sqrt{L_s^2 + L_f^2}}\right)$$

Therefore, the maximum toe-off angle can be obtained as

$$|\alpha| = 180^\circ - \angle P_8P_3P_5 - \angle P_8P_3O \qquad \text{(H.12)}$$

REFERENCES.

Beckett, R., and K. Chang. 1968. "An Evaluation of the Kinematics of Gait by Minimum Energy." J. *Biomechanics.* 1: 147-159.

Elftman, H. 1966. "Biomechanics of Muscle." *J. Bone Jt Surg.(A)* 48: 363-377.

Fenn, W. 1930. "Frictional and Kinetic Factors in the Work of Sprint Running." *Am. J. Physiol.* 92: 583-611

Fenn, W. 1930. "Work against Gravity and Work due to Velocity Changes in Running." *Am. J. Physiol.* 93: 433-462.

Greenwood, D. T. 1977. *Chap. 2 Lagrange's Equations. Classical Dynamics.* Englewood Cliffs, NJ: Prentice-Hall. 55.

Inman, V. T. 1966. "Human Locomotion." *Canad. Med. Ass. J.* 94: 1047-1054.

Jacoby, S. L. S., J. S. Kowalik, and J. T. Pizzo. 1972. *Iterative Methods for Nonlinear Optimization Problems.* Englewood Cliffs, NJ: Prentice-Hall.

Lacker, M. H., and et al. 1993. "Calculation of Mechanical Energy Cost in a Simple Model of Human Walking." *IEEE Annual Northeast Bioengineering Conference.* 19: 121-123.

Mochon, S., and T. A. McMahon. 1980. "Ballistic Walking." *J. Biomechanics.* 13: 49-57.

Nelder, J. A., and R. Mead. 1965. Computer Journal, vol.7, pp. 308-313.

Passmore, R., and M. H. Draper. 1965. *Newer Methods of Nutritional Biochemistry.* edited by A. A. Albanese. New York, NY: Academic Press.

Press, W. H., S. A. Teukolsky, W. T. Vetterling, and B. P. Flannery. 1992. *Numerical Recipes in C.* 2nd ed. Cambridge, MA: Cambridge University Press. 408-412.

Ralston, H. J. 1974. "Optimization of Energy Expenditure During Level Walking." *Europ. J. Appl. Physiol.* 33: 293-306.

Veau, B. L. 1977. *Williams and Lissner: Biomechanics of Human Locomotion.* 2nd ed. Philadelphia, PA: W. B. Saunders Company. 205-215.

Wells, D. A. 1967. *Chap. 4 Lagrange's Equations of Motion for a System of Particles. Lagrangian Dynamics.* Schaum's Outline Series. New York, NY: McGraw-Hill. 60-61.